University of Southampton

Two-Phase Flow of Water and Steam in a Liquid Metal Fast Breeder Reactor Pipe

by

Stephen James Kane

Thesis submitted in partial fulfilment for degree of Doctor of Philosophy

Faculty of Mathematical Studies

This thesis was submitted for examination in August 1994.

UNIVERSITY OF SOUTHAMPTON

ABSTRACT

FACULTY OF MATHEMATICAL STUDIES

DEPARTMENT OF MATHEMATICS

Doctor of Philosophy

TWO PHASE FLOW Of WATER AND STEAM IN A LIQUID METAL FAST BREEDER REACTOR PIPE

by Stephen James Kane

This thesis describes the mathematical modelling and analysis of the two phase flow of water and steam in a steam generating pipe contained within the evaporating component of a nuclear power plant. As the fluid is heated the continuous phase (water) is evaporated and steam is produced. The phases adopt different geometrical configurations called flow regimes. The flow regime adopted by the phases depends on the amount of each phase present and also external features such as pipe geometry. The main regions of interest are the subcooled, bubbly and, annular flow regimes. The subcooled flow regime consists of water flowing at temperature below its saturation temperature and can be modelled as a single phase flow. The bubbly is characterised by that the gas phase flows as discrete bubbles in the continuous phase. The bubbly flow regime shall be modelled using a system of averaged two–phase flow equations. Of particular interest is the annular flow regime. The annular flow regime is characterised by the fact that the majority of the liquid phase is present in a thin film along the the pipe wall with the remaining liquid phase being present as droplets in a central gas core. We develop a non-linear singular integro-differential equation to describe the interface between the liquid film and gas core. The annular flow regime is further complicated by an exchange of mass between the film and gas core due to entrainment, deposition of droplets, and evaporation. The loss of mass from the liquid film leads to the phenomenon of dryout where the liquid film ceases to exist.

I don't want to achieve immortality through my work
... I want to achieve it through not dying.

Woody Allen.

TABLE OF CONTENTS

LIST OF FIGURES

ACKNOWLEDGEMENTS

I would like thank my supervisor Alistair Fitt for all his help and guidance. I would also like to thank all the members of the Industrial Applied Mathematics group, especially Bob Craine.

I would like to acknowledge the financial support of SERC and Nuclear Electric in the form of CASE Studentship.

LIST OF SYMBOLS

A	Average cross-sectional area (m^2)
c_p	Specific heat capacity $(KJ/Kg\,K)$
C_D	Drag coefficient
D	Hydraulic diameter (m)
E	Energy source (J)
F_D	Drag force (N)
H	Coefficient of surface heat transfer $(Kw/m^2\,K)$
h	Enthalpy (J/Kg)
K	Thermal conductivity $(Kw/m\,K)$
p	Pressure (N/m^2)
q	Heat flux (Kw/m^2)
r	Radial coordinate (m)
r_b	Average bubble radius (m)
r_c	Radius of curvature (m)
R	Gas constant $(KJ/mol\,^\circ C)$
R_0	Universal gas constant $(KJ/mol\,^\circ C)$
T	Temperature (K)
T_k	Shear stress in phase k (N/m^2)
t	Time variable (s)
v, ν, ω	Velocity (m/s)

W	Interfacial work
Z	Compressibility factor
α_k	Void fraction of phase k
Δp	Pressure drop (N/m^2)
Γ	Rate of production of steam $(Kg/m^3\,s)$
κ	Thermal diffusivity (m^2/s)
λ	Latent heat of vaporisation$(KJ/Kg\,s)$
μ	Dynamic Viscosity $(Kgm^{-1}s^{-1})$
ρ	Density (Kg/m^3)
σ	Surface tension (N/m)
τ	Stress (N/m^2)
ϕ	Velocity potential (m^2/s)

Dimensionless Groups

$Fr = \frac{v}{\sqrt{gL}}$	Froude number
$N_{Gz} = \frac{\rho c_p v r^2}{K}$	Graetz number
$Nu = \frac{H a}{K}$	Nusselt number
$N_{Pe} = \frac{\rho c_p v r}{K}$	Peclet number
$N_{pch} = \frac{\Gamma L}{\rho v}$	Phase change number
$N_p = \frac{p}{\rho v^2}$	Pressure group
$Pr = \frac{\mu c_p}{k}$	Prandtl number
$Re = \frac{\rho v L}{\mu}$	Reynolds number

$Re_{2p} = \frac{2 r_b \rho \lvert v_1 - v_2 \rvert}{\mu_m}$	Two-phase Reynolds number

Subscripts

i	Interfacial
1	Gas phase
2	Liquid phase
m	Mixture variable
s	Saturation point
w	Value of variable at the wall interface

Superscripts

Re	Reynolds stresses
i	Inner variable
o	Outer variable

Chapter 1

INTRODUCTION

1.1 Physical Background

The purpose of this thesis is to study the two-phase flow of water and steam in the steam generating pipes of a nuclear reactor plant and to model the different flow regimes which occur as the fluid is evaporated along the length of the steam generating pipes. In this section we shall outline the physical background to the problem and give some details on the development of nuclear reactors and their advantages and disadvantages.

Generally speaking, there are three main types of nuclear reactors. These are classed as gas cooled, liquid cooled, or reactors where the coolant is a liquid metal. The coolant is the material which is employed to take the thermal energy (heat) away from the nuclear reactor. In this thesis we shall mainly be considering liquid metal cooled reactors. The choice of coolant is of the utmost importance to the reactor designers for reasons of efficiency, safety and cost. It was found that liquid metals made excellent coolants since they have good thermal transport properties and the size of the piping and other pieces of major equipment could then be kept to a minimum.

Gas Cooled Reactors (GCR), Pedersen (1978), use either carbon dioxide or helium as the coolant. The main advantages of a gas cooled reactor are that the coolant is very easy to handle, there is a cheap and abundant supply of carbon dioxide and the coolant can operate at high temperatures without pressurisation. The disadvantages with gas cooled reactors are that both gases have low heat transfer properties and require large heat transfer surfaces. The poor heat transfer properties of the gases mean that they are not as efficient as liquid metal coolants. Also, since large heat transfer surfaces are required, the size of the piping and other pieces of major equipment cannot be kept to a minimum in a gas cooled reactor, making them more expensive to build than Liquid Metal Fast Breeder Reactors.

Both ordinary and heavy water(H_2^2O) have been used as coolants in liquid cooled reactors since they have good heat removal properties. The major disadvantage of water as a coolant is that the system needs to operate at pressures far greater than atmospheric to raise the boiling temperature of the coolant. Water is also very corrosive at high temperatures meaning that the pipes have to be coated with zirconium alloys or stainless steel. This increases greatly the production costs of the steam generating pipes.

In the 1960's, as outlined by Mclain , the metals of interest for the liquid metal coolant were sodium, potassium, lithium, lead, bismuth and mercury. The choice of coolant is determined by which of the metals satisfies the greatest number of the following properties:

- Low vapour pressure at the operating temperature
- Boiling point of approximately 1500deg F at atmospheric pressure
- Low melting point

- Excellent heat transfer coefficient
- Radiation stability
- Thermal stability
- A low thermal neutron capture cross-section
- Short term induced radioactivity
- Low cost
- Require low pumping power
- Non-toxic
- Non-reactive with water or air

The low system pressure permits the design of pipes with low stress levels and decreases the chance of pipe rupture. Having a liquid metal that boils at $1500\,^{\circ}F$ atmospheric pressure is an advantage since most liquid metals are limited to a boiling temperature of $1200\,^{\circ}F$ at atmospheric pressure and therefore cannot transfer so much heat to the boiler. Also, if the system is operating at atmospheric pressure it considerably reduces the risk of a LOCA (loss of coolant accident) due to the pipes rupturing. If at atmospheric pressure the pipes do rupture then the severity of the damage caused by the loss of coolant is far less than if the system was operating at a pressure greater then atmospheric pressure. The liquid metal coolant also needs to have low thermal neutron capture cross-section meaning that is less likely to become radioactive than metals with a higher thermal neutron capture cross-section. It is important that the coolant does not become radioactive, since if there is a loss of

coolant accident caused by rupture of the pipes, the radioactive material may escape into the atmosphere. This situation may be complicated further if the coolant is reactive with water or air since an explosion may occur causing further damage to the environment.

By a process of elimination it was found that sodium had most of the properties listed above. Sodium does have drawbacks, however, for it is reactive with both water and air. On the positive side molten sodium has a high specific heat capacity and high thermal and electrical conductivity. Another problem associated with using liquid metals as coolants is their corrosive effect on the pipes. However, with a suitable choice of pipe material, such as steel, the corrosion rate may be limited to less than 0.0001 in/yr.

The type of reactor we shall be dealing with is a liquid metal fast breeder reactor with a '*once through*' boiler. From now on we shall refer to this by the abbreviation LMFBR. A once through boiler differs from other boilers in that the water that has been evaporated is not recirculated through the boiler, thus lowering the chance that the water will become radioactive.

The central structure in all nuclear power plants is the nuclear *reactor* or *core* as it is sometimes known. The nuclear core contains fuel rods containing an isotope of Uranium, usually U_{235}. The fuel rods are bombarded with neutrons. Absorption of a neutron by a *heavy* material such as Uranium or Plutonium causes the nucleus to split into two massive fragments with a large release of thermal energy. The process by which a heavy material splits into lighter materials is known as *fission*, as opposed to the process of *fusion* where two lighter materials combine together to form a heavy material. As well as the Uranium splitting into lighter materials, two neutrons are produced. Only one of these neutrons is needed to substain the reaction. The number

of *free* neutrons within the reactor is limited by the use of control rods. Control rods are constructed of carbon and can be lowered into the reactor to absorb some of the neutrons. If the losses of neutrons can be reduced sufficiently the possibility exists for new fuel to be generated in quantities as large or even larger than the amount consumed. This process of producing new fuel is known as *breeding* and hence the name breeder reactors.

Sodium cooled reactors usually have two heat exchangers. This is because the molten sodium that transports heat away from the reactor core becomes radioactive and so there is an intermediate heat exchanger loop where heat from the radioactive sodium is transferred to more molten sodium. This molten sodium then passes to the primary heat exchanger where it is used to heat the water and steam in the steam generating pipes. The purpose of the intermediate heat exchanger is for safety reasons, to prevent any radioactive sodium being released into the atmosphere if any problems occur during the steam generating process. A schematic diagram of a once through liquid metal fast breeder reactor plant is shown in figure 1.1.

The design life of steam generating pipes within a liquid metal fast breeder reactor is about thirty years. The integrity of the pipes is therefore clearly important for safety reasons. Calculations carried out by General Electric, and presented by Magee, Casey et al (1976), predicted fatigue lives of less then thirty years for the steam generating pipes. These calculated fatigue lives were clearly unacceptable when compared to the expected design lives of the pipes. This led General Electric to develop more accurate ways to estimate the fatigue life of the pipes and also to raise the question of what causes the pipes to crack.

Nuclear Electric Ltd also became interested in this problem when they became involved with the European Fast Breeder Reactor Project. The European fast breeder

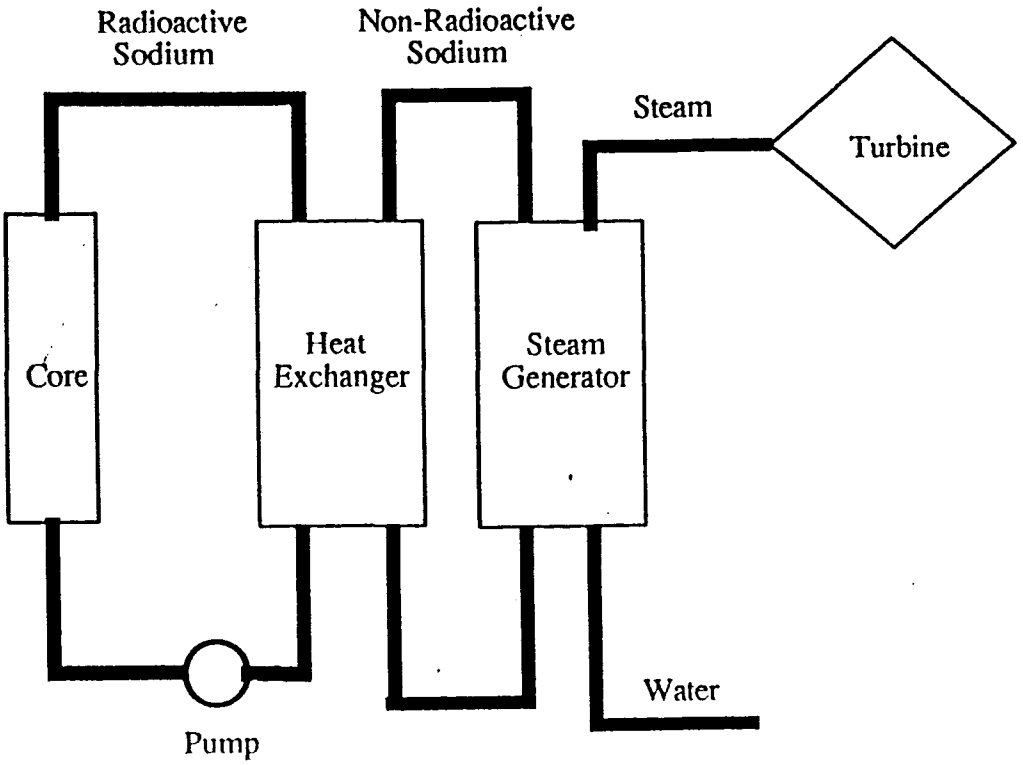

Figure 1.1: Schematic layout of LMFBR plant

reactor was based on a liquid metal fast breeder reactor (LMFBR) with a once-through boiler. Initial work was carried out by Atthey, Scruton, and Chojnowski (1988) with particular emphasis on the heat transfer mechanisms involved and how these mechanisms are affected by the motion of the dryout front. Initial experimental work was undertaken at Kraftwerk union and reported upon by Atthey et al (1988).

The evaporating component of the nuclear reactor consists of a bundle of vertical steam generating pipes surrounded by an outer casing. Molten sodium is pumped in at the top of the casing and subcooled water is pumped up through an inlet at the base of the steam generating pipes. The water enters the steam generating pipes at

a temperature of about $240\,^{\circ}C$ and with an inlet pressure of 200 Bar. The molten sodium has an inlet temperature of approximately $600\,^{\circ}C$ and an outlet temperature of about $350\,^{\circ}C$. There is an exchange of heat between the countercurrent flowing molten sodium and the water in the steam generating pipes due to the difference in temperature between the fluid and the molten sodium. As the water is heated so it begins to vaporize and we obtain a two-phase flow consisting of water and steam. The various geometrical configurations adopted by the two phases are called flow regimes or flow patterns. The flow patterns are determined by the amount of each phase present and external effects such as the orientation of the pipe and whether the pipe is being heated.

For the purpose of this work we shall only be considering two-phase flows in uniformly heated vertical pipes. By uniformly heated we mean that the heating is uniform around the circumference of the pipe. We will mainly be considering the case where the pipes are electrically heated, since in practice it is easier to obtain experimental observations from an electrically heated test rig than one that is heated by a liquid metal. Experimental evidence indicates that the principal two-phase flow regimes present in such a vertical pipe are:

- Single phase liquid flow
- Bubbly flow
- Slug flow
- Annular flow
- Drop flow
- Single phase vapour flow.

Some texts such as Collier (1972) and Whalley (1987) list other flow regimes such as wispy annular and churn turbulent regimes, which may occur under certain flow conditions between some of the aforementioned flow regimes. Some texts also refer to slug flow as plug flow. For a list of alternative names for the flow regimes the reader is referred to Chisholm (1983).

The purpose of this thesis is to model the upward vertical flow of water and steam in a steam generating pipe and to model the process of dryout. Dryout occurs in the annular flow regime and is of fundamental importance to the nuclear power industry since it can cause the steam generating pipes to crack and eventually rupture. A full description of the dryout mechanism is given in §1.2.4, the section describing the annular flow regime. The flow regimes are also shown diagrammatically in figure (1.2). Note that for clarity the flow regimes in figure (1.2) have not been drawn to scale.

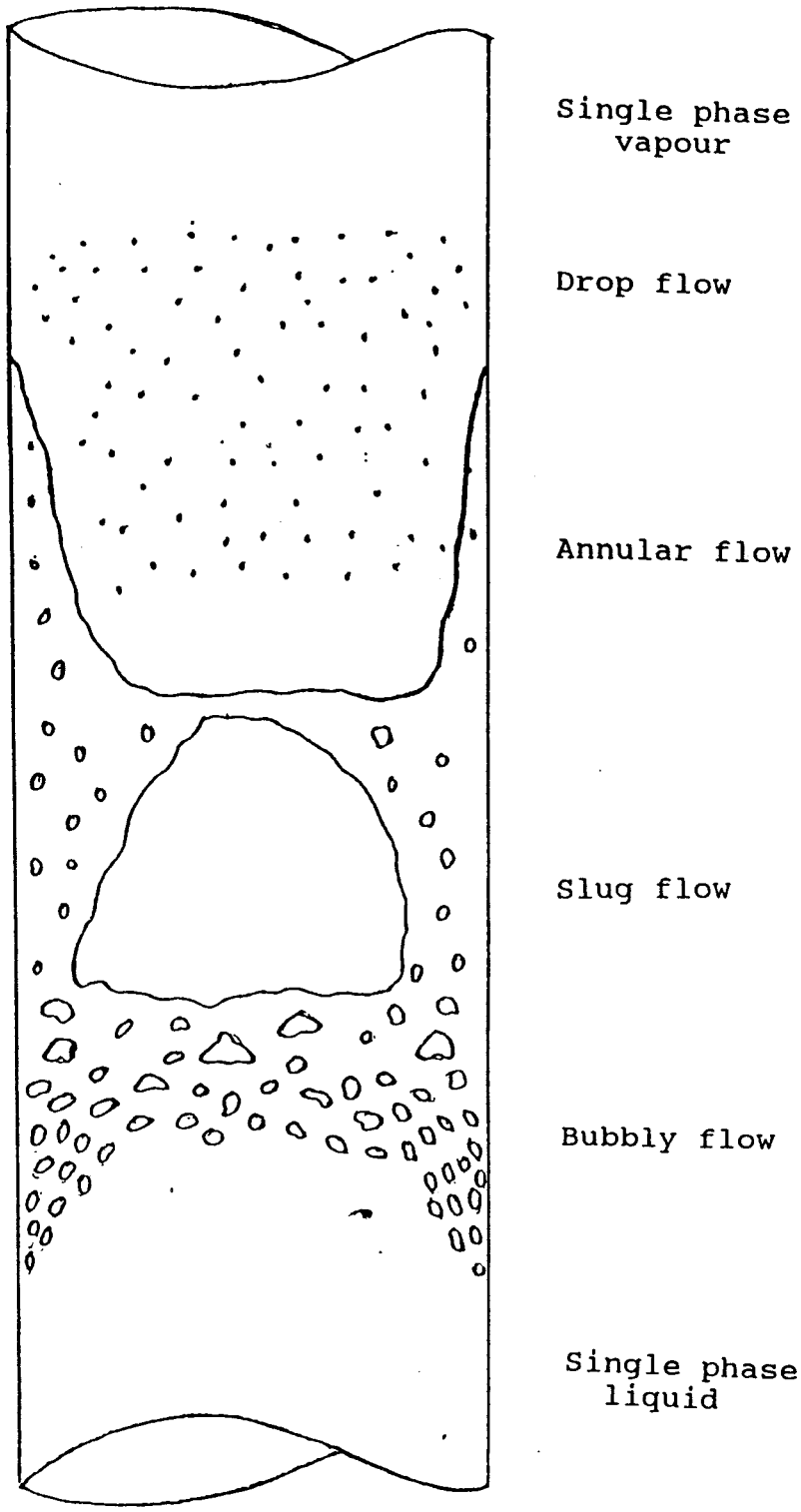

Figure 1.2: Vertical two-phase flow patterns

1.2 Two-Phase Flow Regimes

1.2.1 Single Phase Flow

Water is pumped into the evaporator pipe through an inlet at the base. The water is initially at a temperature of $240\,^{\circ}C$, which is considerably less than its boiling temperature, and an inlet pressure of 200 Bar. The boiling temperature of the water is high because the steam generating pipes are at such a high pressure. The water is either heated by the countercurrent flow of molten sodium in a LMFBR or electrically heated in the test rig. The water is at a lower temperature than the pipe walls and therefore heat is conducted into the water. As long as the internal pipe wall temperature remains below the temperature required for bubble nucleation the heat transfer mechanism is that of single phase convective heat transfer.

1.2.2 Bubbly Flow

The bubbly flow regime consists of the vapour phase flowing as discrete bubbles in the continuous liquid phase. The bubbles vary from being small and spherical to large and cap shaped. The bubbles are produced by the evaporation of the surrounding liquid. They are formed at nucleation sites which may either be impurities in the liquid or pits, scratches or cavities along the pipe walls. In certain situations the bubbles themselves may act as nucleation sites. The bubbly flow regime is usually initiated when there is still some subcooled liquid present and the heat transfer process is therefore known as subcooled nucleate boiling.

The transition from the bubbly regime to the next regime occurs when the gas flow increases and the bubbles get closer together so that collisions occur more fre-

quently. These collisions lead to bubble coalescence and to the formation of larger bubbles, which themselves then collide producing even larger bubbles. Once these larger bubbles have a diameter comparable to the inner pipe diameter the flow regime has undergone the transition to slug flow.

The bubbly flow that we shall consider will be one involving a change of state. Bubbly flows involving no change of state also exist and have been studied, for example by Lisseter and Fowler (1992). They showed how a set of scales could be developed for a realistic bubbly flow model and these scales were then used to non-dimensionalize the equations. By examining the non-dimensionalized equations they were able to neglect some terms and simplify the model. Their simplified model compared favourably with experimental data. The work of Lisseter and Fowler showed that it is possible to develop simple but realistic models for bubbly flows.

1.2.3 Slug Flow

Slug flow consists of large spherical cap bubbles with diameters comparable to the diameter of the pipe. These large spherical cap bubbles are often referred to as '*Taylor*' bubbles or as '*bullet shaped*' bubbles. The large gas bubbles are separated from the pipe wall by a thin, slowly descending liquid film. The bulk of the liquid is in the form of slugs which separate the spherical cap bubbles from each other. These liquid slugs may have small gas bubbles entrained in them. The lengths of the spherical cap bubbles vary but are usually two to three times the diameter of the pipe in length. A transition from slug flow to annular flow occurs when the large gas bubbles begin to break up. The heat transfer mechanism for the slug regime is saturated nucleate boiling. Slug flows are also be found in heat exchanger pipes and in gas-oil pipelines.

1.2.4 Annular Flow

The annular flow regime consists of a thin liquid film along the pipe wall with a central gas core. The gas core is entrained with liquid droplets which flow along with the gas core. There is an exchange of mass between the gas core and the liquid film due to:

- entrainment of liquid drops from the liquid film to the gas core
- deposition of liquid drops from the gas core
- evaporation of the liquid film.

The rate of entrainment depends on the structure of the surface waves on the liquid film. One type of entrainment is caused by the shearing off of the crests of large amplitude surface waves by the gas flow. These waves can have amplitudes which are $3 - 5$ times greater then the average film thickness. Another method of entrainment is the undercutting of the liquid film by the gas flow. Entrainment may also occur by the bursting of gas bubbles that can sometimes exist in the liquid film. For a more detailed discussion of surface waves that occur in annular two phase flow see Ishii et al.(1975)

The rate of deposition is directly proportional to the concentration of liquid droplets entrained in the gas core flow. The evaporation rate depends on the heat flux being supplied to the liquid film from an external heating source.

The annular flow regime finishes when dryout occurs. Dryout is the point at which complete evaporation of the liquid film occurs. At the dryout position there is a sharp increase in the wall temperature because the thermal conductivity of the vapour

phase is an order of magnitude less than that of the liquid phase. Determination of the dryout point is complicated by the fact that the liquid film can reform, thus quenching or rewetting the wall causing the wall temperature to drop. In fact, this process of dryout and rewetting can occur periodically causing thermal stresses to be set up in the pipe wall which may lead to cracks forming in the walls. The integrity of the pipes is therefore greatly affected by the process of dryout and a good understanding of dryout is vital in being able to predict the lifetimes of steam generating pipes.

For the purposes of our work we shall consider a system where there is an exchange of mass in the annular flow regime. This not always the case for annular two-phase flows. For example, the petrochemical industry is interested in the annular flow of oil and natural gas in pipelines where there is no mass exchange. A physical model for an annular two-phase flow without mass exchange is presented by Oliemans et al (1986). Their model is based upon the experimental observation that the the film thickness remains approximately constant along the length of the pipe. This is an important physical example since it shows that dryout cannot occur unless there is some form of mass exchange present within the system.

A process closely related to dryout is that of burnout, which can occur in pool boiling. In pool boiling, the boiling occurs at the heated surface and the fluid being heated is stagnant. The process of burnout is the same as dryout except for the fact that in dryout the fluid is being forced to flow. Thus dryout occurs in forced convective flows and burnout in pool boiling. Some texts also refer to the process of dryout as either, CHF-*critical heat flux*, DNB-*departure from nucleate boiling*, or simply as *boiling crisis*.

Another important phenomenon which may occur in the annular flow regime is that of *flooding* and *flow reversal*. These two processes are usually seen experimentally

by injecting liquid through an inlet into a vertical pipe. The liquid forms a thin film along the pipe wall and flows in a downward direction due to gravity. Gas is then pumped in through the base of the pipe so that it is flowing in the opposite direction to the liquid film. As the gas flow rate is increased the surface of the liquid film becomes disturbed and ripples begin forming on the surface of the film. As the gas flow rate is increased large waves form on the liquid film. These waves eventually *bridge* the pipe and partially block it. Some of the liquid from this blockage is then propelled above the liquid inlet by the gas flow forming droplets. This process is known as *flooding*. When the gas flow rate is increased further the liquid film begins to be pulled up the pipe by the gas flow. Eventually all the liquid is pulled up by the gas flow and a co-current annular flow is formed. If the gas flow rate is now gradually reduced a situation is reached where the liquid film is said to *hang* at the liquid inlet. This means that the entire liquid film is located above the liquid inlet. If the gas flow rate is reduced further then the liquid film begins to flow down the pipe and a counter-current annular flow is formed. This process is termed *flow reversal*. It was shown by Fowler and Lisseter (1992) that a two-fluid model for the annular flow regime involving realistic phase interaction could be used to predict when flooding and flow reversal are likely to occur.

1.2.5 Drop and Single Phase Vapour Flow

The drop flow regime is characterised by the fact that the liquid phase is entrained as discrete liquid droplets in the gas phase. This regime is also termed the *liquid deficient region* as the flow is mainly composed of the gas phase. If the pipe is sufficiently long all the liquid phase will eventually evaporate and the flow will just consist of vapour. This regime is termed single phase vapour flow.

1.2.6 Different Pipe Geometries

All the previously described flow regimes have been for vertical upflow in a cylindrical pipe. Other pipe geometries that exist include two phase flow in rectangular pipes, where the liquid tends to collect in the corners of the pipe. Sometimes to improve the heat transfer a helically twisted tape will be inserted in cylindrical pipes. This has the effect of *throwing* the liquid onto to the walls of the pipe ensuring good heat transfer since the thermal conductivity of water is far greater than that of steam. A similar effect is obtained by using helically shaped pipes, which also has the effect of minimising the space required for the evaporator.

1.2.7 Horizontal Two-Phase Flow

All the previously described flow regimes have been for vertical two-phase flows. Corresponding flow patterns exist for flows in horizontal pipes. The horizontal bubbly two phase flow regime differs from the vertical one since the gas bubbles tend to gather along the top of the horizontal pipe, whereas in vertical bubbly flow the bubbles are evenly distributed across the cross-section of the pipe. A similar occurrence happens with horizontal slug flow since the large Taylor bubbles gather at the top of the horizontal pipe. Horizontal annular flow is very similar to vertical annular flow except that the liquid film at the bottom of the horizontal pipe is thicker than the liquid film along the top of the pipe.

1.3 Closing Remarks

Our approach to modelling the flow of steam and water in a steam generating pipe will to be to consider each flow regime separately and then produce a global model for the flow. The aim of modelling each of the flow regimes is to be able to formulate analytical relationships for quantities such as pressure drops and lengths of the flow regimes and then be able to estimate the importance of each flow regime in the global flow.

An important feature to take into account in our model will be the exchange of mass between the two phases. This will vary from regime to regime and will depend on the flow conditions. It will have particular relevance in the annular flow regime where the evaporation of a thin film along a heated plate will be modelled. From the latter model we hope to be able to predict the shape of the liquid gas interface close to the dryout point.

Chapter 2

METHODS OF MULTIPHASE FLOWS

2.1 Introduction

In this chapter we shall outline some of the theories of multiphase flows, with specific emphasis on the different modelling techniques developed to model multiphase flows. We shall also define all of the physical quantities that will be required in later chapters.

A multiphase flow is simply the flow of several phases which need not be in different physical states. The simplest form of a multiphase flow is a two-phase flow. Examples of two-phase flows are

liquid-gas - boiling condensation processes
gas-liquid - atomizers
gas-solid - fluidised beds
liquid-liquid - liquid-liquid extractions
liquid-solid - flow of suspensions

In such a large class of problems many diverse mechanisms are important in the different flows. The models used for these different flows do have common features, such as interfacial drag.

Historically, among the first multiphase systems to be investigated were geophys-

ical flows involving sediments and, also, the motion of clouds. At the start of the century work was undertaken on the shape beds of particles take when subjected to a fluid flow. This lead to an investigation of the stability of the interface between two liquids and to an understanding of sedimentation. The need to extract hydrocarbons from inside the earth's crust led to a detailed investigation into two– phase flow in a porous medium. In the 1960's, with the emergence of commercial nuclear power, came the need to model water and steam flows. Problems first encountered when modelling fluid-fluid flows, unlike fluid-particle systems, were mainly due to the fact that the shape of the interface between the fluids may change shape leading to interactions between the fluids. The need to model water and steam flows is still very important today for reasons of nuclear safety and improving the efficiency of heat transfer in steam generating pipes.

Some authors, for example Wallis (1969), use the term two-component flow to indicate that the two phases consist of different materials. So, for example, the flow of air and water would be considered a two-component flow, whereas the flow of water and steam would be termed a two-phase flow.

For the purpose of this work we shall be concentrating on the flow of water and steam in steam generating pipes located in the evaporation component of a Liquid Metal Fast Breeder reactor. Our model will be complicated by the fact that a change of phase occurs because the water is evaporated as it flows. For this reason the flow model will include an exchange of mass between the two phases. Although we will only be modelling a one dimensional two-phase flow the techniques developed may be extended to model general multiphase flows in higher dimensions. Two general approaches have been developed for modelling multiphase flows; one consists of modelling the dynamics of a single particle and extending the model to a multi-particle system, whilst the other concerns the development of continuum models. For the

purpose of this work we shall be developing a continuum model.

There have been several methods developed for modelling multiphase flows. These methods have been widely reported upon in such texts as Wallis (1969), Collier (1972), Soo (1967,1990), Whalley (1987) and Drew and Wood (1988). The seminal book by Wallis tends to concentrates on gas–liquid flows using cross-sectionally averaged equations. In addition he introduced constitutive relationships by quoting appropriate experiments. The work by Soo is principally concerned with particle fluid systems. Both Collier and Whalley tend to concentrate on the flows of liquids and gases, with Whalley giving particular emphasis to physical situations involving boiling processes.

There are a number of different ways that a continuum model may be developed. These include:

- separated flow models
- mixture and homogeneous models
- drift flux models.

Both the drift flux and separated flow models involve formulating a set of equations describing the flow in each phase, whereas the mixture and homogeneous flow models treat the flow as a single component flow. Each of these models is relevant to different physical situations. For example, the homogeneous model has been used successfully to model foams and the drift flux model to describe bubbly flows in wide diameter pipes.

The most general model is the separated flow model and this is the model that we shall be developing. Separated flow models can become very complicated as a large

number of variables may be involved. The equations may be simplified, however, by careful consideration of the physical situation being modelled. In using any of the aforementioned techniques careful consideration needs to be given to which particular flow regime is being modelled, since the equations of motion for the flow will vary from regime to regime.

In the following sections we shall explain in detail the separated flow model and outline the drift flux and mixture models.

2.2 Separated Flow Model

The separated flow model involves formulating a set of equations that describe the motion of each phase. Separated flow models vary a great deal in complexity depending on the particular flow being modelled. When modelling two-phase flows we need to take into consideration, for instance, whether both phases are compressible, if there is an exchange of mass between the phases, and whether we are considering a single-pressure or a two-pressure model. For the purpose of our modelling we shall be using a two–pressure model. The motivation behind developing two-pressure models is that single-pressure models do not always result in a hyperbolic set of partial differential equations which, in turn, can lead to an ill-posed initial value problem. Single pressure models are based on the assumption that the pressures in each phase are in equilibrium.

Before considering the details of two-phase flow averaging we give a short example to show just how much care is required. Suppose we write down a system of equations

for an unsteady one dimensional incompressible inviscid two phase flow :

$$\frac{\partial}{\partial t}(\alpha_1\rho_1) + \frac{\partial}{\partial x}(\alpha_1 v_1 \rho_1) = 0, \tag{2.1}$$

$$\frac{\partial}{\partial t}(\alpha_2\rho_2) + \frac{\partial}{\partial x}(\alpha_2 v_2 \rho_2) = 0, \tag{2.2}$$

$$\frac{\partial}{\partial t}(\alpha_1\rho_1 v_1) + \frac{\partial}{\partial x}\left(\alpha_1\rho_1 v_1^2\right) + \alpha_1\frac{\partial p_1}{\partial x} = 0, \tag{2.3}$$

$$\frac{\partial}{\partial t}(\alpha_2\rho_2 v_2) + \frac{\partial}{\partial x}\left(\alpha_2\rho_2 v_2^2\right) + \alpha_2\frac{\partial p_2}{\partial x} = 0. \tag{2.4}$$

The above equations are Euler equations for each phase. We have four equations with five unknowns α_1, v_1, v_2, p_1, and p_2. To close the system we need to apply a constraint on the system to reduce the number of unknown variables to four. A popular choice to close the system is to use a *one-pressure model* and take $p_1 = p_2 = p$, where p is the averaged bulk pressure. The above system of equations may then be written in the form

$$A\omega_t + B\omega_x = 0, \tag{2.5}$$

where $w = (\alpha_1, v_1, v_2, p)^T$ and the matrices A and B are defined by

$$A = \begin{pmatrix} \rho_1 & 0 & 0 & 0 \\ -\rho_2 & 0 & 0 & 0 \\ \rho_1 v_1 & \rho_1\alpha_1 & 0 & 0 \\ -\rho_2 v_2 & 0 & \rho_2\alpha_2 & 0 \end{pmatrix}, \tag{2.6}$$

$$B = \begin{pmatrix} \rho_1 v_1 & \rho_1\alpha_1 & 0 & 0 \\ -\rho_2 v_2 & 0 & \rho_2\alpha_2 & 0 \\ \rho_1 v_1^2 & 2\rho_1\alpha_1 v_1 & 0 & \alpha_1 \\ -\rho_2 v_2^2 & 0 & 2\rho_2\alpha_2 v_2 & \alpha_2 \end{pmatrix}. \tag{2.7}$$

The characteristics of this system are obtained by solving the equation

$$|B - \lambda A| = 0, \tag{2.8}$$

for λ. The characteristics are found to be $\lambda = 0$ (twice), due to the fact that both phases are incompressible, with the remaining two characteristics are given by the solution of

$$\alpha_1\rho_2\left(v_1-\lambda\right)^2+\alpha_2\rho_1\left(v_2-\lambda\right)^2=0\,. \tag{2.9}$$

This shows that the system of equations will be elliptic (have complex characteristics) unless the condition $v_1 = v_2$ is satisfied. Boundary value problems are associated with elliptic systems whereas problems that depend on initial data and boundary conditions are associated with hyperbolic systems. Hyperbolic systems of equations have real distinct characteristic values. Two–phase flow problems are usually associated with hyperbolic systems, since we would expect the flow at any instance to depend on the histories of the inlet and other boundary conditions.

If a single pressure model for a two phase flow is to be physically reasonable model (i.e. hyperbolic) we must also impose that the velocities of the two phases are equal. For many flows this is not a valid assumption to make, since for vertical two-phase annular flow, for example the gas phase velocity is several orders of magnitude greater then the velocity of the liquid phase present in the liquid film.

For a detailed discussion of the differences between single- and two-pressure models see Ransom and Hicks (1984) and Stewart and Wendroff (1984). The main conclusions stated by Ranson and Hicks concerning two pressure models are that under some circumstances two pressure models, are hyperbolic, and provide greater physical detail than single pressure models.

2.2.1 Averaging

When modelling multiphase flows we use averaged equations which may then be used to predict average flow quantities. Employment of averaged multiphase equations allow us to predict such quantities as the average bubble velocity and the pressure drop across the bubbly flow region which for most practical applications is adequate.

For the purposes of our model we shall begin by formulating the exact equations of motion for each of the two phases with suitable boundary conditions and jump conditions at the interfaces between the phases. We shall then apply the averaging processes to formulate an averaged set of equations for the flow.

There are several types of averaging used in the formulation of the averaged multiphase flow equations. The four most commonly used averages are the time average, space average, weighted average and ensemble average. The time and space averages for a continuous quantity, $f(\boldsymbol{x},t)$, are defined respectively by :

$$\langle f\rangle(\boldsymbol{x},t) = \frac{1}{T}\int_{t-T}^{t} f(\boldsymbol{x},t')dt', \tag{2.10}$$

$$\langle f\rangle(\boldsymbol{x},t) = \frac{1}{L^3}\int_{x_1-\frac{1}{2L}}^{x_1+\frac{1}{2L}}\int_{x_2-\frac{1}{2L}}^{x_2+\frac{1}{2L}}\int_{x_3-\frac{1}{2L}}^{x_3+\frac{1}{2L}} f(\boldsymbol{x}',t)dx_3'dx_2'dx_1', \tag{2.11}$$

where t and x_i $(i=1\ldots3)$ are the time and space variables respectively. The parameter T appearing in equation (2.10) is a time scale for the flow. The most important average is the ensemble average, which is obtained by summing together all the observed values and then dividing by the total number of observations .This averaging is taken over a number of realisations of the flow. For a continuous quantity $f(\boldsymbol{x},t)$ the ensemble average is defined by

$$\langle f\rangle(\mathbf{x},t) = \int_M f(\mathbf{x},t;\mu)\, dm(\mu)\ . \tag{2.12}$$

where M is the set of all processes and $m(\mu)$ the measure of observing process μ. In general the averaged equations we shall be employing have been obtained by application of the ensemble average. The other averaging techniques are only appropriate in special situations as an approximation to the ensemble average.

Before applying the averaging techniques it is worth noting that all the aforementioned averages satisfy the following rules, as quoted by Drew (1983), which are used in formulating the averaged multiphase flow equations:

$$\langle f+g\rangle = \langle f\rangle + \langle g\rangle \,, \tag{2.13}$$

$$\langle \langle f\rangle g\rangle = \langle f\rangle \langle g\rangle \,, \tag{2.14}$$

$$\left\langle \frac{\partial f}{\partial t}\right\rangle = \frac{\partial \langle f\rangle}{\partial t}, \tag{2.15}$$

$$\left\langle \frac{\partial f}{\partial x_i}\right\rangle = \frac{\partial \langle f\rangle}{\partial x_i}, \tag{2.16}$$

$$\langle c\rangle = c. \tag{2.17}$$

In the preceding rules f and g are functions of the space and time variables, c a constant. Angled brackets are used to represent the averaging process. Equations (2.13) and (2.14) are known as Reynold's rules, equation (2.15) is Leibnitz rule and equation (2.16) is Gauss' rule.

The averaging is usually achieved by the introduction of a phase indicator function. The phase indicator function is defined by

$$X_k(\boldsymbol{x},t) = \begin{cases} 1 & \text{if } \boldsymbol{x} \text{ is in phase k at time t} \\ 0 & \text{other}\,. \end{cases} \tag{2.18}$$

For a more general discussion of the phase indicator function see for example Drew(1983).

To obtain a set of averaged two-phase equations the exact equations of motion for

the flow are multiplied by the phase indicator function and the resulting equations are then averaged. In formulating the averaged equations the previous rules for averages are applied. In averaging the equations we need to use the following relationship

$$\frac{\partial X_k}{\partial t} + v_i.\nabla X_k = 0\,, \tag{2.19}$$

where v_i is the velocity of phase k on the interface between the different phases. Proof of the relationship (2.19) is given by Drew (1983) and involves intergrating the left-hand side of equation (2.19) multiplied by a function with compact support over volume and time.

For example, to average the conservation of mass equation, we multiply through by the phase indicator function and then average the equation. Following Drew (1983), and using the rules outlined in equations (2.13)–(2.16) and (2.19), we obtain:

$$\left\langle X_k \frac{\partial \rho}{\partial t} + X_k \nabla(\rho v) \right\rangle = 0\,, \tag{2.20}$$

$$\left\langle \frac{\partial (\rho X_k)}{\partial t} - \rho \frac{\partial X_k}{\partial t} + \nabla(\rho X_k v) - \rho v \nabla . X_k \right\rangle = 0\,, \tag{2.21}$$

$$\left\langle \frac{\partial (\rho X_k)}{\partial t} + \rho v_i . \nabla X_k + \nabla(\rho X_k v) - \rho v \nabla . X_k \right\rangle = 0\,, \tag{2.22}$$

$$\frac{\partial \langle \rho X_k \rangle}{\partial t} + \nabla(\langle \rho X_k v \rangle) = \rho(v - v_i).\nabla \langle X_k \rangle\ . \tag{2.23}$$

The term $\rho\,(v - v_i)\,.\nabla\,\langle X_k \rangle$ is the rate of production of mass by phase k per unit volume and is usually denoted by Γ_k. We define the void fraction of phase k to be $\langle X_k \rangle$. The void fraction is usually denoted by α_k and is the time averaged fraction of the cross-sectional area or volume which is occupied by phase k.

To formulate the averaged conservation of mass equation in a more recognisable form we introduce the phase and mass weighted variables. The phasic average of a

variable ϕ is defined as

$$\tilde{\phi}_k = \frac{\langle X_k \phi \rangle}{\alpha_k}, \tag{2.24}$$

and the mass weighted average of a variable ψ is defined as

$$\tilde{\psi}_k = \frac{\langle X_k \rho \psi \rangle}{\alpha_k \tilde{\rho}_k}. \tag{2.25}$$

If we introduce the above averaged variables into the averaged conservation of mass equation,(2.22), we obtain the more familiar equation

$$\frac{\partial (\alpha_k \tilde{\rho}_k)}{\partial t} + \nabla . (\alpha_k \tilde{\rho}_k \tilde{v}_k) = \Gamma_k. \tag{2.26}$$

A similar procedure may be used to develop averaged equations for conservation of momentum, energy and enthalpy.

For ease of notation we will no longer indicate the average of a variable ϕ by $\tilde{\phi}$, but simply as ϕ. The reader should assume that all variables have been averaged unless stated otherwise.

2.2.2 Equations of Two-Phase Flow

When all the conservation equations have been averaged we are left with a system of partial differential equations describing the average behaviour of each phase. For this thesis we shall only consider a one dimensional model, although all the analysis does extend to two and three dimensional problems. The one dimensional set of equations is obtained from the ensemble averaged three dimensional equations by averaging over the cross-section of the flow. The area average of the ensemble-averaged variable $\bar{f}$ is defined by

$$\left\langle \bar{f}(\mathbf{x}, t) \right\rangle = \frac{1}{A(z)} \int \int_{A(z)} \bar{f}(\mathbf{x}, t)\, dA\,, \tag{2.27}$$

where we have assumed the flow is purely in the z direction with a cross-sectional area $A(z)$. As previously mentioned the equations describing the flow can be simplified by careful consideration of the physical situation being modelled.

The following set of averaged one-dimensional equations were first presented by Drew and Wood (1985). These equations differ from previous models in that previous models have bypassed the averaging process and postulated conservation equations from first principles.

The standard notation for two phase flows is for the liquid and gas phase variables to have the subscripts 1 and 2 respectively. For modelling a two phase flow the conservation equations for mass and momentum are required along with a conservation equation for energy internal energy or enthalpy. Equations (2.30)–(2.32) are not independent but merely alternatives.

Mass

$$\frac{\partial\left(\alpha_k\,\rho_k\right)}{\partial t}+\frac{1}{A}\frac{\partial}{\partial z}\left(\alpha_k\rho_k v_k\right)=\Gamma_k \tag{2.28}$$

Momentum

$$\begin{aligned}&\frac{\partial\left(\alpha_k\rho_k v_k\right)}{\partial t}+\frac{1}{A}\frac{\partial}{\partial z}\left(AC_{vk}\alpha_k\rho_k v_k^2\right)= \\ &\quad\frac{1}{A}\frac{\partial}{\partial z}\left(A\alpha_k(T_k+T_k^{Re})\right)+M_k+\alpha_k\rho_k g_z+v_{ki}^m\,\Gamma_k+\frac{4}{D}\alpha_{kw}T_{kw}\end{aligned} \tag{2.29}$$

Energy

$$\begin{aligned}&\frac{\partial}{\partial t}\left(\alpha_k\rho_k\left(u_k+\frac{1}{2}v_k^2+u_k^{Re}\right)\right)+\frac{1}{A}\frac{\partial}{\partial z}\left(AC_{ek}\alpha_k\rho_k v_k\left(u_k+\frac{1}{2}v_k^2+u_k^{Re}\right)\right) \\ &\quad=\frac{1}{A}\frac{\partial}{\partial z}\left(A\alpha_k\left[(T_k-T_k^{Re})v_k-q_k-q_k^{Re}\right]\right)-\frac{\xi_h}{A}\alpha_{kw}q_{kw} \\ &\qquad+E_k+W_k+\left[u_{ki}+\frac{1}{2}\left(v_{ki}^e\right)^2\right]\Gamma_k+\alpha_k\rho_k\left(r_k+g_z v_k\right)\,.\end{aligned} \tag{2.30}$$

Internal energy

$$\frac{\partial(\alpha_k\rho_k u_k)}{\partial t}+\frac{1}{A}\frac{\partial}{\partial z}(AC_{uk}\alpha_k\rho_K v_k u_k) \tag{2.31}$$
$$=-\frac{1}{A}\frac{\partial}{\partial z}A\alpha_k\left(q_k+\hat{q}_k^{Re}\right)-\frac{\xi_h}{A}\alpha_{ke}q_{kw}+E_k+u_{ki}\Gamma_k$$
$$+\alpha_k\rho_k r_k+\alpha_k\tau_k\frac{\partial v_k}{\partial z}+\alpha_k D_k-\alpha_k p_k\frac{\partial v_k}{\partial z}+P_k$$

Enthalpy

$$\frac{\partial(\alpha_k\rho_k h_k)}{\partial t}+\frac{1}{A}\frac{\partial}{\partial z}(AC_{hk}\alpha_k\rho_k v_k h_k)=-\frac{1}{A}\frac{\partial}{\partial z}\left(A\alpha_k\left(q_k+\hat{q}_k^{Re}\right)\right) \tag{2.32}$$
$$-\frac{\xi_h}{A}\alpha_{ke}q_{kw}+E_k+\alpha_k\rho_k\tau_k$$
$$+h_{ki}\Gamma_k+\alpha_k\tau_k\frac{\partial v_k}{\partial z}+\alpha_k D_k+\hat{P}_k+\alpha_k\left(\frac{\partial p_k}{\partial t}+v\frac{\partial p_k}{\partial z}\right).$$

The remaining relationship defining the flow is the entropy inequality given by

$$\frac{\partial\alpha_k\rho_k s_k}{\partial t}+\frac{1}{A}\frac{\partial}{\partial z}(AC_{sk}\alpha_k\rho_k s_k v_k)\geq\frac{1}{A}\frac{\partial}{\partial z}A\alpha_k\left(\phi_k+\phi_k^{Re}\right) \tag{2.33}$$
$$\frac{\xi_h}{A}\alpha_{kw}\phi_{kw}+S_k+s_{ki}\Gamma_k+\alpha_k\rho_k\sigma_k\,.$$

The entropy inequality can be used to check the validity of constitutive equations. Suppose a constitutive equation is used in the inequality such that the inequality is violated for some values of the parameters. Then, if the initial conditions of the system are set such that these values of parameters are present at the start of the flow then the entropy will decease. A decrease in entropy violates the second law of thermodynamics. So constitutive relationships that violate the entropy inequality are incorrect.

Although energy, mass and momentum are conserved across the phase interface the properties of the phases are discontinuous across the interface. So in addition to the equations (2.28)-(2.32) we also require a set of jump conditions to relate the

properties of the two phases at the interface. The jump conditions, as presented by Drew and Wood (1985), are:

$$\Gamma_1 + \Gamma_2 = 0 \tag{2.34}$$

$$M_1 + M_2 + v_{1i}^m \Gamma_1 + v_{2i}^m \Gamma_2 = m \tag{2.35}$$

$$E_1 + W_1 + E_2 + W_2 + \left[u_{1i} + \frac{1}{2}(v_{1i}^e)^2\right] \Gamma_1 + \left[u_{2i} + \frac{1}{2}(v_{2i}^e)^2\right] \Gamma_2 = \epsilon \tag{2.36}$$

The variables E_k, M_k and W_k are the interfacial energy, momentum and work. The velocities with superscripts e and m are the interfacial velocities for energy and momentum respectively. As well as the jump conditions, equations (2.34)-(2.36), we also require a set of constitutive relationships to close the model. Constitutive relationships describe how the two phases interact with each other. For example, constitutive equations are required for the stresses in each phase, the pressure differences and the interfacial force density. The constitutive relationships depend on which flow regime is being modelled and what materials the phases are composed of. Another important requirement of the constitutive equations is that they must be consistent with the equations of motion and the jump conditions. Also, the constitutive equations should be material frame indifferent, that is they should be independent under a change of coordinate system. Constitutive equations are usually obtained by first proposing a mathematical form for the constitutive equation and then checking it experimentally. The empirical results may then be used to adjust the proposed form.

Throughout equations (2.28)–(2.32) there are many constants denoted by the general form C_{ab}. These constants are called profile parameters and arise because when averaging the equations it is assumed that the average of a product equals the product of the averages. The latter is incorrect, i.e.

$$\langle f\, g \rangle \neq \langle f \rangle \langle g \rangle\,, \tag{2.37}$$

but by the introduction of profile parameters, it is assumed that

$$\langle f\, g\rangle = C_{fg}\langle f\,\rangle\langle g\rangle\,. \tag{2.38}$$

The profile parameters are usually determined from empirical observations.

The void fraction of phase k is denoted by α_k and is defined as the time averaged fraction of the cross-sectional area, or the volume, which is occupied by phase k. Throughout this work we shall use α_1 and α_2 to represent the liquid and gas void fractions respectively. From the definition of void fraction we have the relationship

$$\alpha_1 + \alpha_2 = 1\,. \tag{2.39}$$

If $\alpha_1 = 1$ then flow just consists of liquid and if $\alpha_2 = 1$ the flow just consists of vapour.

The cross-sectional area of the pipe is denoted by the letter A. Note that A will be a function of the axial variable z if the pipe in which the fluid is flowing in constricts or dilates. Note for the one-dimensional approximation to hold the cross-sectional area must vary only slowly or not at all.

In many two-phase flows there is an exchange of mass between the two phases either by evaporation or condensation depending on whether the fluid is being heated or cooled. The rate of production of mass per unit cross-sectional area is denoted by Γ_k. Upon adding together the conservation of mass equations for each phase we obtain

$$\frac{\partial}{\partial t}\left(\alpha_1\rho_1 + \alpha_2\rho_2\right) + \frac{1}{A}\frac{\partial}{\partial z}A\left(\alpha_1\rho_1 v_1 + \alpha_2\rho_2 v_2\right) = \Gamma_1 + \Gamma_2\,. \tag{2.40}$$

Therefore for the total mass to be conserved within the flow we must have

$$\Gamma_1 + \Gamma_2 = 0\,. \tag{2.41}$$

Note that this is just the jump condition (2.34).

The velocity of phase k is denoted by v_k. It is important to note that this is the actual averaged velocity of the phase and not the superficial phase velocity. The superficial velocity of the phase is the velocity of that phase if it was travelling alone in the pipe. The superficial velocity is more commonly used as a variable in the drift flux model and will be developed further when we consider the drift flux model. The other velocities that appear are interfacial velocities which have the subscript i. The difference in the velocity at the interface in three dimensional flows is given by the jump condition

$$\overline{\rho\psi\left(v-v_i\right)\cdot\nabla X_k}=C_\psi\overline{\rho_{ki}}\overline{\psi_k i}\left(\overline{v_{ki}}^{\psi}-\overline{v_i}\right)\cdot\nabla\overline{\alpha_k}=\overline{\psi_{ki}\Gamma_k}\,. \tag{2.42}$$

Since the tangential components of the velocities are continuous the jump in the velocity v_{ki} must occur in the averaged normal direction. So the interfacial velocity in three dimensions is obtained by taking the dot product of the above jump condition with $\nabla\alpha_k$ and then rearranging to obtain

$$\overline{v_{ki}}^{\psi}=\overline{v_i}+\frac{\overline{\Gamma_k}\nabla\overline{\alpha_k}}{C_\psi\overline{\rho_{ki}}|\nabla\overline{\alpha_k}|^2}\,. \tag{2.43}$$

The one dimensional interfacial velocities are assumed to have the same form as the three dimensional velocities There are interfacial velocities for momentum, energy and work defined by

$$v_{ki}^{\psi}=v_i+\frac{\Gamma_k}{C_\psi\rho_{ki}|\partial\alpha_k/\partial z|}\,. \tag{2.44}$$

Where the superscripts m, e and w indicate the interfacial velocity for momentum, energy and work respectively.

The interfacial force due to the stresses acting on the interface is given by the quantity M_k, which is defined by

$$M_k=p_{ki}\nabla\alpha_k-\tau_{ki}\cdot\nabla\alpha_k+M_k'\,. \tag{2.45}$$

The term M_k' represents all the forces that are not directly related to the phase distribution such as the drag, Basset and virtual mass force. The Basset force is a force experienced by bubbles due to the formation of a boundary layer on the bubble.

We now briefly define the remaining variables from equations (2.28)–(2.33). The term T_k is the stress and is related to the shear stress τ_k and the pressure p_k by

$$\tau_k = T_k + p_k \,, \tag{2.46}$$

The internal energy of phase 'k'is denoted by u_k and the enthalpy and entropy by h_k and s_k. The interfacial energy, momentum and work are denoted respectively by E_k, M_k and W_k. The interfacial energy and work are related via the jump condition (2.36). The term q_k is the heat flux.

Variables that have the superscript Re are known as Reynolds stress and are due to turbulence. Variables with a subscript w represent perimeter averaged variables and take account for fluid close to the wall. Variables with subscript i are the values of the variables along the interface between the phases.

2.3 Mixture and Homogeneous Models

An important simplification of the separated flow model is the mixture model. The mixture model is a simplification of the two fluid model in that it replaces the two fluid equations with a one component *pseudo* fluid model. The variables for the mixture model are averaged variables based on the two fluid variables. The easiest way to formulate the mixture model is by adding the relevant conservation equations (2.28)–(2.32) and then deciding on sensible mixture variables. For example, for the

mixture conservation of mass we add together equations (2.28) for $k = 1, 2$ to obtain

$$\frac{\partial}{\partial t}(\alpha_1 \rho_1 + \alpha_2 \rho_2) + \frac{\partial}{\partial z}(\alpha_1 \rho_1 v_1 + \alpha_2 \rho_2 v_2) = 0\,. \tag{2.47}$$

This equation is then simplified by the introduction of the mixture variables for density and velocity. A suitable choice of mixture variables for density and velocity are respectively

$$\rho_m = \alpha_1 \rho_1 + \alpha_2 \rho_2\,, \tag{2.48}$$

$$v_m = \frac{\alpha_1 \rho_1 v_1 + \alpha_2 \rho_2 v_2}{\alpha_1 \rho_1 + \alpha_2 \rho_2}\,. \tag{2.49}$$

It should be noted that other authors have developed different forms for the mixture density and velocity. The conservation of mass equation in terms of the mixture variables is therefore

$$\frac{\partial \rho_m}{\partial t} + \frac{\partial}{\partial z}(\rho_m v_m) = 0\,. \tag{2.50}$$

The mixture equations for momentum and energy are formulated in the same way by adding the respective balance equations and then deciding upon mixture variables. For a complete set of mixture equations and definitions of all the mixture variables see either Drew and Wood (1985) or, for a more classical approach, Atkin and Craine (1975). The mixture model is usually a good approximation to the flow if the fluids are well mixed.

Closely related to mixture theory is homogeneous flow theory. To be able to approximate the flow using homogeneous flow theory the two phases must be well mixed and travelling at the same velocity. So homogeneous flow theory is a simplification of mixture theory and the balance equations can be obtained from the mixture equations by setting $u_1 = u_2 = u_m$. The homogeneous flow model has been used to calculate the pressure gradient for two phase flows. For a more detailed discussion of the applications of homogeneous flow theory see Wallis (1969) and Whalley (1987).

2.4 Drift Flux Model

The drift flux model has been used successfully in modelling bubbly flows, slug flows and fluid particle systems such as fluidised beds. The drift flux model was developed by Wallis, and his book published in 1969 still remains a seminal reference for the drift flux model. A good introduction to the this model can also be found in Whalley (1987). The drift flux model is most relevant for flows where the velocity of the gas phase is well defined. This particular model can be confusing due to the large number of variables used.

To understand the drift flux model we need to distinguish between superficial phase velocities and actual phase velocities. The superficial phase velocity is the velocity of that particular phase if it were flowing alone in the pipe. The superficial velocity is thus defined as

$$V_j = \frac{G_j}{\rho_j}, \tag{2.51}$$

where G_j is the mass flux of phase j and ρ_j the density of phase j. The mass flux is defined by

$$G_j = \alpha_j \rho_j v_j . \tag{2.52}$$

By combining equations (2.51) and (2.52) we are able to relate the superficial velocities and the actual velocities via the equation,

$$v_j = \frac{V_j}{\alpha_j} . \tag{2.53}$$

Another important quantity is v_s, the slip velocity, which is defined as the difference between the actual gas phase velocity and the actual liquid phase velocity. In terms of the superficial velocities and gas void fraction, the slip velocity is defined by

$$v_s = \frac{V_2}{\alpha_2} - \frac{V_1}{1-\alpha_1} . \tag{2.54}$$

Rearrangement of 2.54 yields

$$v_s\alpha_2\left(1-\alpha_2\right) = V_2\left(1-\alpha_2\right) - V_1\alpha_2\,. \tag{2.55}$$

The drift flux of the gas phase relative to the liquid phase is therefore defined to be

$$j_{21} = v_s\alpha_2\left(1-\alpha_2\right)\,. \tag{2.56}$$

The drift flux represents the volumetric flux of a component relative to a surface moving at the average velocity. The drift velocity of the gas phase relative to the mean flow and the drift velocity of the liquid phase to the mean flow are defined respectively by

$$v_{2j} = v_2 - j\,, \tag{2.57}$$

$$v_{1j} = v_1 - j\,, \tag{2.58}$$

where j is defined as

$$j = V_1 + V_2\,. \tag{2.59}$$

Although the drift flux model has been used to model flows, we will not be developing it further since for our flow we do not have detailed experimental results to define the velocity of the gas phase as a function of the other flow parameters.

2.5 Closing Remarks

From the equations developed in this chapter it is evident that correct averaging of the equations is of upmost importance to the model. The other important process is the formulation of the constitutive relationships. Most constitutive relationships are developed from experimental data. They are then checked to ensure that they are consistent with the averaged equations by insisting that they satisfy the entropy

inequality. The particular model used depends on the flow being considered. For example if two phases are well mixed then the mixture model would be the first model to be considered. A more complicated separated flow model could be introduced when the general features of the flow are understood.

One of the major difficulties with multiphase models is the large number of variables involved. The complexity of the equations can usually be reduced by using asymptotic methods to determine which terms involved in the equations are small and may therefore be neglected. This helps us to develop realistic but simple models for the different flow regimes.

Having reviewed the physical details of LMFBR's, two-phase flows, and the different flow regimes, we will now start to look specifically at each region in a heat exchanger pipe.

Chapter 3

SUBCOOLED FLOW REGIME

3.1 Introduction

In this chapter we shall study the subcooled flow regime, which is the region of flow where the water is at a temperature below its boiling temperature. The subcooled region is the first flow regime and occurs at the base of the steam generating pipe. The subcooled water is pumped in at the base of the pipe at a constant velocity and is heated by the countercurrent flow of molten sodium which flows in a casing surrounding the steam generating pipes. In test rigs the steam generating pipes are heated electrically, since it is easier to measure physical quantities such as external heat flux and wall temperature.

We shall assume that the start of the transition from subcooled flow to bubbly flow occurs when the temperature of the fluid reaches the boiling temperature at some point within the flow. With this assumption we shall be able to estimate the length of subcooled region and judge its global importance to the flow.

We will consider two situations, one where the fluid is heated by a constant heat flux and another where the heat transfer is modelled by Newton's law, so that the heat supplied to the fluid is directly proportional to the temperature difference between the channel wall and the fluid. In calculations we shall assume that all the physical

quantities of the fluid (i.e. specific heat capacity, thermal diffusivity etc.) remain constant which is a reasonable approximation for water.

3.2 Energy Equation For Single Phase Liquid

Experimentally the flow in the subcooled regime is sometimes observed to be turbulent and other times laminar. For this analysis we shall be just be considering the situation where the flow is laminar. Ignoring viscous dissipation, the energy equation for an inviscid incompressible fluid is

$$\rho c_p \left(\frac{\partial T}{\partial t} + (\mathbf{q}.\nabla)T \right) = K \nabla^2 T \,, \tag{3.1}$$

where $\mathbf{q}$ is the velocity of the fluid and $T = T(r, \theta, z)$ the temperature of the fluid. We shall initially model the flow using cylindrical coordinates and also assume that the pipe is uniformly heated around its circumference. This is not exact since the liquid sodium will be cooler at the bottom of the pipe than at the top, having given up some of its heat to the fluid. The thermal conductivity K is a measure of the efficiency of the material at conducting heat.

Since the fluid is heated uniformly around the circumference of the steam generating pipe we can assume that the temperature is angular independent and only varies in the axial and radial directions. We also assume that the flow is steady, and the fluid is flowing with a constant velocity ω in the axial direction and there is no flow in the radial direction. With these assumptions we can write down the relevant reduced version of the energy equation (3.1)

$$\rho c_p \, \omega \frac{\partial T}{\partial z} = K \left(\frac{\partial^2 T}{\partial r^2} + \frac{1}{r} \frac{\partial T}{\partial r} + \frac{\partial^2 T}{\partial z^2} \right) . \tag{3.2}$$

In an effort to simplify equation (3.2) we introduce the following non-dimensional variables

$$T = T_0 \hat{T}, \tag{3.3}$$

$$z = L\hat{z}, \tag{3.4}$$

$$r = a\hat{r}, \tag{3.5}$$

where T_0 is the initial inlet temperature, L is a typical length scale in the axial direction and a is the pipe radius. The non–dimensionalised version of equation (3.2) is therefore

$$\frac{\partial \hat{T}}{\partial z} = \frac{1}{N_{Gz}} \left(\frac{\partial^2 \hat{T}}{\partial \hat{r}^2} + \frac{1}{\hat{r}} \frac{\partial \hat{T}}{\partial \hat{r}} \right) + \frac{\alpha}{N_{Pe}} \frac{\partial^2 \hat{T}}{\partial \hat{z}^2}. \tag{3.6}$$

The non-dimensional groups introduced in the above equation are the Peclet number, aspect ratio and Graetz number, defined respectively by

$$N_{Pe} = \frac{\rho c_p \omega a}{K}, \tag{3.7}$$

$$\alpha = \frac{a}{L}, \tag{3.8}$$

$$N_{Gz} = N_{Pe}\,\alpha = \frac{\rho c_p \omega a^2}{KL}. \tag{3.9}$$

For the physical situation under consideration the Peclet number typically has the value 7.4×10^4 and the aspect ratio a value of 7×10^{-3}. Thus the Graetz number has a value of 518. The values of the physical parameters used in calculating these non-dimensional groups are located in Appendix A. By comparing the magnitudes of the non-dimensional groups it may shown that

$$\frac{1}{N_{Gz}} \gg \frac{\alpha}{N_{Pe}}. \tag{3.10}$$

This means that to lowest order any terms multiplied by $\frac{\alpha}{N_{Pe}}$ may be neglected. To

lowest order the non-dimensional equation (3.6) therefore reduces to

$$\frac{\partial \hat{T}}{\partial \hat{z}} = \frac{1}{N_{Gz}} \left(\frac{\partial^2 \hat{T}}{\partial \hat{r}^2} + \frac{1}{\hat{r}} \frac{\partial \hat{T}}{\partial \hat{r}} \right) . \tag{3.11}$$

Before dealing with the complexities of the full axially symmetric case, we note that a further simplification is to consider the two dimensional energy equation instead of the axially symmetric energy equation. All the simplifications carried out on the axially symmetric energy equation also hold for the two dimensional case, which can be written

$$\frac{\partial \hat{T}}{\partial \hat{z}} = \frac{1}{N_{Gz}} \frac{\partial^2 \hat{T}}{\partial \hat{x}^2} . \tag{3.12}$$

3.3 Constant Heat Flux

3.3.1 Two Dimensional Problem

For the two dimensional case with prescribed heat flux we need to solve the energy equation with the following boundary conditions:

$$K \frac{\partial T}{\partial x} = q \quad \text{on } x = a , \tag{3.13}$$

$$K \frac{\partial T}{\partial x} = -q \quad \text{on } x = -a . \tag{3.14}$$

In equations (3.13)–(3.14), q is the constant external heat flux applied at the boundary of the channel. The problem is shown diagrammatically in figure 3.1.

Since the problem is symmetric about $x = 0$ we need only solve the problem in the region $0 < x < a$. By using symmetry we may replace the second boundary condition with

$$K \frac{\partial T}{\partial x}(0, z) = 0 \quad \text{on } x = 0 . \tag{3.15}$$

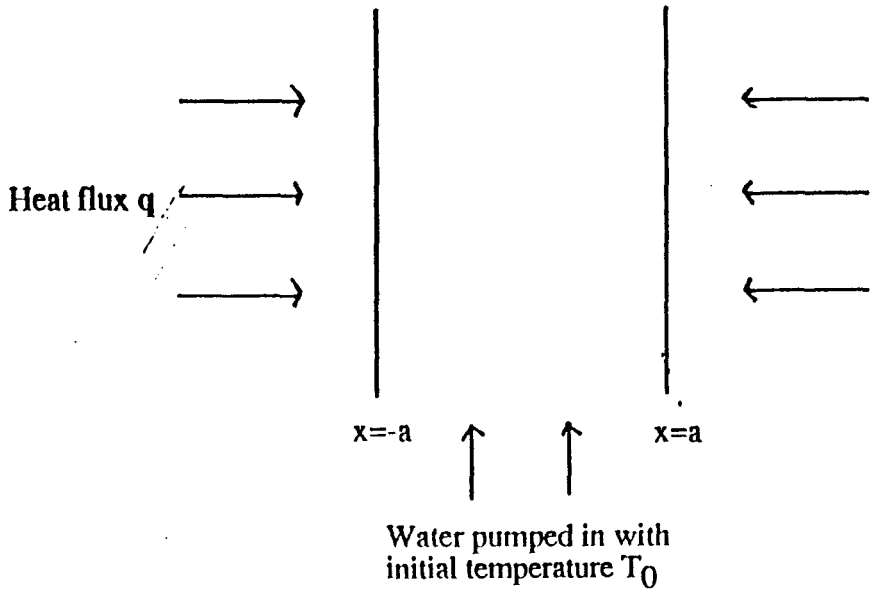

Figure 3.1: Schematic layout of 2-dimensional problem

The boundary value problem for the two dimensional case in the region $0 < x < a$ may then be written as

$$\rho c_p \omega \frac{\partial T}{\partial z} = K \frac{\partial^2 T}{\partial x^2}, \tag{3.16}$$

$$T = T_0 \quad \text{on } z = 0, \tag{3.17}$$

$$K \frac{\partial T}{\partial x} = q \quad \text{on } x = a, \tag{3.18}$$

$$K \frac{\partial T}{\partial x} = 0 \quad \text{on } x = 0. \tag{3.19}$$

We seek a solution of the form

$$T(x,z) = f(x,z) + \phi(x,z), \tag{3.20}$$

where $f(x,z)$ is a function that satisfies the partial differential equation (3.16) but

also renders the boundary conditions (3.18) and (3.19) homogeneous. By inspection such a function is seen to be

$$f(x,z) = T_0 + \frac{qz}{a\rho c_p \omega} + \frac{qx^2}{2Ka}. \tag{3.21}$$

The problem in terms of $\phi(x,z)$ may then be written as

$$\rho c_p \omega \frac{\partial \phi}{\partial z} = K \frac{\partial^2 \phi}{\partial x^2}, \tag{3.22}$$

$$\phi(x,0) = -\frac{qx^2}{2Ka}, \tag{3.23}$$

$$\frac{\partial \phi}{\partial x}(0,z) = 0, \tag{3.24}$$

$$\frac{\partial \phi}{\partial x}(a,z) = 0. \tag{3.25}$$

The boundary value problem defined by equations (3.22)–(3.25) may then be solved by using the separation of variable technique. The solution for the two dimensional heat flux case can therefore be written

$$T(x,z) = T_0 + \frac{q}{K}\left(\frac{\kappa z}{a\omega} - \frac{a}{6} + \frac{x^2}{2a} - \frac{2a}{\pi^2}\sum_{n=1}^{\infty}\left(\frac{(-1)^n}{n^2}\cos\left(\frac{n\pi x}{a}\right)\exp -\frac{n^2\pi^2\kappa z}{a^2\omega}\right)\right). \tag{3.26}$$

For ease of notation in equation (3.26) we have introduced the quantity κ, the thermal diffusivity. The thermal diffusivity is defined by

$$\kappa = \frac{K}{\rho c_p}. \tag{3.27}$$

We may now use equation (3.26) to calculate the length of the subcooled region. To do this we assume that the transition from subcooled flow to bubbly flow occurs when the temperature of the water at some point in the channel reaches the saturation temperature. Experiments were carried out by the Kreftwerk Union using an electrically heated pipe of axial length $6m$ and inner radius $7mm$. A heat flux of $595Kw\ m^2$

was supplied to the pipe. The Kreftwerk experiments were reported on by Atthey et al (1988). The water had an pressure of 200 bar, implying that the saturation temperature of the water is $365\,^{\circ}C$. The inlet temperature of the water was $240\,^{\circ}C$.

Since the heat flux is being applied at the boundary of the channel we may assume that the water will first reach its saturation temperature at some point along the channel wall. By setting $x = 7 \times 10^{-3}m$ in equation (3.26) and varying z we were able to calculate that the transition from subcooled flow to bubbly flow occurred a distance of $0.15m$ from the channel inlet. The variation of temperature along the channel wall with respect to the distance from the channel inlet is shown in figure 3.2. An explicit formula for calculating the length of the subcooled region is obtained in the next section by the use of asymptotic methods.

Next, calculations were performed to determine how the temperature of the water varied across the channel by keeping z fixed and varying x. We found that the bulk of the water remained at its inlet temperature of $240\,^{\circ}$ C and that only a layer of water about 1mm thick along the channel wall was heated. The variation of the water temperature near the wall is shown in figure 3.3.

3.3.2 Asymptotic Analysis of Two Dimensional Constant Heat Flux Case

Two dimensional subcooled flow with a prescribed constant heat flux at the walls is governed by equations (3.16)–(3.19). Although we have an exact analytical solution it is not very easy to analyse since it involves an infinite summation. However, from the analytical solution we were able to see that only the temperature of a very thin layer of water next to the channel wall was changing significantly, and this suggests the existence of a boundary layer along the channel wall. This implies that

we might obtain a simpler approximate solution to the problem by the application of asymptotic methods. To study the problem asymptotically we need first of all to non-dimensionalise equations (3.17)–(3.19). A suitable set of non-dimensional variables are

$$T = T_0(1+\theta)\,, \tag{3.28}$$

$$z = LZ\,, \tag{3.29}$$

$$x = aX\,, \tag{3.30}$$

where T_0 is the inlet temperature, a is the half the width of the channel and L is typical length in the axial direction. Upon the introduction of the non-dimensional variables the system of equations (3.16)–(3.19) reduces to

$$\frac{\partial\theta}{\partial Z} = \varepsilon\frac{\partial^2\theta}{\partial X^2}\,, \tag{3.31}$$

$$\frac{\partial\theta}{\partial X} = 0 \quad \text{on } X=0\,, \tag{3.32}$$

$$\frac{\partial\theta}{\partial X} = \lambda \quad \text{on } X=1\,, \tag{3.33}$$

$$\theta = 0 \quad \text{on } Z=0\,, \tag{3.34}$$

where ε and λ are defined respectively by

$$\varepsilon = \frac{1}{N_{Gz}} = \frac{1}{Pe\,\alpha}\,, \tag{3.35}$$

$$\lambda = \frac{qa}{KT_0}\,. \tag{3.36}$$

The critical balance determines that λ is of order $\varepsilon^{-1/2}$.

From the structure of equation (3.31), it is obvious that there is a boundary layer at $X=1$ since if we treat the problem as regular perturbation with small parameter ε we can not satisfy all the boundary conditions. The problem therefore needs to be

approached as singular perturbation problem. To study such problems we need to construct an inner solution for the rapid variation of temperature within the boundary layer and an outer solution for the variation of temperature away from the boundary layer.

Outer Problem

The outer expansion is given by the solution of the following equations

$$\frac{\partial \theta}{\partial Z} = 0, \tag{3.37}$$

$$\frac{\partial \theta}{\partial X} = 0 \quad \text{on } X = 0, \tag{3.38}$$

$$\theta = 0 \quad \text{on } Z = 0. \tag{3.39}$$

The solution to this problem is simply

$$\theta^o = 0, \tag{3.40}$$

where we have used a superscript o to indicate that this is the solution for the outer problem.

Inner Problem

For the inner problem we need to change to boundary layer variables. Since the boundary layer is located at $X = 1$ we need to expand the independent variable about $X = 1$. A suitable change of variable is therefore

$$\xi = \frac{1 - X}{\varepsilon^{\upsilon}}, \tag{3.41}$$

where υ is to be determined. Since we are now solving the problem for the boundary layer we may neglect the boundary condition at $X = 0$ so that the problem becomes

$$\frac{\partial \theta}{\partial Z} = \varepsilon^{1-2\upsilon} \frac{\partial^2 \phi}{\partial \xi^2}, \tag{3.42}$$

$$\frac{\partial \theta}{\partial \xi} = -\varepsilon^{v}\lambda \quad \text{on } \xi = 0\,, \tag{3.43}$$

$$\theta = 0 \quad \text{on } Z = 0\,. \tag{3.44}$$

The correct balance therefore occurs when $v = \frac{1}{2}$. The boundary layer equations then reduce to

$$\frac{\partial \theta}{\partial Z} = \frac{\partial^2 \phi}{\partial \xi^2}\,, \tag{3.45}$$

$$\frac{\partial \theta}{\partial \xi} = -\mu \quad \text{on } \xi = 0\,, \tag{3.46}$$

$$\theta = 0 \quad \text{on } Z = 0\,, \tag{3.47}$$

where $\mu = \varepsilon^{1/2}\lambda$ and is $O(1)$. One way to proceed in solving this problem is to introduce similarity variables

$$t = \frac{\xi}{\sqrt{Z}}\,, \tag{3.48}$$

$$\theta = \sqrt{Z}\psi(t)\,. \tag{3.49}$$

These similarity variables can easily be obtained by the method of stretchings. The introduction of similarity variables transforms the partial differential equation (3.45) into an ordinary differential equation with dependent variable ψ and independent variable t. The problem in terms of $\psi(t)$ therefore becomes

$$\frac{\partial^2 \psi}{\partial t^2} + \frac{t}{2}\frac{\partial \psi}{\partial t} - \frac{1}{2}\psi = 0\,, \tag{3.50}$$

$$\frac{\partial \psi}{\partial t} = -\mu \quad \text{on } t = 0\,. \tag{3.51}$$

It should be noted that the boundary condition (3.47) is automatically satisfied by the similarity variables. The general solution of equation (3.50) is

$$\psi(t) = A\,t + B\left(\frac{\sqrt{\pi}t}{2}\text{erf}\left(\frac{t}{2}\right) + \exp\left(-\frac{1}{4}t^2\right)\right)\,, \tag{3.52}$$

where $\mathrm{erf}(x)$ is the error function, defined as

$$\mathrm{erf}\,(x) = \frac{2}{\sqrt{\pi}} \int_0^x \exp(-s^2)\, ds\,. \tag{3.53}$$

Applying the boundary condition defined by equation (3.51) we obtain

$$\psi(t) = -\mu t + B\left[\frac{\sqrt{\pi}t}{2}\mathrm{erf}\left(\frac{t}{2}\right) + \exp\left(-\frac{t^2}{4}\right)\right]. \tag{3.54}$$

To calculate the remaining constant of integration we will need to match the outer solution to the inner solution. The inner solution in terms of ξ and Z is

$$\theta^i = -\mu\xi + B\left[\frac{\sqrt{\pi}}{2}\xi\mathrm{erf}\left(\frac{\xi}{2\sqrt{Z}}\right) + \sqrt{Z}\exp\left(-\frac{\xi^2}{4Z}\right)\right]. \tag{3.55}$$

We have used the superscript i to indicate that θ^i is the inner solution. The matching condition, as quoted in any standard text on asymptotics such as Nayfeh (1981) is that the outer expansion of the inner expansion equals the inner expansion of the outer expansion. This is usually represented by the notation

$$(\theta^i)^o = (\theta^o)^i\,. \tag{3.56}$$

The inner expansion in terms of the outer variable is

$$(\theta^i)^o = -\mu\left(\frac{1-X}{\sqrt{\varepsilon}}\right) + B\left[\frac{\sqrt{\pi}}{2}\left(\frac{1-X}{\sqrt{\varepsilon}}\right)\mathrm{erf}\left(\frac{1-X}{2\sqrt{\varepsilon}\sqrt{Z}}\right) + \sqrt{Z}\exp\left(-\frac{(1-X)^2}{4\sqrt{\varepsilon}\sqrt{Z}}\right)\right]. \tag{3.57}$$

Keeping X fixed and expanding the above to lowest order in ε we obtain

$$(\theta^i)^o = -\frac{\mu(1-X)}{\sqrt{\varepsilon}} + \frac{B\sqrt{\pi}(1-X)}{2\sqrt{\varepsilon}}. \tag{3.58}$$

The inner expansion of the outer expansion is simply zero, which means by equating equation (3.58) with zero we obtain

$$B = \frac{2\mu}{\sqrt{\pi}}. \tag{3.59}$$

The inner expansion is therefore

$$\theta^i = \mu\left(\xi \text{erf}\frac{\xi}{2\sqrt{Z}} + 2\sqrt{\frac{Z}{\pi}}\exp\left(-\frac{\xi^2}{4Z}\right) - \xi\right) . \tag{3.60}$$

Composite Expansion

The composite expansion for the non-dimensional temperature is given by

$$\theta^c = \theta^i + \theta^o - \left(\theta^i\right)^o \tag{3.61}$$

where $(\theta^i)^o$ is the common limit of the outer and inner expansion and we have used the superscript c to indicate that this is the composite solution. The composite expansion for the dimensional temperature is therefore

$$T^c = T_0 + \sqrt{\varepsilon}\lambda T_0\left(\frac{a-x}{\sqrt{\varepsilon}}\,\text{erf}\left(\frac{a-x}{2\sqrt{\varepsilon z}}\right) - \frac{a-x}{\sqrt{\varepsilon}} + 2\sqrt{\frac{z}{\pi}}\exp\left(-\frac{(a-x)^2}{4\varepsilon z}\right)\right) . \tag{3.62}$$

This is a useful approximation to the analytic solution equation (3.26) since it allows us to find a simple formula relating the axial distance along the pipe to the physical parameters.

As previously mentioned we assume that the transition to the bubbly regime occurs when the temperature of the water first reaches the boiling temperature of water. This will occur first at some point along the channel wall. The variation of the water temperature along the channel wall is therefore given by substituting $X = a$ into equation (3.62) to give

$$T_{wi} = T_0\left(1 + 2\lambda\sqrt{\frac{\varepsilon z}{\pi}}\right) . \tag{3.63}$$

A plot of the water temperature along the wall is shown in figure 3.8. Note that it compares favourably with the analytic solution depicted in figure 3.2. The transition

from single phase subcooled flow to bubbly flow occurs when $T_{wi} = T_s$. Upon rearranging equation (3.63) the length of the subcooled region is given by the relationship

$$z = \frac{(T_s - T_0)^2 \pi}{4 T_0^2 \varepsilon} . \tag{3.64}$$

This formula can be recast into more familiar variables by replacing ε with its equivalent physical representation

$$z = \frac{\pi c_p \rho \omega K}{4q^2} (T_s - T_0)^2 . \tag{3.65}$$

Note that equation (3.65) also predicts that the transition to the bubbly flow regime occurs a distance of 0.15m from the channel inlet.

3.3.3 Axially Symmetric Case

The axially symmetric case gives rise to a similar boundary value problem as in the two dimensional case. The axially symmetric problem to lowest order is

$$\rho c_p \omega \frac{\partial T}{\partial z} = K \left(\frac{\partial^2 T}{\partial r^2} + \frac{1}{r} \frac{\partial T}{\partial r} \right) , \tag{3.66}$$

$$T(r, 0) = T_0 , \tag{3.67}$$

$$K \frac{\partial T}{\partial r} = q \quad \text{on } r = a , \tag{3.68}$$

$$K \frac{\partial T}{\partial r} = 0 \quad \text{on } r = 0 , \tag{3.69}$$

where r is the radial coordinate and z the axial coordinate. Following the same procedure as in section (1.3.1) we look for a solution of the form

$$T(r, z) = f(r, z) + \phi(r, z) , \tag{3.70}$$

where $f(r,z)$ satisfies the differential equation but also makes the boundary conditions homogeneous. By inspection such a function is seen to be

$$f(r,z) = T_0 + \frac{2qz}{a\rho c_p \omega} + \frac{qr^2}{2Ka}. \tag{3.71}$$

This transforms the boundary value problem to

$$\rho c_p \omega \frac{\partial \phi}{\partial z} = K\frac{\partial^2 \phi}{\partial r^2} + \frac{1}{r}\frac{\partial \phi}{\partial r} \tag{3.72}$$

$$\phi = -\frac{qr^2}{2Ka} \quad \text{on } z = 0, \tag{3.73}$$

$$\frac{\partial \phi}{\partial r} = 0 \quad \text{on } r = a, \tag{3.74}$$

$$\frac{\partial \phi}{\partial z}(0,z) = 0 \quad \text{on } r = 0. \tag{3.75}$$

This boundary value problem can once again be solved by separation of variables. Using a similar procedure to that used for the two-dimensional problem the solution is given by

$$T(r,z) = T_0 + \frac{q}{K}\left(\frac{2\kappa z}{\omega a} + \frac{r^2}{2a} - \frac{a}{4} - \sum_{n=1}^{\infty} \frac{2a}{\alpha_n^2} \frac{J_0\left(\frac{\alpha_n r}{a}\right)}{J_0(\alpha_n)} \exp -\frac{\alpha_n^2 \kappa z}{a^2 \omega}\right). \tag{3.76}$$

Here α_n are the roots of the equation

$$J_1(\alpha_n) = 0. \tag{3.77}$$

Note that $J_0(x), J_1(x)$ are Bessel functions of the first kind of order zero and one respectively. In general Bessel functions of the first kind of order ν satisfy the equation

$$\frac{\partial^2 J}{\partial r^2} + \frac{1}{r}\frac{\partial J}{\partial r} + \left(1 - \frac{\nu^2}{r^2}\right) J = 0. \tag{3.78}$$

To calculate the length of the subcooled region we find the point at which the water along the wall reaches its saturation temperature. We calculated this distance to be

$0.15m$ from the channel inlet. The variation of water temperature along the channel wall is shown in figure 3.4.

As with the two dimensional case only a thin layer of water along the pipe wall showed any significant increase in temperature. The variation of temperature in the radial direction at a distance of $0.15m$ from the inlet is shown in figure 3.5. This agrees with the previous result of § 3.3.2.

3.3.4 General Solution

Solutions to generalised versions of the previous boundary value problems considered above are possible through the application of Duhamel's theorem, which for this particular problem has the following form taken from Carslaw and Jaeger (1946):

> If $T = f(x, z)$ represents the temperature of a fluid, with initial temperature zero and surface heat flux equal to unity, then the solution to the problem when the surface heat flux is $q(z)$ is given by
>
> $$T(x, z) = \int_0^z q(\tau) \frac{\partial}{\partial \tau} f(x, z - \tau) d\tau \, .$$

So, for example, applying Duhamel's theorem to the two dimensional case with a heat flux $q(z)$ at the surface $x = a$ gives the general solution

$$T(x, z) = T_0 + \int_0^z \frac{q(\tau)}{K} \frac{\partial}{\partial \tau} \left(\frac{\kappa (z - \tau)}{a\omega} - \frac{2a}{\pi^2} \sum_{n=1}^{\infty} \frac{(-1)^n}{n^2} \cos\left(\frac{n\pi x}{a}\right) \exp - \frac{n^2 \pi^2 \kappa (z - \tau)}{a^2 \omega} \right) d\tau \, . \tag{3.79}$$

By applying equation (3.79) it would be possible to model more complex situations where the heat flux depended on the axial distance along the channel from the inlet.

3.4 Comments on Heating by Constant Heat Flux

Both the two dimensional case and the fully axially symmetric case predict that the length of the subcooled regime will be $0.15m$. This compares favourably with the results obtained by Atthey (1992). Both cases show that only the fluid close to the wall is being heated significantly. This allowed us to develop a simple formula based on asymptotic techniques for the length of the subcooled regime.

3.5 Heating by Newton's law

3.5.1 Newton's Law

Newton's law states that the heat flux across a surface is directly proportional to the temperature difference between the surface and the surrounding medium.

This statement is equivalent to applying the following boundary condition along the channel wall

$$K \frac{\partial T}{\partial x} = H(T(a,z) - T_a)\,, \tag{3.80}$$

where H is the coefficient of surface heat transfer. For our analysis we shall assume that H is constant although in reality it is typically a function of the flow velocity and the temperature.

3.5.2 Two Dimensional Case

For the two dimensional case we need to solve the energy equation with a Newton's law boundary condition:

$$\rho c_p \omega \frac{\partial T}{\partial z} = K \frac{\partial^2 T}{\partial x^2}, \tag{3.81}$$

$$T = T_0 \quad \text{on } z = 0, \tag{3.82}$$

$$\frac{\partial T}{\partial x} = -h(T(a,z) - T_a) \quad \text{on } x = a, \tag{3.83}$$

$$\frac{\partial T}{\partial x} = 0 \quad \text{on } x = 0, \tag{3.84}$$

where $h = \frac{H}{k}$. The boundary condition can be made homogeneous by introducing the change of variable

$$\phi = T(x,z) - T_a. \tag{3.85}$$

The boundary value problem for ϕ then becomes

$$\rho c_p \omega \frac{\partial \phi}{\partial z} = \frac{\partial^2 \phi}{\partial x^2}, \tag{3.86}$$

$$\phi = T_0 - T_a \quad \text{on } z = 0, \tag{3.87}$$

$$\frac{\partial \phi}{\partial x} = -h\phi \quad \text{on } x = a, \tag{3.88}$$

$$\phi_x(0,z) = 0. \tag{3.89}$$

This boundary problem for $\phi(x,z)$ can now be solved by separation of variables to give

$$T(x,z) = T_a + \sum_{n=1}^{\infty} \frac{2ha(T_o - T_a)}{p_n^2 + h^2a^2 + ah} \frac{\cos(\frac{p_n x}{a})}{\cos p_n} \exp\left(-\frac{p_n^2 z}{a^2 \alpha w}\right). \tag{3.90}$$

In equation (3.90) p_n are the roots of the transcendental equation,

$$p_n \tan p_n = ha. \tag{3.91}$$

This equation has an infinite amount of roots that can be located by application of a numerical procedure such as Newton's method. Some of the roots for specific values of ha are located in Carslaw and Jaeger (1946). To calculate the value of H we used the equation

$$q = H(T_a - T_f)\,, \tag{3.92}$$

In equation (3.92) T_a denotes the ambient temperature, which we take to be equal to the maximum wall temperature of 480 ° C, and T_f is the average temperature of the water. For a first approximation we assume the average temperature of the water is 240 ° C. The value of h is obtained by dividing the surface heat transfer coefficient by the thermal conductivity of the water (ie $h = \frac{H}{k}$). This gives a value for ha of approximately 27. Since the fluid near the wall of the channel will heat up more quickly then the rest of the fluid, we assume that the water would first reach its saturation temperature along the channel wall. We let $r = 7 \times 10^{-3}$m, where 7×10^{-3}m is the radius of the channel, and then vary z until we find the point at which the water first reaches its saturation temperature. According to this simplified model, this determines the transition to bubbly flow to be a distance $0.5m$ along the pipe.

We then repeated the calculation but took $T_f = 280$ ° C, which gave the quantity ha a value of about 33. This time the transition point was calculated to be at a distance of about $0.35m$ along the channel. The variation of water temperature along the channel wall is shown in figure 3.6. We then calculated how the temperature of the water varied radially at a fixed axial distance. As in the constant heat flux case we found that only a layer of water of thickness 1mm along the channel wall was being heated and the bulk of the water was remaining at its inlet temperature. The temperature profile for variation of water temperature in the radial direction at a distance of $0.35m$ from the pipe inlet is shown in figure 3.7

3.5.3 Asymptotic Analysis of the Two Dimensional Case

The analytic solution obtained in the previous section is not very easy to analyse since it involves summing an infinite series and finding roots of a transcendental equation. The analytic solution does indicate though that there is a thermal boundary layer along the channel wall as only the fluid near the channel wall shows any significant increase in temperature. To analyse the boundary layer we first need to non-dimensionalise equations (3.81)–(3.84). To do this we introduce the following non-dimensional variables

$$\theta = \frac{T - T_0}{T_a - T_0}, \tag{3.93}$$

$$x = aX, \tag{3.94}$$

$$z = LZ, \tag{3.95}$$

where T_0 and T_a are the inlet and maximum wall temperatures respectively. The x variable has been scaled with half the channel width and the z variable with a typical length in the axial direction. The non-dimensional problem can then be written as

$$\frac{\partial \theta}{\partial Z} = \varepsilon \frac{\partial^2 \theta}{\partial X^2}, \tag{3.96}$$

$$\theta = 0 \quad \text{on } Z = 0, \tag{3.97}$$

$$\frac{\partial \theta}{\partial X} = -Nu(-1 + \theta) \quad \text{on } X = 1, \tag{3.98}$$

$$\frac{\partial \theta}{\partial X} = 0 \quad \text{on } X = 0. \tag{3.99}$$

In the above system ε is equal to $\frac{1}{N_{Gz}}$, where N_{Gz} is the Graetz number defined previously by equation (3.9). The non-dimensional constant Nu is the Nusselt number defined by

$$Nu = \frac{Ha}{K}. \tag{3.100}$$

The critical balance determines that the Nusselt is of order $\varepsilon^{-1/2}$.

As stated previously this is not a regular perturbation problem since there exists a boundary layer at $X = 1$. To look at this problem asymptotically we need to find an outer solution far away from the boundary layer and an inner solution which incorporates the boundary layer.

Outer Problem

The outer expansion is obtained by solving the following equations

$$\frac{\partial \theta}{\partial Z} = 0, \tag{3.101}$$

$$\theta = 0 \quad \text{on } Z = 0, \tag{3.102}$$

$$\frac{\partial \theta}{\partial X} = 0 \quad \text{on } X = 0. \tag{3.103}$$

The solution to this problem is simply

$$\theta^o = 0, \tag{3.104}$$

where we have used the superscript o to indicate that this is an outer solution.

Inner Problem

In order to investigate the inner solution we need to introduce the boundary layer variable defined by

$$\xi = \frac{1 - X}{\varepsilon^{1/2}}. \tag{3.105}$$

The inner problem can then be written as

$$\frac{\partial \theta}{\partial Z} = \frac{\partial^2 \theta}{\partial \xi^2}, \tag{3.106}$$

$$\theta = 0 \quad \text{on } Z = 0, \tag{3.107}$$

$$\frac{\partial \theta}{\partial \xi} = \varepsilon^{1/2} Nu\,(-1 + \theta). \tag{3.108}$$

To complete the inner solution we need a matching condition, which for this problem is

$$\theta \to 0 \quad \text{as } \xi \to \infty . \tag{3.109}$$

One approach to solving this problem is take the Laplace transform with respect to the Z variable. The Laplace transform is defined in the usual way by

$$\bar{\theta}(\xi, s) = \mathcal{L}\left[\theta(\xi, z)\right] = \int_0^\infty e^{-z\,s}\theta(\xi, z)\, dz . \tag{3.110}$$

The transformed problem can then be written down as

$$\frac{\partial^2 \bar{\theta}}{\partial \xi^2} - s\bar{\theta} = 0 , \tag{3.111}$$

$$\frac{d\bar{\theta}}{d\xi} - \mu\bar{\theta} = -\frac{\mu}{s} \quad \text{on } \xi = 0 \tag{3.112}$$

$$\bar{\theta} \to 0 \quad \text{on } \xi \to \infty . \tag{3.113}$$

In the above system of equations we have introduce the the quantity μ defined by

$$\mu = Nu\varepsilon^{1/2} . \tag{3.114}$$

Since Nu is of order $\varepsilon^{1/2}$ then μ is of order 1. The solution to equation (3.111) which satisfies the boundary conditions (3.112) and (3.113), is

$$\bar{\theta} = \frac{\mu\, e^{-\sqrt{s}\xi}}{s\left(\sqrt{s} + \mu\right)} \tag{3.115}$$

To obtain $\theta(\xi, Z)$ we need to apply the inverse Laplace transform. The inverse of (3.115) as quoted by Carslaw and Jaeger (1946), is

$$\theta^i(\xi, Z) = \operatorname{erfc}\left(\frac{\xi}{2\sqrt{Z}}\right) - \exp\left(\mu\xi + \mu^2 Z^2\right) \operatorname{erfc}\left(\frac{\xi}{2\sqrt{Z}} + \mu\sqrt{Z}\right) , \tag{3.116}$$

where $\operatorname{erfc}(x)$ is the complementary error function and we have used the superscript i to indicate that this is an inner solution

Composite Expansion

The composite expansion is given by

$$\theta^c = \theta^i + \theta^o - (\theta^i)^o \tag{3.117}$$

where the last term represents the outer limit of the inner expansion and the superscript c indicates that it is a composite expansion. The composite dimensional expansion of the temperature is therefore

$$T^c = T_0 + (T_a - T_0)\left[\text{erfc}\left(\frac{a-x}{2a\sqrt{\varepsilon z}}\right) - e^{h(a-x)+\varepsilon h^2 a^2 z^2}\text{erfc}\left(\frac{a-x}{2a\sqrt{\varepsilon z}} + \varepsilon^{1/2} ha\sqrt{z}\right)\right], \tag{3.118}$$

From the composite expansion we can now obtain an explicit formula describing the temperature of the water along the channel wall by substituting $x = a$ into equation (3.118). The water temperature distribution along the channel wall is therefore given by the expression

$$T_{wi} = T_a - (T_a - T_0)e^{\varepsilon h^2 a^2 z}\text{erfc}\left(ha\sqrt{\varepsilon z}\right). \tag{3.119}$$

A plot of the asymptotic expansion of the water temperature along the wall is shown in figure 3.9. Note that equation (3.118) also predicts that the transition to bubbly flow occurs $0.35m$ from the pipe inlet.

3.5.4 Axially Symmetric Case

The axially symmetric case gives rise to a similar boundary value problem as in the two dimensional case. The axially symmetric problem to lowest order is

$$\rho c_p \omega \frac{\partial T}{\partial z} = K\left(\frac{\partial^2 T}{\partial r^2} + \frac{1}{r}\frac{\partial T}{\partial r}\right), \tag{3.120}$$

$$T = T_0 \quad \text{on } z = 0\,, \tag{3.121}$$

$$\frac{\partial T}{\partial r} = -h(T - T_a) \quad \text{on } r = a\,, \tag{3.122}$$

$$\frac{\partial T}{\partial r} = 0 \quad \text{on } r = 0\,. \tag{3.123}$$

As with the previous boundary values problem, the problem can be made homogeneous by the substitution

$$\phi(r, z) = T(r, z) - T_s\,. \tag{3.124}$$

The boundary value problem in terms of $\phi(x, z)$ is therefore

$$\rho c_p \omega \frac{\partial \phi}{\partial z} = K\left(\frac{\partial^2 \phi}{\partial r^2} + \frac{1}{r}\frac{\partial \phi}{\partial r}\right), \tag{3.125}$$

$$\phi = (T_0 - T_a) \quad \text{on } z = 0\,, \tag{3.126}$$

$$\frac{\partial \phi}{\partial r} = -h\phi \quad \text{on } r = a\,, \tag{3.127}$$

$$\frac{\partial \phi}{\partial r} = 0 \quad \text{on } r = 0\,. \tag{3.128}$$

This system is solved using separation of variables, giving a solution

$$T(x, z) = T_s + \sum_{n=1}^{\infty} \frac{2ha(T_0 - T_s)}{p_n^2 + a^2h^2} \frac{J_0\left(\frac{p_n r}{a}\right)}{J_0(p_n)} \exp\left(-\frac{p_n^2 z}{a^2 \alpha w}\right), \tag{3.129}$$

where p_n are the roots of the equation

$$pJ_1(p) = ahJ_0(p)\,. \tag{3.130}$$

This transcendental equation has an infinite number of roots which can be calculated using a numerical scheme, such as the bisection method. Using the same method as in the previous section with $T_f = 240\,^\circ C$ we again calculated the transition point to be a distance of about $0.5m$ along the channel. However when we took the average temperature of the fluid to be $280\,^\circ C$ the transition to bubbly flow occurred $0.35m$ from the pipe inlet. The temperature variations along the wall and in the radial direction are shown in figures 3.10 and 3.11 respectively.

3.5.5 General Solution

Applying Duhamel's theorem as previously defined in § 3.3.4 we can calculate the general solution for the two dimensional system. So, for example, for the two dimensional case we have the general solution,

$$T(x,z) = T_0 + \int_0^z (T_s(\tau) - T_0)\frac{\partial}{\partial \tau}\left(\sum_{n=1}^{\infty} \frac{2ha}{p_n^2 + a^2h^2}\frac{J_0\left(\frac{p_n x}{a}\right)}{J_0(p_n)} e^{-\frac{p_n^2(z-\tau)}{a^2 a w}}\right)d\tau\,. \qquad (3.131)$$

This is the solution to the problem where the surrounding temperature is not constant but depends on z.

3.6 Discussion

From the analysis carried out in this chapter we have been able to calculate the length of the subcooled regime for two forms of heating, constant heat flux and heating by Newton's law. The two forms of heating give different lengths since heating by Newtons law depends on the temperature difference between the fluid and the wall. As the fluid gets hotter the temperature difference decreases and therefore less heat flows from the wall to the fluid. This implies that the length of the subcooled regime should be greater for the Newton case then the for the constant heat flux case. This argument is verified by our analysis.

The model could be made more complex by not assuming that the fluid velocity remains constant throughout the subcooled regime. Further work could be to study non-uniform heating of the pipe in which the external heat flux varies around the cross-section of the pipe.

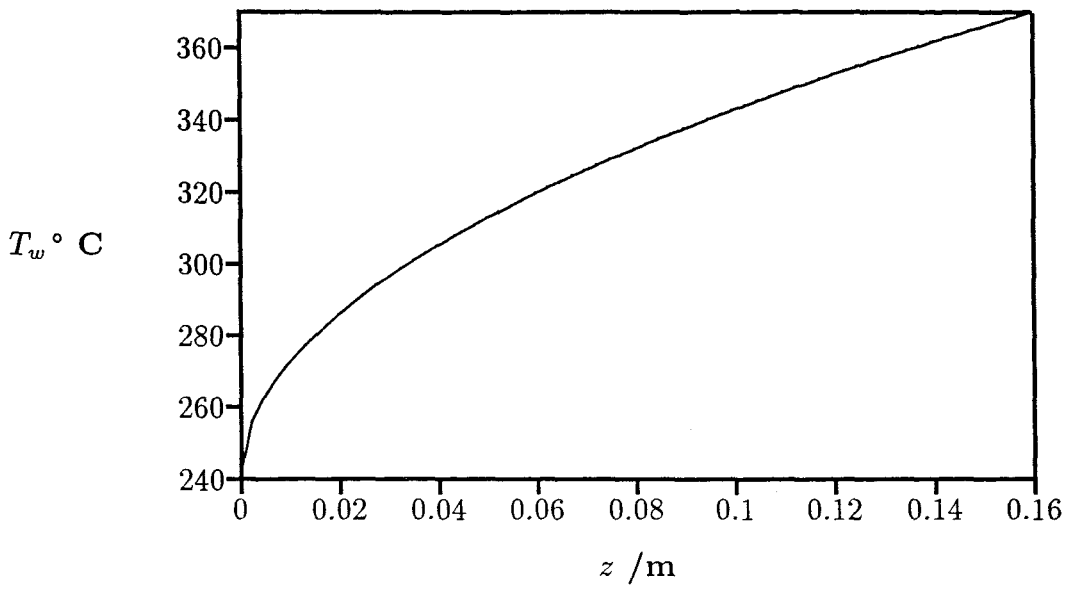

Figure 3.2: Variation of water temperature along channel wall for constant heat flux, two dimensional geometry

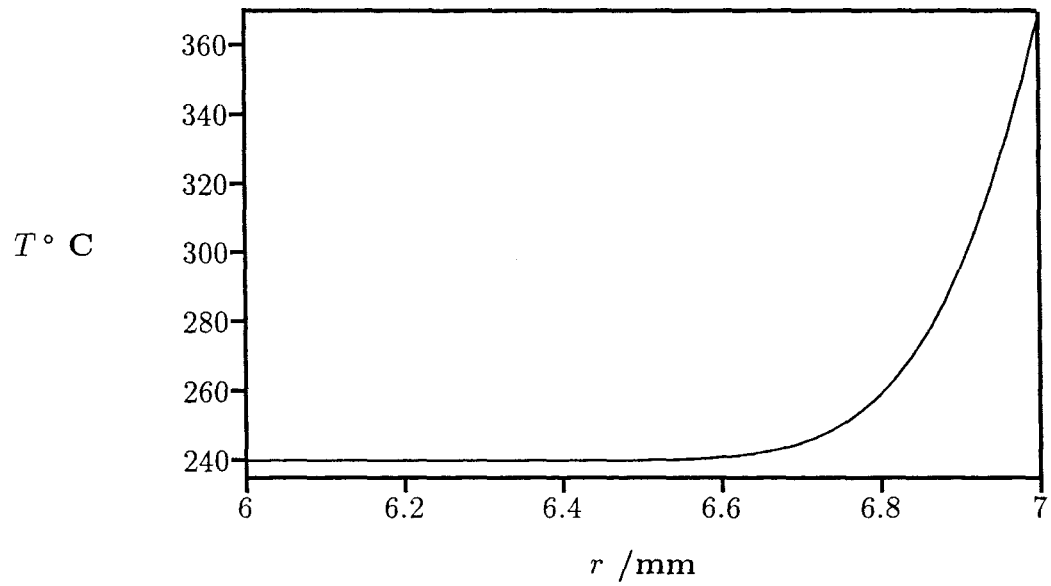

Figure 3.3: Variation of water temperature in radial direction for constant heat flux, two dimensional geometry

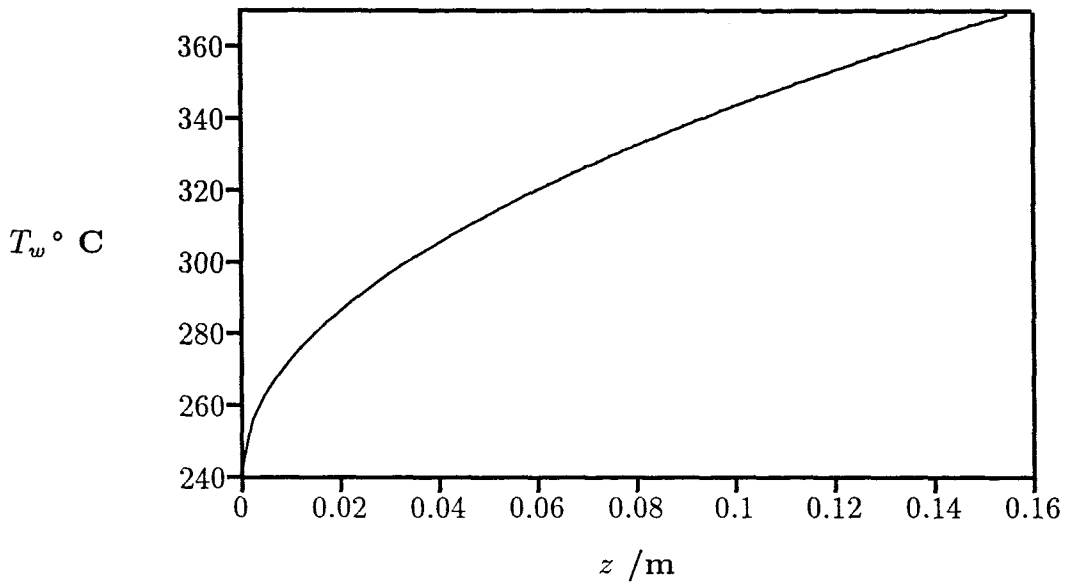

Figure 3.4: Variation of water temperature along channel wall for constant heat flux, axially symmetric geometry.

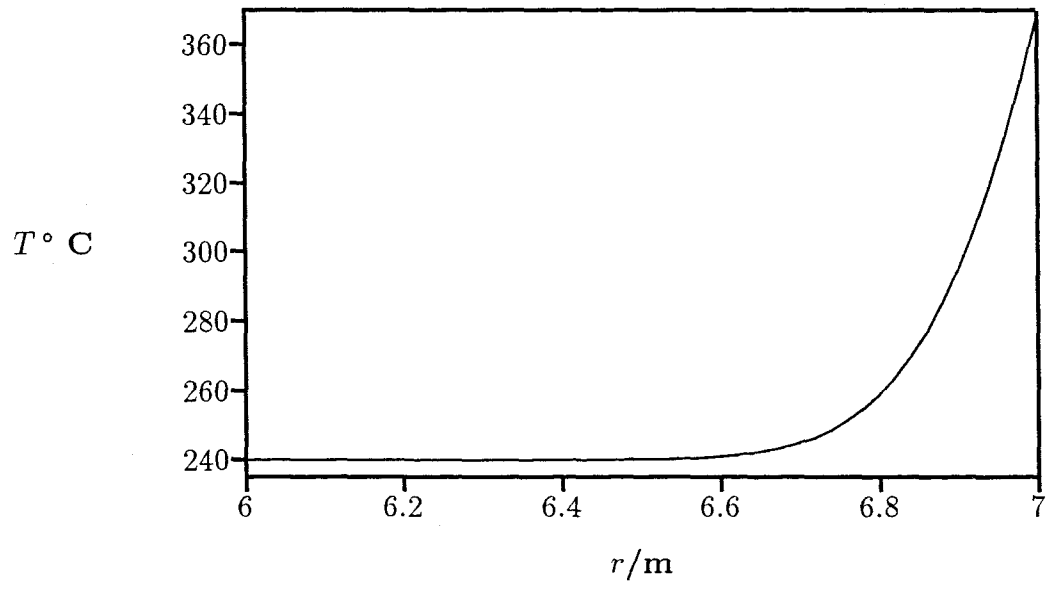

Figure 3.5: Variation of water temperature in radial direction for constant heat flux, axially symmetric geometry

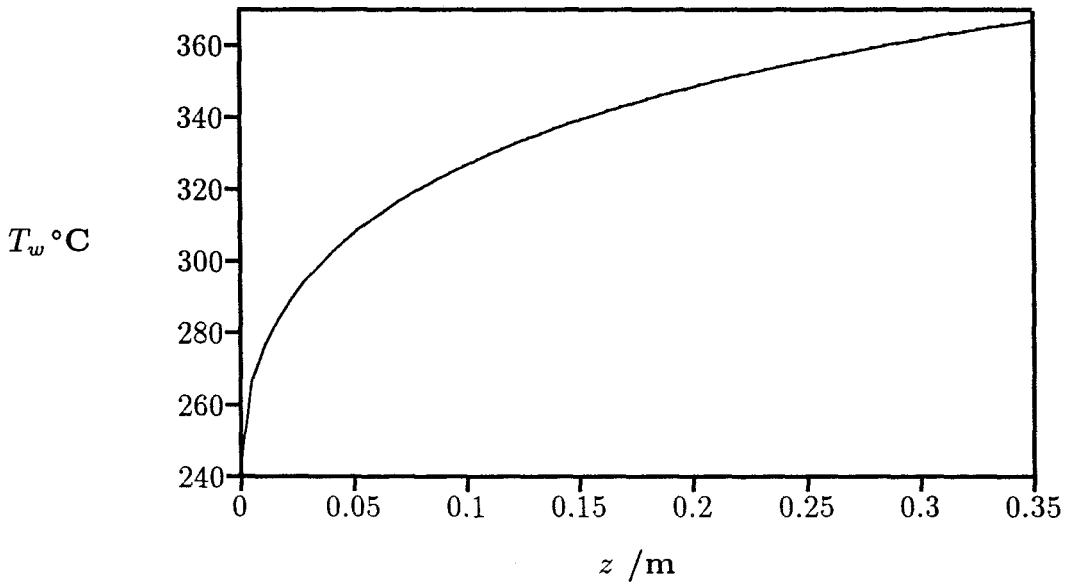

Figure 3.6: Variation of water temperature along channel wall for Newton heating, two dimensional geometry

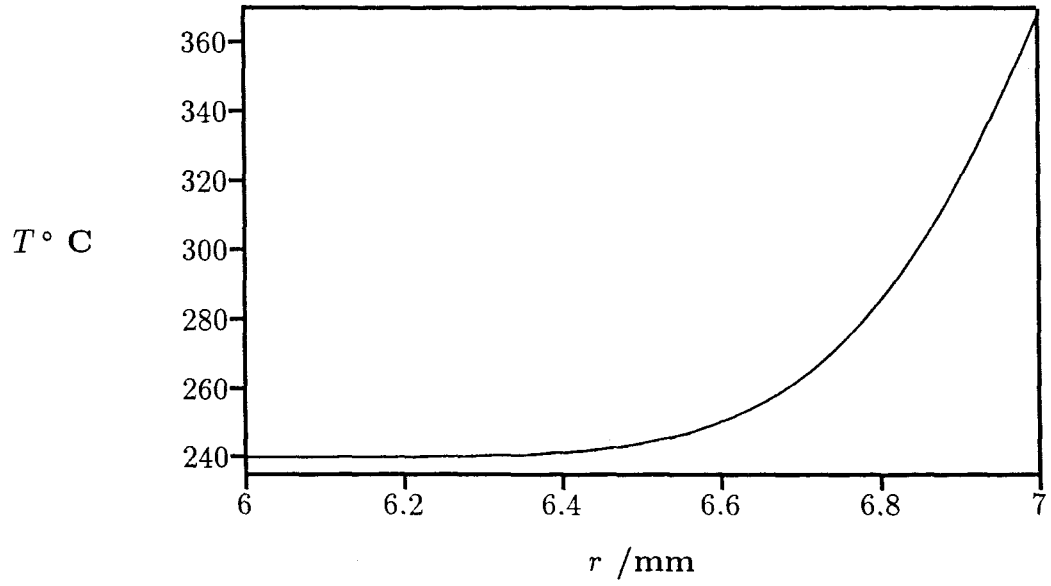

Figure 3.7: Variation of water temperature in radial direction for Newton heating, two dimensional geometry

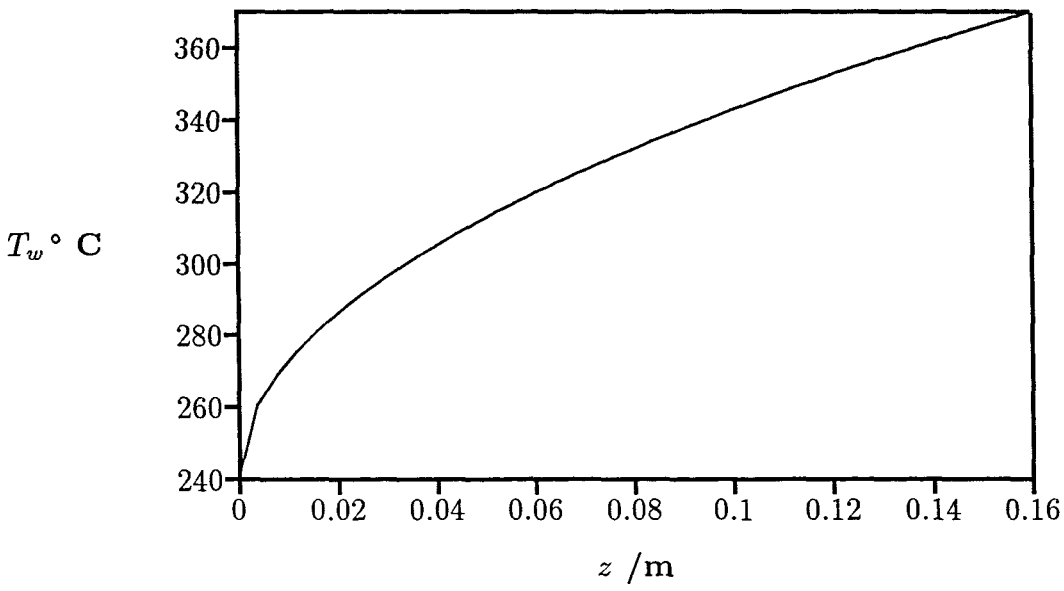

Figure 3.8: Asymptotic solution for the variation of water temperature along the wall for constant heat flux, two dimensional geometry

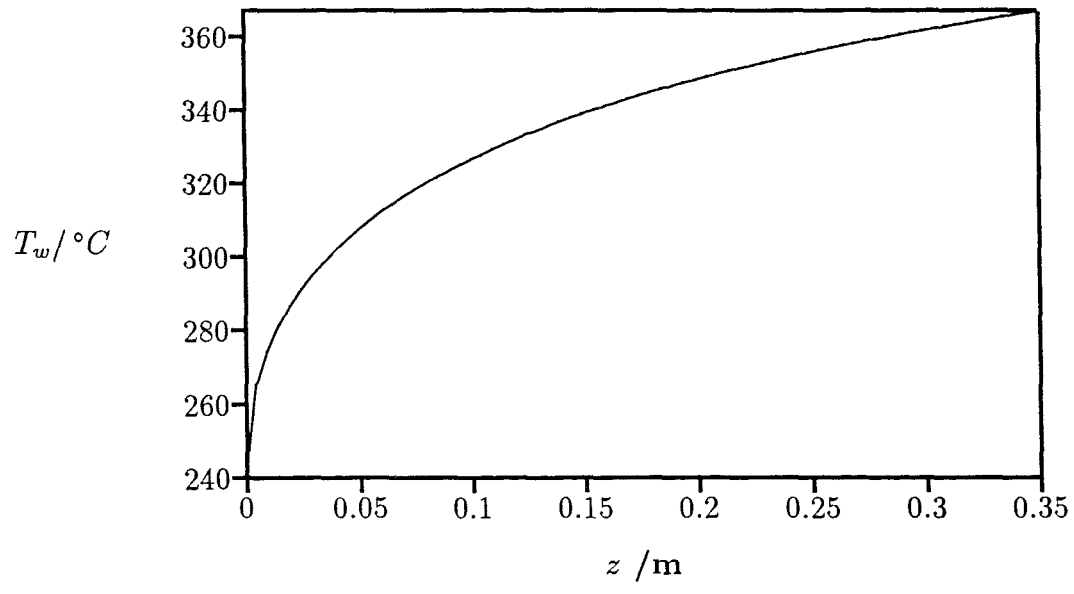

Figure 3.9: Asymptotic solution for the variation of water temperature along the wall for Newton heating, two dimensional geometry

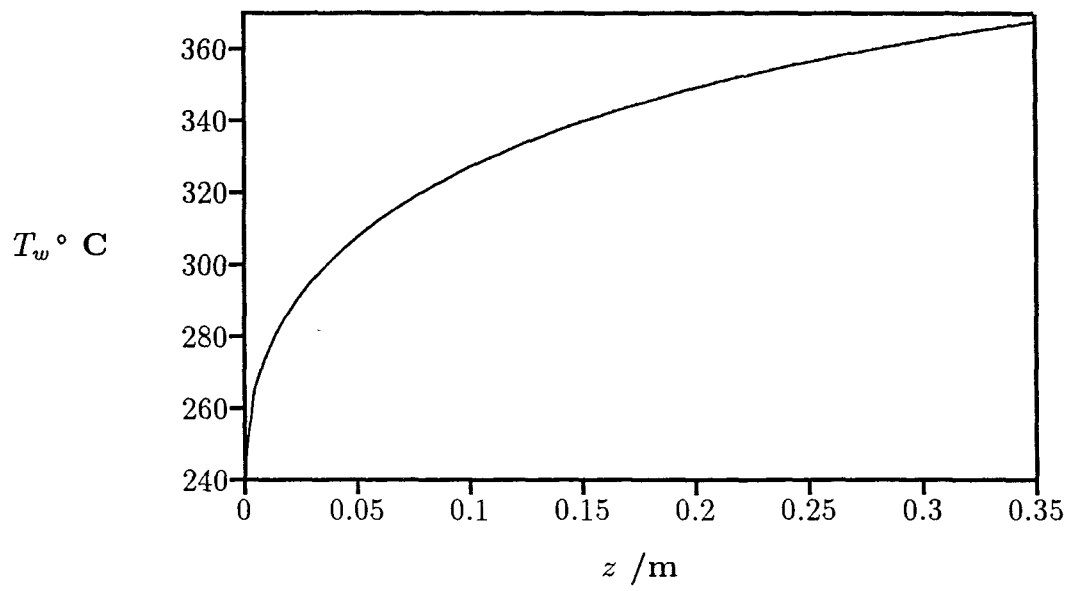

Figure 3.10: Variation of water temperature along channel wall for Newton heating, axially symmetric geometry

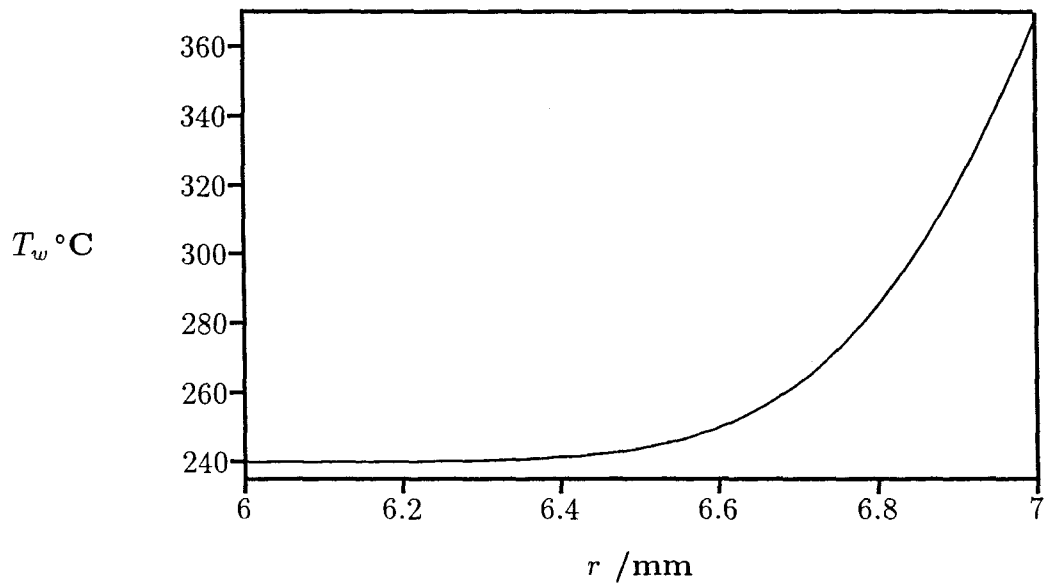

Figure 3.11: Variation of water temperature in radial direction for Newton heating, axially symmetric geometry

Chapter 4

BUBBLY AND SLUG FLOW REGIMES

4.1 Introduction

The gas phase flows as discrete bubbles in the continuous liquid phase. The bubbles are formed at nucleation sites along the channel walls. This type of nucleation is termed heterogeneous nucleation and is due to the fact that the channel walls are not entirely smooth but contain minute pits where bubbles can be formed. It should be noted that bubbles may also act as nucleation sites themselves. To model the bubbly flow regime it will be necessary to formulate a set of equations for each of the two phases. Since the steam generating pipe is being heated our model must to take into account the exchange of mass between the two phases due to the evaporation of the liquid phase.

As the number of bubbles increases so does the probability that the bubbles will collide and conglomerate to form bigger *bullet* shaped bubbles. These *bullet* shaped bubbles are often referred to as Taylor bubbles, as for example in Mao and Dukler (1991) and Chisholm (1983). The collision process continues until bubbles are produced which have a diameter just less than the diameter of the channel. Once this has occurred the flow regime is assumed to have changed from bubbly flow to slug flow. Between the large Taylor bubbles *slugs* of water are entrained with smaller

bubbles. As the Taylor bubbles flow up the channel a thin film of liquid flows around the bubble in the opposite direction to the overall flow.

Navarro-Valenti, Clausse, Drew and Lahey(1991) and Taitel, Bornea and Dukler (1980), observed that the transition from bubbly to slug flow takes place when the gas void fraction, α_2, has a value of approximately 0.3. We shall use this fact to help us calculate the length of the bubbly regime and the pressure drop across the bubbly regime.

4.2 The Bubbly Flow Regime

4.2.1 Constitutive Relationships

To utilise the two-phase flow equations developed in chapter 2 on pages 27– 28 we need to supply the constitutive equations that are relevant to the bubbly flow regime. As previously mentioned, the constitutive equations describe how the two phases interact with each other. Therefore we will need to develop equations describing such interactions as the drag force experienced by the steam bubbles and the interfacial pressure difference between the two phases.

Interfacial Pressure

For two-phase flows where the effect of surface tension is important the simple relationship between the continuous and dispersed interfacial pressures is

$$p_{2i} - p_{1i} = \frac{2\sigma}{r_c}. \tag{4.1}$$

In the above expression σ(N/m) is the surface tension and r_c is the radius of curvature of the gas/liquid interface. For the purpose of our modelling we will be assuming that the effects of surface tension are negligible and therefore the interfacial pressures are equivalent and equation (4.1) reduces to

$$p_{1i} = p_{2i} \,. \tag{4.2}$$

Drew and Wood (1983) suggest that the pressure of the continuous phase may be related to the continuous interfacial pressure by

$$p_{1i} = p_1 - \xi \rho_1 \left(v_1 - v_2\right)^2 \,, \tag{4.3}$$

where the last term is known as Lamb's term and ξ is a dimensionless constant which for most applications, is taken to have a value of 0.25, as quoted by Prosperetti and Satrape (1990). The dispersed phasic pressure is assumed to be equal to the dispersed interfacial pressure, that is

$$p_{2i} = p_2 \,. \tag{4.4}$$

By combining equations (4.2)–(4.4) we are able to relate the continuous and dispersive pressures by the equation

$$p_1 = p_2 + \xi \rho_1 \left(v_1 - v_2\right)^2 \,. \tag{4.5}$$

The above equation is a simple formula relating the continuous and dispersive pressures that we will use to close the equations of two phase flow. Note that by using equation (4.5) we are formulating a two pressure model.

Interfacial Force

The one-dimensional interfacial force term defined by Drew and Wood (1988) is given by

$$M_k = p_{ki}\frac{\partial \alpha_k}{\partial z} - \tau_{ki}\frac{\partial \alpha_k}{\partial z} + M_k' \,, \tag{4.6}$$

where p_{ki} and τ_{ki} are respectively the interfacial pressure and viscous stress of phase k. The interfacial force is due to the stress acting on the interface between the two phases. For the dispersed phase M_2' is the sum of all the interfacial terms not directly related to the phase distribution. For the purpose of this work we will only be considering the effects of the drag force. The equation for M_2' is therefore

$$M_2' = F_D \,, \tag{4.7}$$

where F_D is the force on the bubbles due to drag. To calculate M_1' we need to apply the jump condition defined by equation (2.35). As we will be neglecting the effects of surface tension, the momentum source term due to surface tension, m, can be neglected. The jump condition (2.35), upon the introduction of (4.6), reduces to

$$M_1' + M_2' + p_{1i}\frac{\partial \alpha_1}{\partial z} + p_{2i}\frac{\partial \alpha_2}{\partial z} + \Gamma\left(v_{2i} - v_{1i}\right) = 0 \,. \tag{4.8}$$

This expression can be simplified further since the interfacial velocities are equal and, by using equation (2.39) to relate the void fractions for the continuous and dispersive phase, we obtain

$$M_1' + M_2' + \left(p_{2i} - p_{1i}\right)\frac{\partial \alpha_2}{\partial z} = 0 \,. \tag{4.9}$$

As we are neglecting the effects of surface tension the interfacial pressures are equivalent and we obtain the relationship

$$M_1' = -M_2' \,. \tag{4.10}$$

The interfacial force terms for the continuous and dispersive phases are therefore respectively

$$M_1 = p_{1i}\frac{\partial \alpha_1}{\partial z} - F_D\,, \tag{4.11}$$

$$M_2 = p_{2i}\frac{\partial \alpha_1}{\partial z} + F_D\,. \tag{4.12}$$

Interfacial Drag

The interfacial drag term appears as one of the interfacial force terms in equation (2.45). The interfacial drag depends strongly on which flow regime is being modelled and on the materials that make up the two-phase flow. In two-phase flows the drag force is directly proportional to the square of the difference of phasic velocities. In developing an equation to describe the interfacial drag one needs to determine the drag coefficient, C_D. The two-phase interfacial drag as defined by Zuber and Ishii (1976), and also Drew and Wood (1988), is

$$F_D = \frac{3}{8}\frac{C_D}{r_b}\alpha_2\rho_1\left(v_1 - v_2\right) \mid v_1 - v_2 \mid\,. \tag{4.13}$$

In the expression (4.13) r_b is the average bubble radius. The drag coefficient is a function of the two-phase Reynolds number, Re_{2p}, which is defined through

$$Re_{2p} = \frac{2r_b\rho_1 \mid v_1 - v_2 \mid}{\mu_m}\,. \tag{4.14}$$

In expression (4.14) μ_m is the mixture viscosity defined by

$$\frac{\mu_m}{\mu_1} = \left(1 - \frac{\alpha_2}{\alpha_{2m}}\right)^{\frac{-2.5\alpha_{2m}(\mu_2+0.4\mu_1)}{\mu_2+\mu_1}}\,, \tag{4.15}$$

where α_{2m} is the maximum packing, which for bubbly flows is usually taken to be unity. Following Zuber and Ishii (1976) we may now write down the relevant form of

the drag coefficient for a fluid particle system as

$$C_D = \frac{24}{Re_{2p}} \left(1 + \frac{1}{10} Re_{2p}^{\frac{3}{4}}\right) . \tag{4.16}$$

Distributed Heat Source

When modelling the two-phase flow of water and steam in a steam generating pipe we must take into account the fact that the pipe is being heated and therefore the liquid phase is evaporating. One way of doing this is to introduce a distributed heat source term, r_m, into the model. The distributed heat source is defined as the total heat entering the system per unit mass. The distributed heat source may be related to the external heat flux by treating the flow as a mixture. The total amount of heat entering a cylindrical control volume of length δz is

$$Q = 2\pi a\, q \delta z\, . \tag{4.17}$$

The total mass of fluid contained in a cylindrical control volume of length δz is given by

$$M = \pi a^2 \rho_m\, . \tag{4.18}$$

In equations (4.17) and (4.18) a represents the pipe radius and ρ_m the mixture density. The mixture density has already been defined by equation (2.48). The distributed heat source r_m is then obtained by taking the ratio of equations (4.17) and (4.18), leading to

$$r_m = \frac{2q}{\rho_m a}\, . \tag{4.19}$$

4.2.2 Temperature-Pressure Relationship for Dispersed Phase

We shall model the relationship between the gas pressure and temperature by initially treating the steam as a perfect gas and applying the equation of state for a perfect gas. For a perfect gas we have that the gas pressure is directly proportional to the product of the gas density and temperature. This is referred to as the gas law and is usually defined by

$$p_2 = R\rho_2 T\,, \tag{4.20}$$

where R is the gas constant. The value of the gas constant varies for different gases. The gas constant for a particular gas is given by the ratio of the universal gas constant, R_0, to the molecular weight, M, of the gas in question. For steam the gas constant is given by

$$R = \frac{R_0}{M} = \frac{8.3143}{18} = 0.462 Kg/KJK\,. \tag{4.21}$$

Since, in reality steam is not a perfect gas we introduce a correcting factor to the gas law, called the compressibility factor and denoted by Z. The equation of state for the gas phase with the compressibility factor introduced is

$$p = Z\,R\rho T\,. \tag{4.22}$$

In reality Z is a function of pressure and temperature, but since in the bubbly flow regime the pressure and temperature will not vary much from the saturation temperature and pressure we can take it to be constant. With these assumptions we may calculate the compressibility factor as

$$Z = \frac{p_s}{R\rho_{2s}T_s} = 0.615\,, \tag{4.23}$$

For a more detailed explanation of the equation of state for a perfect gas, and the compressibility factor, the reader is referred to Rodgers and Mayhew (1967).

4.2.3 Temperature-Pressure Relationship for Continuous Phase

To obtain an equation relating the temperature to the pressure we plot the data for the saturation line of water. A plot of the temperature against pressure is shown in figure 4.1. From this it is possible to extrapolate a linear relationship between the temperature and the pressure holding in a region close to the saturation temperature of 365.5 °C. This linear relationship between water temperature and pressure may be cast in the form

$$T = T_s + \chi \hat{p} \tag{4.24}$$

In equation (4.24) T_s is the saturation temperature, and $\hat{p}$ is the pressure relative to the saturation pressure. The gradient of the line χ is calculated directly from the curve depicted in 4.1 and is found to have a value of $0.412 \times 10^{-6}\ °C/Bar$.

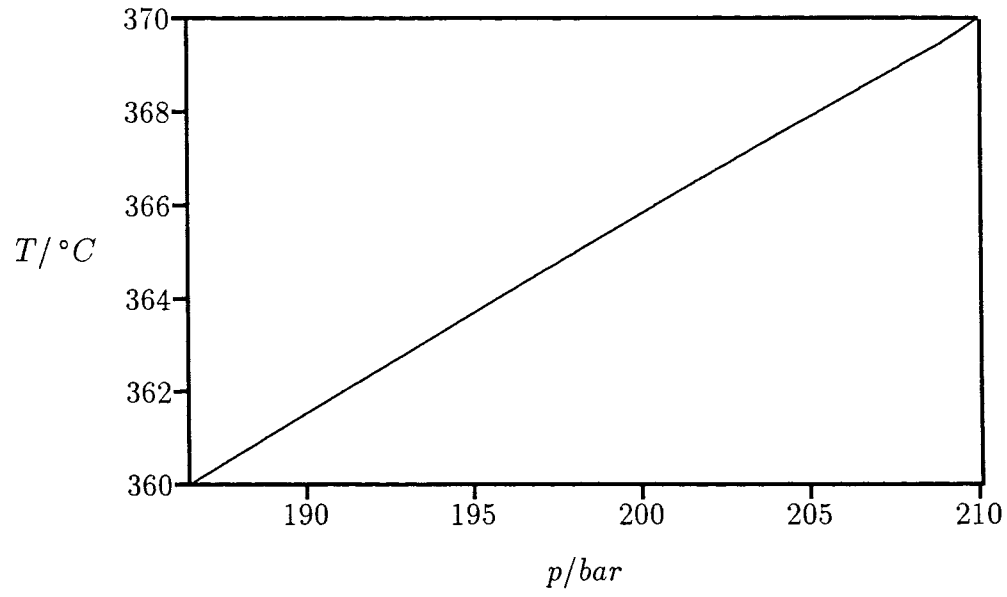

Figure 4.1: Saturation curve for water

4.2.4 Equations of Bubbly Flow Regime

We may now formulate a system of one-dimensional averaged flow equations for the bubbly regime by using the equations defined in chapter 2, (2.28)–(2.32), and the constitutive relationships detailed in this chapter. We have formulated conservation equations of mass and momentum for each phase and an equation for the mixture enthalpy. It's further assumed that the liquid phase is incompressible and that the gas phase is compressible. The unknown variables in the flow equations are the pressure in the gas phase (p_2), gas void fraction (α_2), rate of production of steam (Γ), liquid phase velocity (v_1) and gas phase velocity (v_2). The gas density can be defined as a function of the gas pressure and will be introduced when required at a later point in this chapter.

Conservation of Mass

$$\frac{\partial(\rho_1\alpha_1 v_1)}{\partial z} = -\Gamma(z), \tag{4.25}$$

$$\frac{\partial(\rho_2\alpha_2 v_2)}{\partial z} = \Gamma(z). \tag{4.26}$$

Conservation of Momentum

$$\frac{\partial(\alpha_1\rho_1 v_1^2)}{\partial z} + \alpha_1\left[\frac{\partial p_2}{\partial z} + 2\xi\rho_1(v_1 - v_2)\left(\frac{\partial v_1}{\partial z} - \frac{\partial v_2}{\partial z}\right)\right] + \xi\rho_1(v_1 - v_2)^2\frac{\partial\alpha_2}{\partial z} \tag{4.27}$$

$$= -\Gamma v_1 - \frac{3}{8}\frac{C_D}{r_d}\rho_1\alpha_2(v_2 - v_1) \mid v_2 - v_1 \mid -\alpha_1\rho_1 g$$

$$\frac{\partial(\alpha_2\rho_2 v_2^2)}{\partial z} + \alpha_2\frac{\partial p_2}{\partial z} = \Gamma v_2 + \frac{3}{8}\frac{C_D}{r_d}\rho_1\alpha_2(v_2 - v_1) \mid v_2 - v_1 \mid -\alpha_2\rho_2 g \tag{4.28}$$

Mixture Enthalpy

$$\frac{\partial}{\partial z}(\alpha_1\rho_1 v_1 h_1 + \alpha_2\rho_2 v_2 h_2) =$$

$$\rho_m r_m + \alpha_2 v_2 \frac{\partial p_2}{\partial z} + \alpha_1 v_1 \left[\frac{\partial p_2}{\partial z} + 2\xi\rho_1 (v_2 - v_1) \left(\frac{\partial v_2}{\partial z} - \frac{\partial v_1}{\partial z} \right) \right] . \quad (4.29)$$

The mixture enthalpy equation may be simplified by substituting for the phasic enthalpies and using equations (4.25) and (4.26). In doing this we make the assumption that the water and the steam are at the the same temperature. This assumption means that the water and steam enthalpies are defined respectively by

$$h_1 = c_{p1} (T_s + \chi \hat{p}_2) , \quad (4.30)$$

$$h_2 = c_{p2} (T_s + \chi \hat{p}_2) . \quad (4.31)$$

The mixture enthalpy is therefore defined by

$$\Gamma (c_{p2} - c_{p1}) (T_s + \chi \hat{p}_2) + \alpha_1 \rho_1 v_1 \chi c_{p1} \frac{\partial \hat{p}}{\partial z} + \alpha_2 \rho_2 v_2 \chi c_{p2} \frac{\partial \hat{p}}{\partial z} =$$
$$\frac{2q}{a} + (\alpha_1 v_1 + \alpha_2 v_2) \frac{\partial \hat{p}}{\partial z} + 2\alpha_1 v_1 \rho_1 \xi (v_1 - v_2) \left(\frac{\partial v_1}{\partial z} - \frac{\partial v_2}{\partial z} \right) . \quad (4.32)$$

A further simplification is possible since at the saturation temperature the difference in the water and steam enthalpies is equal to the latent heat of vaporisation. This implies

$$c_{p2} - c_{p1} = \frac{\lambda}{T_s} , \quad (4.33)$$

where λ is the latent heat of vaporization. The mixture enthalpy equation is therefore

$$\Gamma\lambda \left(1 + \frac{\chi}{T_s} \hat{p}_2 \right) + \alpha_1 \rho_1 v_1 \chi c_{p1} \frac{\partial \hat{p}}{\partial z} + \alpha_2 \rho_2 v_2 \chi c_{p2} \frac{\partial \hat{p}}{\partial z} =$$
$$\frac{2q}{a} + (\alpha_1 v_1 + \alpha_2 v_2) \frac{\partial \hat{p}}{\partial z} + 2\alpha_1 v_1 \rho_1 \xi (v_1 - v_2) \left(\frac{\partial v_1}{\partial z} - \frac{\partial v_2}{\partial z} \right) . \quad (4.34)$$

4.2.5 Non-Dimensional Equations

To simplify the equations presented in the previous section we first non-dimensionalise and compare the magnitudes of the non-dimensional groups to see if some terms in

the equations can be omitted. To non-dimensionalise the equations of bubbly flow the following scalings were employed:

$$\Gamma = \Gamma_0 \Gamma' , \qquad \hat{p} = p_s \hat{p}' ,$$
$$\rho_2 = \rho_1 \rho_2' , \qquad v_1 = v_0 v_1' ,$$
$$v_2 = v_0 v_2' , \qquad z = L z' .$$

The non-dimensional equations describing the bubbly flow regime can be written as

$$\frac{\partial (\alpha_1 v_1')}{\partial z'} = -N_{pch} \Gamma' \tag{4.35}$$

$$\frac{\partial (\rho_2' \alpha_2 v_2')}{\partial z'} = N_{pch} \Gamma' \tag{4.36}$$

$$\frac{\partial (\alpha_1 v_1'^2)}{\partial z'} + N_p \alpha_1 \frac{\partial \hat{p}'}{\partial z'} + 2\xi \alpha_1 (v_1' - v_2') \left(\frac{\partial v_1'}{\partial z'} - \frac{\partial v_2'}{\partial z'} \right) + \xi (v_1' - v_2')^2 \frac{\partial \alpha_1}{\partial z'} \tag{4.37}$$

$$= -N_{pch} \Gamma' v_1' - N_{CD} \alpha_2 (v_1' - v_2') \mid v_1' - v_2' \mid - \frac{1}{N_{Fr}^2} \alpha_1$$

$$\frac{\partial (\rho_2' \alpha_2 v_2'^2)}{\partial z'} + N_p \alpha_2 \frac{\partial \hat{p}'}{\partial z'} = N_{pch} \Gamma' v_2' + N_{CD} \alpha_2 (v_1' - v_2') \mid v_1' - v_2' \mid - \frac{1}{N_{Fr}^2} \alpha_2 \rho_2' \tag{4.38}$$

$$N_{pch} \Gamma' [1 + N_1 \hat{p}_2'] = N_2 - N_4 \alpha_1 v_1' \frac{\partial \hat{p}'}{\partial \hat{z}} - N_5 \alpha_2 v_2' \rho_2' \frac{\partial \hat{p}'}{\partial \hat{z}} \tag{4.39}$$

$$+ N_3 (\alpha_1 v_1' + \alpha_2 v_2') \frac{\partial \hat{p}'}{\partial z'} + 2 N_7 \xi v_1' (v_1' - v_2') \left(\frac{\partial v_2'}{\partial z'} - \frac{\partial v_1'}{\partial z'} \right)$$

By combining the non-dimensional forms of equations (4.22) and (4.24) we can construct an equation for the density of the gas phase which is simply a function of the non-dimensionalised gas pressure. The non-dimensional gas density is now defined by

$$\rho_2' = \frac{N_6 (1 + \hat{p}')}{(1 + N_1 \hat{p}')} . \tag{4.40}$$

In equations (4.35)–(4.40) the N_α's are non-dimensional numbers which depend on the physical parameters. The non-dimensional numbers and their orders of magnitude are

$$N_{pch} = \frac{\Gamma_s L}{\rho_1 v_0} \sim 1000\,, \tag{4.41}$$

$$N_p = \frac{p_s}{\rho_1 v_0^2} \sim 8333\,, \tag{4.42}$$

$$N_{CD} = \frac{3C_D L}{8r_b} \tag{4.43}$$

$$N_{Fr} = \frac{v_0}{\sqrt{g\,L}} \sim 0.26\,, \tag{4.44}$$

$$N_1 = \frac{\chi p_s}{T_s} \sim 0.225\,, \tag{4.45}$$

$$N_2 = \frac{2q}{\rho_1 v_0 \lambda}\frac{L}{a} \sim 1.45\,, \tag{4.46}$$

$$N_3 = \frac{p_s}{\rho_1 \lambda} \sim 56.77\,, \tag{4.47}$$

$$N_4 = \frac{c_{p1}\chi p_s}{\lambda} \sim 2.95\,, \tag{4.48}$$

$$N_5 = \frac{c_{p2}\chi p_s}{\lambda} \sim 2.82\,, \tag{4.49}$$

$$N_6 = \frac{\rho_{2s}}{\rho_1} \sim 0.18\,, \tag{4.50}$$

$$N_7 = \frac{v_0^2}{\lambda} \sim 7 \times 10^{-3}\,. \tag{4.51}$$

The values used to calculate the magnitudes of the above non-dimensional numbers are listed in Appendix A. The value of the drag number, N_{CD}, will be discussed in section §4.3 since it depends on the magnitude of the difference between the gas and liquid phase velocities.

4.3 Bubble Velocity

The main assumption we make in modelling the bubbly flow regime is that the bubbles flow up the channel with the continuous phase at approximately the same velocity. This is a reasonable approximation to make since at high pressures the surface tension of the bubbles tends rapidly to zero. For more details on the relationship between bubble rise velocity and pressure the reader is referred to Whalley (1987). This approximation allows us to introduce the following perturbation,

$$v_2' = v_1' + \varepsilon_1 v \,. \tag{4.52}$$

We could also introduce a similar perturbation as above for the pressure, but since we expect the change in pressure will be small the effect of this perturbation on the pressure will be negligible. On physical grounds we would expect the drag force on the bubbles to be important and therefore require that, to lowest order, the drag terms remain in the conservation of momentum equations. This means we need to choose ε_1 to have a value such that

$$N_{CD}\varepsilon_1^2 \sim N_p \,. \tag{4.53}$$

For our simplified study we shall treat the drag coefficient as a constant. The drag coefficient is a function of the two-phase Reynolds number which depends on the difference in the continuous and dispersive velocities, meaning that the drag coefficient is a function of ε_1. Using these assumptions we obtain

$$N_{CD} \sim \frac{1 \times 10^5}{\varepsilon_1} + O(\varepsilon^{-1/4}) \,. \tag{4.54}$$

To satisfy the condition outlined in equation (4.53) we must have $\varepsilon_1 = O(10^{-2})$. For ease of notation from this point onwards we shall drop the prime notation for

non-dimensional variables and the reader should assume that all variables are non-dimensional unless stated otherwise. The two phase flow equations to lowest order in ε_1 are defined by:

$$\frac{\partial \alpha_1 v_1}{\partial z} = -N_{pch}\Gamma \tag{4.55}$$

$$\frac{\partial \rho_2 \alpha_2 v_1}{\partial z} = N_{pch}\Gamma \tag{4.56}$$

$$\frac{\partial (\alpha_1 v_1^2)}{\partial z} + N_p \alpha_1 \frac{\partial \hat{p}}{\partial z} = N_{pch}\Gamma v_1 + \alpha_2 v \mid v \mid -\frac{1}{N_{Fr}^2}\alpha_1 \tag{4.57}$$

$$\frac{\partial (\rho_2 \alpha_2 v_1^2)}{\partial z} + N_p \alpha_2 \frac{\partial \hat{p}}{\partial z} = -N_{pch}\Gamma v_1 - \alpha_2 v \mid v \mid -\frac{1}{N_{Fr}^2}\alpha_2 \rho_2 \tag{4.58}$$

$$N_{pch}\Gamma \left[1 + N_1 \hat{p}_2\right] = N_2 + \left(N_3 v_1 - N_4 \alpha_1 v_1 - N_5 \left(1 - \alpha_1\right) \rho_2 v_1\right) \frac{\partial \hat{p}_2}{\partial z} \tag{4.59}$$

The initial conditions for the dimensional equations, taken relative to the start of the bubbly region, are

$$v_1(0) = 1\,,$$

$$\hat{p}(0) = 0\,,$$

$$\alpha_2(0) = 0\,,$$

$$v = 0\,.$$

4.4 Simplified Bubbly Flow Model

The complexity of the problem can further be simplified together by adding the non-dimensional conservation of momentum equations for each phase to give a system of equations which is now independent of the variable v. The combined momentum

equation can then be integrated exactly to determine the pressure as a function of the gas velocity. The system of equations now under consideration is:

$$\frac{\partial \alpha_1 v_1}{\partial z} = -N_{pch}\Gamma\,, \tag{4.60}$$

$$\frac{\partial}{\partial z}\left(\left(1-\alpha_1\right)\rho_2 v_1\right) = N_{pch}\Gamma\,, \tag{4.61}$$

$$v_1\frac{\partial v_1}{\partial z} + N_p v_1\frac{\partial \hat{p}_2}{\partial z} = -N_{fr}\,, \tag{4.62}$$

$$N_{pch}\Gamma\left[1+N_1\hat{p}_2\right] = N_2 + \left(N_3 v_1 - N_4\alpha_1 v_1 - N_5\left(1-\alpha_1\right)\rho_2 v_1\right)\frac{\partial \hat{p}_2}{\partial z}\,, \tag{4.63}$$

$$\rho_2 = \frac{N_6\left(1+\hat{p}_2\right)}{1+N_1\hat{p}_2}\,. \tag{4.64}$$

To make progress with this model we introduce the following perturbation series

$$\hat{p}_2 = \hat{p}_{20} + \varepsilon_2\hat{p}_{21} + \cdots\,, \tag{4.65}$$

$$v_1 = v_{10} + \varepsilon_2 v_{11} + \cdots\,, \tag{4.66}$$

$$\alpha_1 = \alpha_{10} + \varepsilon_2\alpha_{11} + \cdots\,, \tag{4.67}$$

$$\Gamma = \Gamma_0 + \varepsilon_2\Gamma_1 + \cdots\,, \tag{4.68}$$

$$\rho_2 = \rho_{20} + \varepsilon_2\rho_{21} + \cdots\,. \tag{4.69}$$

Strictly speaking ρ_2 is a known function of p_2, but we have included a perturbation series for ρ_2 to simplify the algebra. Comparing the magnitudes of the non-dimensional groups defined in equations (4.41)–(4.50) we can see that a suitable choice for ε_2 is

$$\varepsilon_2 = \frac{1}{N_p}\,. \tag{4.70}$$

By substituting the perturbation series into the simplified model we will obtain a zero order problem where ε_2 is absent, and a first order problem where only terms of order ε_2 are considered.

$O(1)$ Problem

$$\frac{\partial}{\partial z}(\alpha_{10}v_{10}) = -N_{pch}\Gamma_0\,, \tag{4.71}$$

$$\frac{\partial}{\partial z}(\rho_{20}(1-\alpha_{10})v_{10}) = N_{pch}\Gamma_0\,, \tag{4.72}$$

$$\frac{\partial \hat{p}_2}{\partial z} = 0\,, \tag{4.73}$$

$$N_{pch}\Gamma_0[1+N_1\hat{p}_{20}] = N_2 + (N_3 v_{10} - N_4\alpha_{10}v_{10} - N_5(1-\alpha_{10})\rho_{20}v_{10})\frac{\partial \hat{p}_{20}}{\partial z} \tag{4.74}$$

$$\rho_{20} = \frac{N_6(1+\hat{p}_{20})}{1+N_1\hat{p}_{20}}\,. \tag{4.75}$$

Integrating equation (4.73) and applying the relevant initial condition we obtain

$$\hat{p}_{20} = 0\,. \tag{4.76}$$

In terms of the non-dimensional gas pressure we have

$$p_{20} = 1\,. \tag{4.77}$$

The above result can then be used to simplify the problem significantly as it simply means that to lowest order the gas density and rate of production of steam are constant. The problem therefore reduces to

$$\frac{\partial(\alpha_{10}v_{10})}{\partial z} = -N_2\,, \tag{4.78}$$

$$N_6\frac{\partial}{\partial z}(1-\alpha_{10})v_{10} = N_2\,, \tag{4.79}$$

$$\Gamma_0 = \frac{N_2}{N_{pch}}\,, \tag{4.80}$$

$$\rho_{20} = N_6\,. \tag{4.81}$$

The problem has reduced to solving a pair of simultaneous differential equations for the lowest order terms in the asymptotic expansion of the liquid void fraction and

the liquid velocity. The solution to equations (4.78)–(4.79) with the relevant initial conditions is

$$v_{10} = 1 + \beta z, \tag{4.82}$$

$$\alpha_{10} = \frac{1 - N_2 z}{1 + \beta z}. \tag{4.83}$$

For ease of notation we have introduced the variable β defined by

$$\beta = \left(\frac{1 - N_6}{N_6}\right) N_2. \tag{4.84}$$

Combining equations (4.83) and (2.39) yields the following relationship for the gas void fraction:

$$\alpha_{20} = \frac{N_2 z}{N_6 (1 + \beta z)}. \tag{4.85}$$

It should be noted that all the aforementioned results are for non-dimensional variables.

$O(\varepsilon_2)$ Problem

The next order terms in the perturbation series are given by the solution of the system of equations:

$$\frac{\partial}{\partial z}(\alpha_{10} v_{11} + \alpha_{11} v_{10}) = -N_{pch} \Gamma_1, \tag{4.86}$$

$$\frac{\partial}{\partial z}((1 - \alpha_{10}) v_{11} \rho_{20} + (1 - \alpha_{10}) v_{10} \rho_{21} - \alpha_{11} v_{10} \rho_{20}) = +N_{pch} \Gamma_1, \tag{4.87}$$

$$v_{10} \frac{\partial v_{10}}{\partial z} + v_{10} \frac{\partial \hat{p}_{21}}{\partial z} = -N_{Fr}, \tag{4.88}$$

$$N_{pch} [\Gamma_1 + \Gamma_0 \hat{p}_{21}] = (N_3 v_{10} - N_4 \alpha_{10} v_{10} - N_5 (1 - \alpha_{10}) \rho_{20} v_{10}) \frac{\partial \hat{p}_{21}}{\partial z}, \tag{4.89}$$

$$\rho_{21} = N_6 (1 - N_1) \hat{p}_{21}. \tag{4.90}$$

Using the results obtained for the first order problem, equation (4.88) can be integrated directly to give a relationship for $\hat{p}_{21}$ in terms of the axial distance from the

start of the bubbly regime. This relationship (after some rearrangement) is

$$\hat{p}_{21} = -\beta z - \frac{N_{Fr}}{\beta} \log\left(1 + \beta z\right) . \tag{4.91}$$

In obtaining the above relationship the boundary condition $\hat{p}_{21} = 0$ was used. Equation (4.91) can now be used to obtain a relationship for Γ_1 in terms of the axial distance from the initiation of the bubbly flow regime. After some simplification the aforementioned relation is

$$\Gamma_1 = \frac{N_2}{N_{pch}} \left[\beta z - \frac{N_{Fr}}{\beta} \ln\left(1 + \beta z\right)\right] \tag{4.92}$$

$$-\frac{1}{N_{pch}} \left[N_3 - N_4 + \left(\beta + N_2 \left(N_4 - N_5\right)\right) z\right] \times \left[\beta + \frac{N_{Fr}}{1 + \beta z}\right]$$

To evaluate α_{11} and v_{11} we need to integrate equations (4.86) and (4.87) with respect to z, giving

$$\alpha_{10} v_{11} + \alpha_{11} v_{10} = -G(z) , \tag{4.93}$$

$$N_6 \left(1 - \alpha_{10}\right) v_{11} + \left(1 - \alpha_{10}\right) v_{10} \rho_{21} + N_6 \alpha_{11} v_{10} = G(z) . \tag{4.94}$$

In equations (4.93)–(4.94) the function $G(z)$ is obtained from integration of equation (4.92) and can be expressed

$$G(z) = \left(\frac{N_2 N_4 N_{Fr}}{\beta^2} - \frac{N_2 N_{Fr}}{\beta^2} - \frac{N_3 N_{Fr}}{\beta} - \frac{N_2 N_{Fr} z}{\beta} + \frac{N_4 N_{Fr}}{\beta} - N_{Fr}\right.$$

$$\left. - \frac{N_2 N_5 N_{Fr}}{\beta^2}\right) \ln(1 + \beta z) + \left(\frac{N_2 \beta}{2} + \frac{N_2 N_5 \beta}{2} - \frac{N_2 N_4 \beta}{2}\right) z^2 \tag{4.95}$$

$$- \left(-N_3 \beta + N_4 \beta - \beta^2 + \frac{N_2 N_5 N_{Fr}}{\beta} + \frac{N_2 N_{Fr}}{\beta} - \frac{N_2 N_4 N_{Fr}}{\beta}\right) z$$

From the previous analysis for the $O(1)$ problem α_{10} and v_{10} are known functions of z. This allows us to solve equations (4.93)–(4.94) for α_{11} and v_{11}. After some

simplification v_{11} and α_{11} are defined by

$$v_{11} = \frac{\beta}{N_2} G(z) - (1-\alpha_{10})\, v_{10}\rho_{21}\,, \tag{4.96}$$

$$\alpha_{11} = -\frac{G(z)}{v_{10}} \left(1+\frac{\beta}{N_2}\right) + \frac{1}{N_6}\alpha_{10}(1-\alpha_{10})\,\rho_{21}\,, \tag{4.97}$$

Respectively by substituting for $G(z)$, α_{10}, and v_{10} we obtain

$$v_{11} = \frac{\beta}{N_2}\left(\left(\frac{N_2\,N_4\,N_{Fr}}{\beta^2} - \frac{N_2\,N_{Fr}}{\beta^2} - \frac{N_3\,N_{Fr}}{\beta} - \frac{N_2\,N_{Fr}\,z}{\beta}\right.\right.$$

$$\left.+N_6\,N_2\,(1-N_1)\left(\frac{\beta+N_2}{\beta^2}\right) + \frac{N_4\,N_{Fr}}{\beta} - N_{Fr} - \frac{N_2\,N_5\,N_{Fr}}{\beta^2}\right)\ln(1+\beta z) \tag{4.98}$$

$$+\left(\frac{N_2\,\beta}{2} + \frac{N_2\,N_5\,\beta}{2} - \frac{N_2\,N_4\,\beta}{2} - N_6\,N_2\,(1-N_1)\,(\beta+N_2)\right)z^2$$

$$\left.-\left(-N_3\,\beta + N_4\,\beta - \beta^2 + \frac{N_2\,N_5\,N_{Fr}}{\beta} + \frac{N_2\,N_{Fr}}{\beta} - \frac{N_2\,N_4\,N_{Fr}}{\beta}\right)z\right)\,,$$

$$\alpha_{11} = \frac{1}{N_6}\left(\frac{1-N_2\,z}{1+\beta\,z}\right)\left(\frac{N_2\,z}{1+\beta\,z}\right)(1-N_1)\left(-\beta z - \frac{N_{Fr}}{\beta}\log(1+\beta z)\right)$$

$$-\left(\left(\frac{N_2\,N_4\,N_{Fr}}{\beta^2} - \frac{N_2\,N_{Fr}}{\beta^2} - \frac{N_3\,N_{Fr}}{\beta} - \frac{N_2\,N_{Fr}\,z}{\beta} + \frac{N_4\,N_{Fr}}{\beta} - N_{Fr}\right.\right.$$

$$\left.-\frac{N_2\,N_5\,N_{Fr}}{\beta^2}\right)\ln(1+\beta z) + \left(\frac{N_2\,\beta}{2} + \frac{N_2\,N_5\,\beta}{2} - \frac{N_2\,N_4\,\beta}{2}\right)z^2 \tag{4.99}$$

$$\left.-\left(-N_3\,\beta + N_4\,\beta - \beta^2 + \frac{N_2\,N_5\,N_{Fr}}{\beta} + \frac{N_2\,N_{Fr}}{\beta} - \frac{N_2\,N_4\,N_{Fr}}{\beta}\right)z\right)$$

$$\times\left(1+\frac{\beta}{N_2}\left(\frac{1-N_2\,z}{1+\beta\,z}\right)\right)\frac{1}{1+\beta\,z}\,.$$

4.4.1 Analysis of Simplified Bubbly Flow Model

From the analysis carried out in §4.4 we may now write down the first two terms in the perturbation series for the non-dimensional liquid void fraction, liquid phase velocity, rate of production of steam and pressure in the gas phase, as functions of the axial distance, z measured from the start of the bubbly flow regime. After some simplification these quantities are:

Liquid Void Fraction

$$\alpha_1 = \frac{1 - N_2 z}{1 + \beta z} + \varepsilon_2 \left[\frac{1}{N_6} \left(\frac{1 - N_2 z}{1 + \beta z} \right) \left(\frac{N_2 z}{1 + \beta z} \right) (1 - N_1) \left(-\beta z - \frac{N_{Fr}}{\beta} \log (1 + \beta z) \right) \right. \tag{4.100}$$

$$- \left(\left(\frac{N_2 N_4 N_{Fr}}{\beta^2} - \frac{N_2 N_{Fr}}{\beta^2} - \frac{N_3 N_{Fr}}{\beta} - \frac{N_2 N_{Fr} z}{\beta} + \frac{N_4 N_{Fr}}{\beta} - N_{Fr} \right. \right.$$

$$\left. - \frac{N_2 N_5 N_{Fr}}{\beta^2} \right) \ln(1 + \beta z) + \left(\frac{N_2 \beta}{2} + \frac{N_2 N_5 \beta}{2} - \frac{N_2 N_4 \beta}{2} \right) z^2$$

$$\left. - \left(-N_3 \beta + N_4 \beta - \beta^2 + \frac{N_2 N_5 N_{Fr}}{\beta} + \frac{N_2 N_{Fr}}{\beta} - \frac{N_2 N_4 N_{Fr}}{\beta} \right) z \right)$$

$$\left. \times \left(1 + \frac{\beta}{N_2} \left(\frac{1 - N_2 z}{1 + \beta z} \right) \right) \frac{1}{1 + \beta z} \right],$$

Liquid Phase Velocity

$$v_1 = 1 + \beta z + \varepsilon_2 \frac{\beta}{N_2} \left[\left(\frac{N_2 N_4 N_{Fr}}{\beta^2} - \frac{N_2 N_{Fr}}{\beta^2} - \frac{N_3 N_{Fr}}{\beta} - \frac{N_2 N_{Fr} z}{\beta} \right. \right.$$

$$+N_6\,N_2\,(1-N_1)\left(\frac{\beta+N_2}{\beta^2}\right)+\frac{N_4\,N_{Fr}}{\beta}-N_{Fr}-\frac{N_2\,N_5\,N_{Fr}}{\beta^2}\Bigg)\ln(1+\beta z) \quad (4.101)$$

$$+\left(\frac{N_2\,\beta}{2}+\frac{N_2\,N_5\,\beta}{2}-\frac{N_2\,N_4\,\beta}{2}-N_6\,N_2\,(1-N_1)\,(\beta+N_2)\right)z^2$$

$$-\left(-N_3\,\beta+N_4\,\beta-\beta^2+\frac{N_2\,N_5\,N_{Fr}}{\beta}+\frac{N_2\,N_{Fr}}{\beta}-\frac{N_2\,N_4\,N_{Fr}}{\beta}\right)z\Bigg]\,,$$

Rate of Production of Steam

$$\Gamma=\frac{N_2}{N_{pch}}+\varepsilon_2\left[\frac{N_2}{N_{pch}}\left(\beta z-\frac{N_{Fr}}{\beta}\ln(1+\beta z)\right)\right. \quad (4.102)$$

$$\left.-\frac{1}{N_{pch}}\left(N_3-N_4+(\beta+N_2\,(N_4-N_5))\,z\right)\times\left(\beta+\frac{N_{Fr}}{1+\beta z}\right)\right]\,,$$

Gas Pressure

$$p_2=1-\varepsilon_2\left[\beta z+\frac{N_{Fr}}{\beta}\log(1+\beta z)\right]\,. \quad (4.103)$$

As previously mentioned the transition from bubbly to slug flow occurs when the gas void fraction has a value of approximately 0.3, (that is when the liquid void fraction is approximately 0.7). If we just use the first term in the perturbation series for the liquid void fraction we obtain the following simple relationship for the non-dimensional length of the bubbly flow regime

$$z=\frac{1-\alpha_{1\,bs}}{\alpha_{1\,bs}\beta+N_2}\,. \quad (4.104)$$

In the above equation $\alpha_{1\,bs}$ is the liquid void fraction at the bubbly/slug flow transition. Substituting for the values of the parameters in equation (4.104), and redimensionalising, we calculate the length of the bubbly regime to be approximately $0.3\,m$. This seems a sensible value for the length of the bubbly flow region considering the total length of the two phase flow regimes up to the dryout point is approximately one sixth the total length of the pipe. This was also confirmed to be approximately the correct length by Atthey (1992). Plots of the liquid and gas void fractions as a functions of axial distance are shown in figure 4.2. From this plot it is seen that the rate at which the water evaporates decreases as more steam is produced. This is because as well as the thermal energy supplied heating the liquid phase it also heats the gas phase meaning less heat is supplied to the liquid phase slowing down the rate at which steam is being produced.

Now that we have calculated the length of the bubbly flow regime we can calculate the pressure variation in the gas phase. Application of equation (4.103) shows that the gas pressure varies by 0.025 Bars over the length of the bubbly flow regime. The variation in the difference between the gas pressure and the saturation pressure with respect to axial distance is displayed in figure 4.3. Sometimes it is easier experimentally to measure the gas void fraction, by the use of freeze frame photograph for example, and for this purpose we have displayed the variation of gas pressure drop with gas void fraction in figure 4.4.

We are also able to construct profiles of how the liquid phase velocity varies with axial distance and gas void fractions. These two profiles are displayed in figures (4.5) and (4.6). These two plots show that the liquid velocity increases as the the liquid void fraction decreases. This is due to the fact that the some of the energy supplied thermally is being converted into kinetic energy causing the liquid to increase its velocity

Our analysis can also be applied to look at the variation in the rate of production of steam throughout the regime. The variation of the rate of production of steam with respect to axial distance and void fraction are displayed in figure (4.7) and figure (4.8) respectively. These plots confirm the result deduced from the variation of void fraction with axial distance that the rate at which the rate evaporation occurs decreases as the amount of steam increases.

4.5 Slug Flow

The slug flow regime is characterised by the existence of large gas bubbles whose diameter is comparable to the pipe diameter. The slug flow regime has a more complicated structure then the bubbly and annular flow regimes. This is due to the fact that as the Taylor bubble moves through the liquid phase it pushes the water in front of it to the sides of the pipe forcing the thin layer of water between the Taylor bubble and the pipe wall to flow in the opposite direction to the overall flow. As described by Nakoryakov et al this descending layer of water only changes direction when it interacts with the water travelling in the wake of the Taylor bubble. So the velocity field for the continuous phase in slug flow is far more complicated then for any of the other flow regimes.

The slug flow regime does not undergo a transition directly into the annular flow regime but develops first into the churn flow regime. There is considerable difficulty in identifying the slug/churn transition since there is confusion as to the exact description of the churn regime. As stated by Taitel et al (1980) some define the start of the churn flow regime as being when froth appears within the gas region and others with the instability of the liquid film adjacent to the Taylor bubble.

The transition from churn to annular flow is defined to occur by Taitel et al (1980), when the gas velocity is great enough to support the entrained droplets within the gas core. By balancing the drag and gravity forces on a droplet they were able to develop a simple expression for the minimum gas velocity required to support a droplet. The minimum velocity is given by the expression

$$U_G = \frac{2}{\sqrt{3}} \left(\frac{g\,(\rho_L - \rho_G)\,d}{\rho_G\,C_d} \right)^{1/2}, \tag{4.105}$$

where C_d is the coefficient of frag and d the diameter of the droplet. The droplet size is usually determined by balancing the the surface tension that holds the droplet together with the impact force required by the gas to break up the droplet.

Griffith and Wallis (1961) proposed an alternative model for the transition directly from the slug regime to annular regime. Their model simply assumed that the transition occurred when the Taylor bubbles become very *long*. When this model was compared with experimental data it was found that it predicted a gas velocity lower then expected. So it was proposed that their model, instead of predicting the transition from slug to annular, may actually predicted the transition to the churn regime.

The important information from the slug flow regime is that upon transition to the annular flow regime the gas velocity is at least an order of magnitude greater then the liquid velocity. This is due to the effects of flow reversal on the liquid layer flowing around the Taylor bubbles. Apart from this fact we are going to ignore the slug flow regime in relation to our problem.

4.6 Closing Remarks

From this work and the work in the previous chapter on the length scales of the flow regimes it is becoming apparent that the dominant flow regime, (ie. the longest regime), is going to be the annular flow regime. This is supported by work carried out by Atthey (1992) in which he proposes that the length from the start of the the subcooled regime to the dryout point is approximately one sixth the total pipe length. The length of the slug flow regime can be estimated by the fact that the length of the Taylor bubbles is approximately twice the diameter of the pipe. It has been observed empirically that the slug flow regime on average consists of five taylor bubbles. So allowing for five Taylor bubbles to exist in the slug flow gives an approximate length for the slug regime of approximately $0.15, m$ (allowing for the liquid slugs between the Taylor bubbles). So in total the length of the subcooled flow, bubbly and slug regimes is about $0.8m$. This means the annular flow regime would be over a meter in length confirming that the annular flow regime is the longest flow regime.

Future work could be to examine the unsteady version of equations (4.25)-(4.32) to see if they form a hyperbolic system of differential equations. Due to the large number of variables involved this calculation could be carried out with the help of a symbolic manipulator such as Maple^{Tm}.

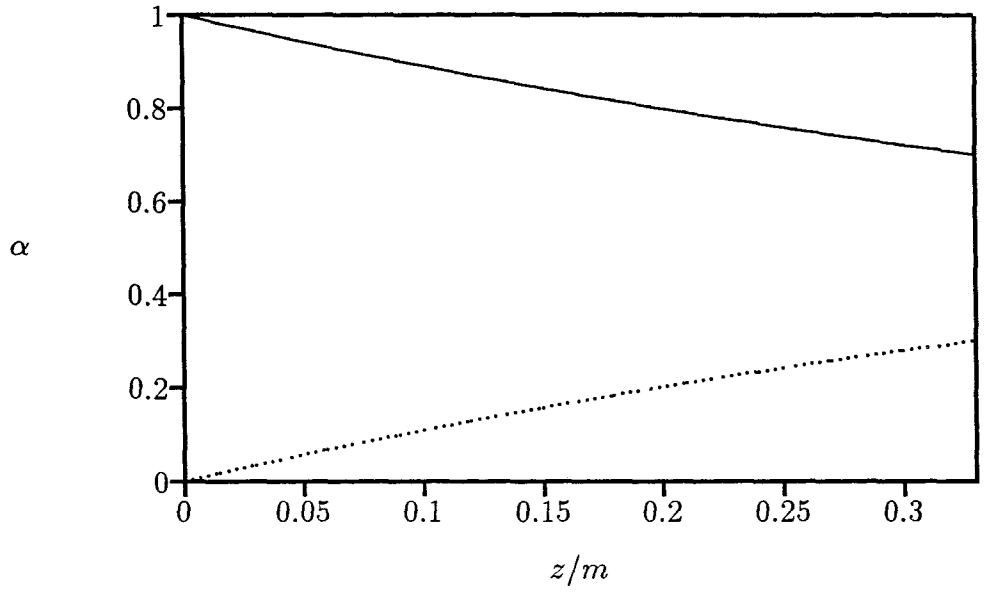

Figure 4.2: Variation of liquid and gas void fractions with respect to axial distance within the bubbly flow regime

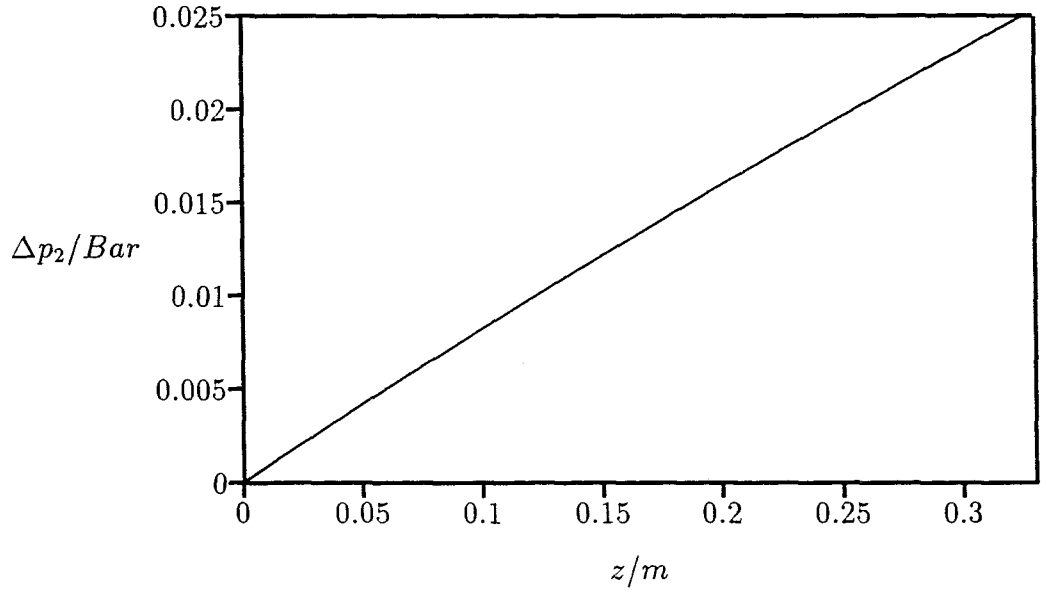

Figure 4.3: Variation of pressure drop in gas phase with respect to axial distance within the bubbly flow regime

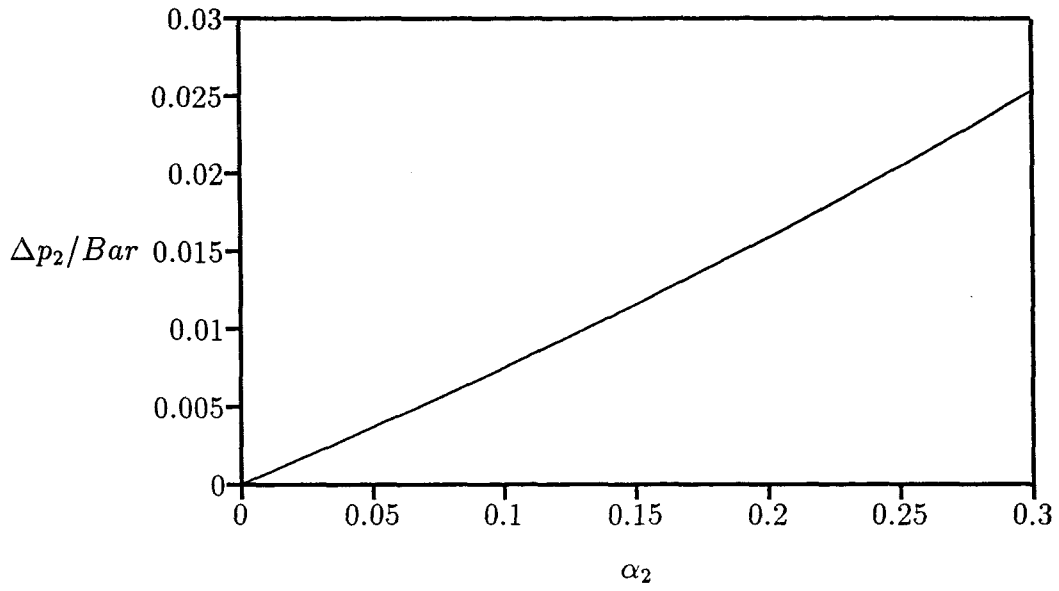

Figure 4.4: Variation of pressure drop in gas phase with respect to gas void fraction

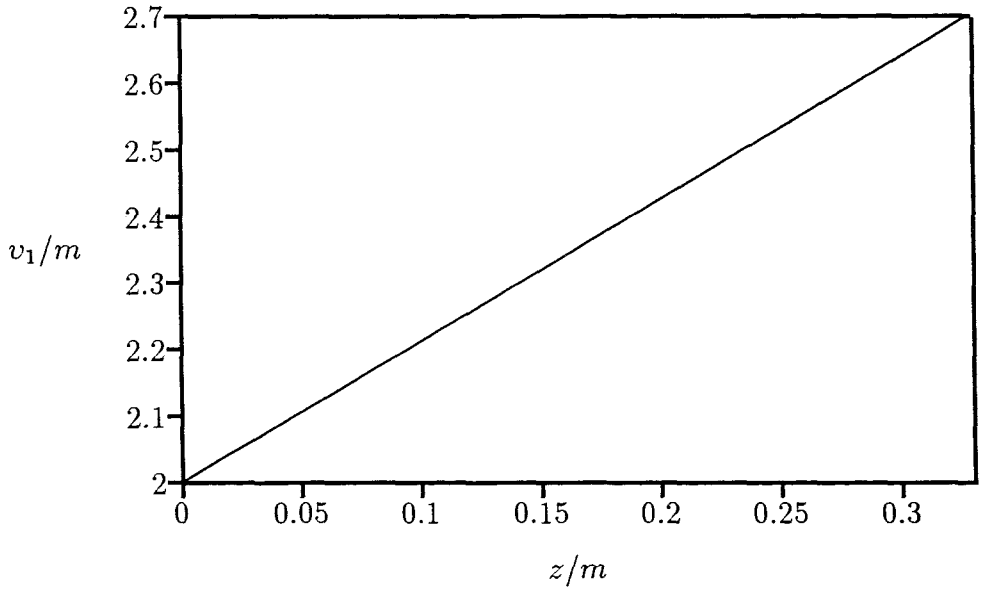

Figure 4.5: Variation of liquid phase velocity with axial distance in the bubbly flow regime

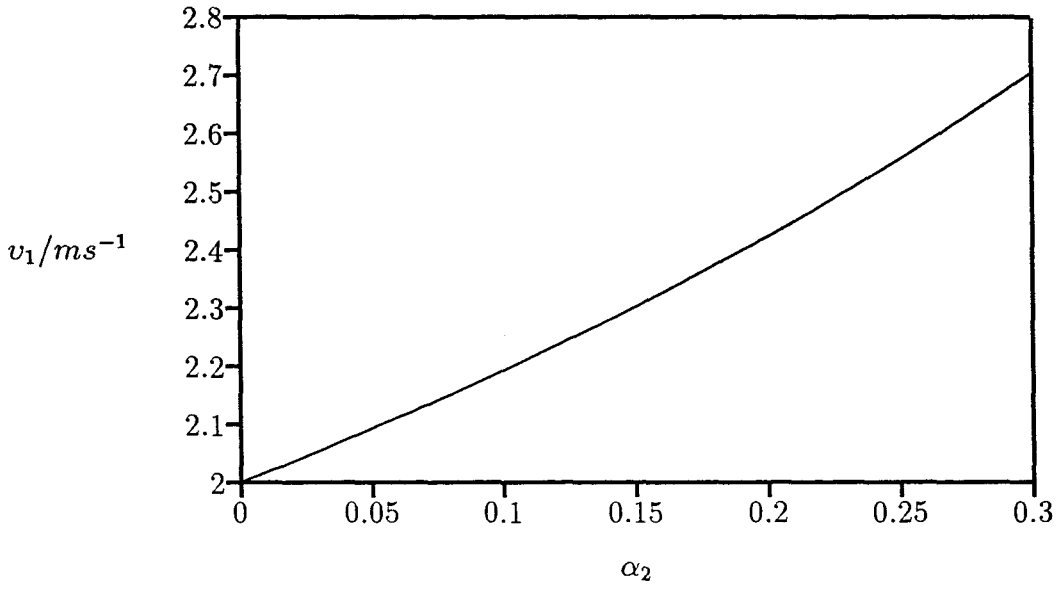

Figure 4.6: Variation of liquid phase velocity with respect to gas void fraction

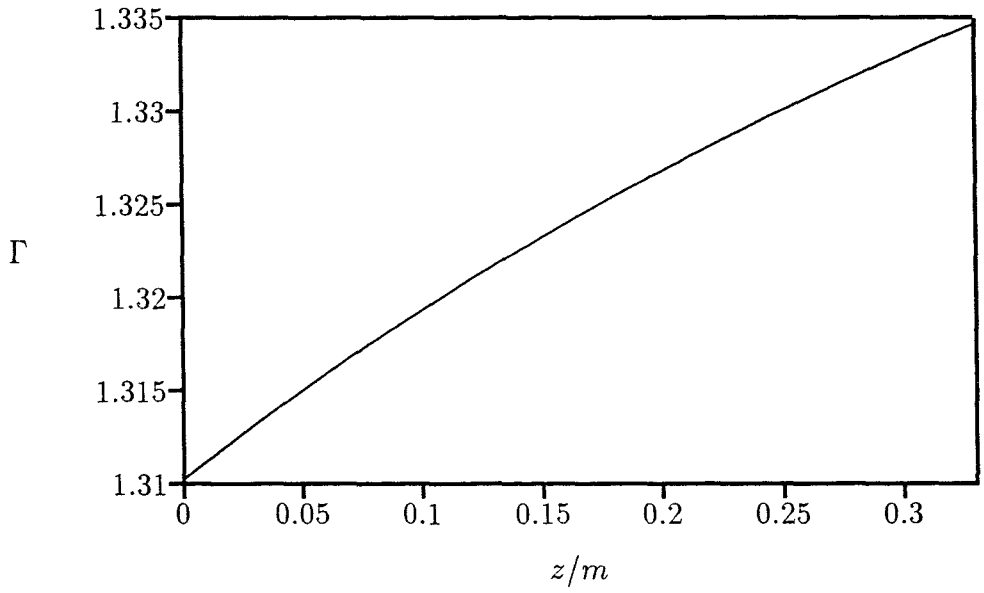

Figure 4.7: Variation of rate of production of steam with respect to axial distance in the bubbly flow regime

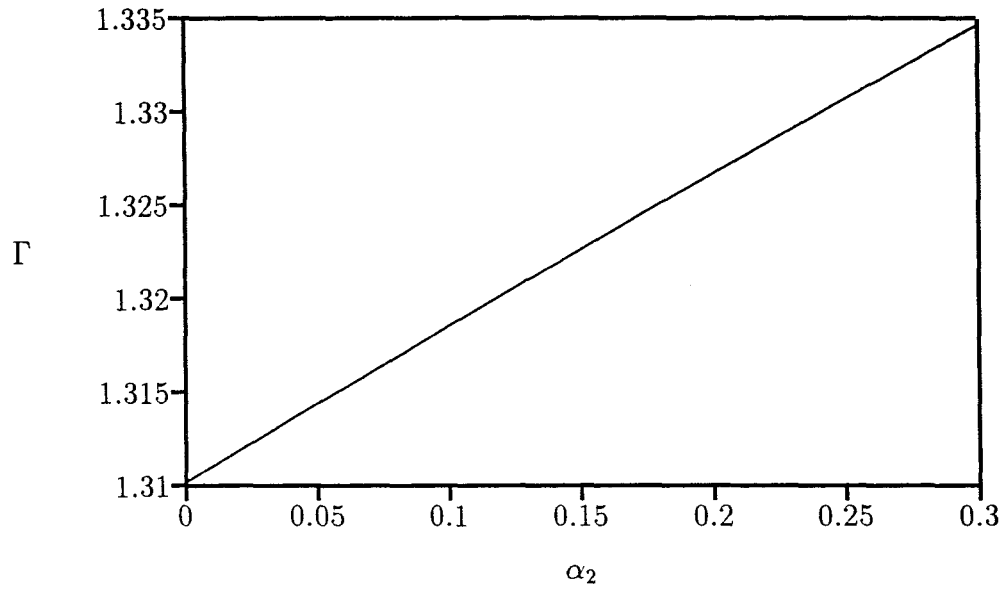

Figure 4.8: Variation of rate of production of steam with respect to gas void fraction

Chapter 5

ANNULAR FLOW

5.1 Introduction

We now analyse the annular flow region. As indicated in the previous chapters, this region forms the largest regime in a steam generating pipe. The annular flow region is also particularly worthy of study since it is in this region that the dryout point occurs.

The annular flow regime is characterised by the fact that most of the liquid phase is present in a thin liquid layer covering the steam generating pipe wall. The remainder of the liquid phase is located as minute liquid droplets within the central gas core. To model the annular flow regime successfully we need to take into account the exchange of mass between the liquid film and gas core. The three mechanisms for mass exchange are

- Entrainment of liquid droplets from the liquid film into the gas core.
- Deposition of liquid droplets from the gas core to the liquid film.
- Evaporation of the liquid phase.

Several mechanisms for entrainment are described by Ishii and Grolmes (1975). A

wavy liquid film may be entrained into a gas flow in a number of different ways, depending on the shape of the interface between the liquid film and gas core. The shape of the interface is influenced by hydrodynamic and surface tension forces. The first form of entrainment, which is commonly observed in experiments on horizontal film flow, for example by Van Rossom (1959), is by the shearing off of the tops of large amplitude waves. The second type of entrainment is caused by undercutting of the liquid flow by a gas flow. A third type of entrainment is caused by gas bubbles being formed in the liquid film, rising to the surface of the liquid film and then bursting, sending droplets of liquid into the gas core. This type of entrainment was shown to exist experimentally by Newitt et al (1954). It was also found that even larger droplets were formed by the surrounding liquid moving into the *crater* formed by the bursting bubble. As the liquid moves into the crater a spike-like filament rises at the centre of the crater. This filament rapidly breaks up into droplets.

From experimental observations, as reported by Whalley (1987), it was found that the rate of deposition of droplets from the gas core to the liquid film is directly proportional to the concentration of liquid droplets in the gas core. This simply means that the more droplets that exist within the gas core the greater the probability that a droplet will hit the liquid film. The relationship between deposition rate and droplet concentration is usually represented by the equation

$$D = k\,C\,, \tag{5.1}$$

where D is the deposition rate, k the deposition mass transfer coefficient and C the concentration of liquid droplets within the gas core. In many texts, for example Whalley (1987), a similar relationship is proposed for the entrainment rate, usually in the form

$$E = k\,C_E\,. \tag{5.2}$$

In the above equation E is the rate of entrainment, k the deposition mass transfer coefficient and C_E the concentration of droplets in the gas core when the entrainment rate and deposition rate are in equilibrium. Although the above relationship is only strictly true when the the deposition rate equals the entrainment rate it is usually assumed to be true for all annular flow regimes involving mass exchange since it is extremely difficult to measure entrainment rates experimentally.

The other mechanism in the mass exchange between the liquid film and gas core is evaporation. Convective boiling which takes place in the liquid film, is the process by which heat is conducted and convected through the thin liquid film. When convective boiling takes place evaporation occurs at the liquid vapour interface and so the evaporation rate depends on the external heat flux supplied to the boiling tubes.

All the aforementioned mass exchange mechanisms determine where the position of dryout will occur. For our analysis we will be concentrating on the effect of evaporation on both the thickness of the liquid film and the position at which dryout occurs.

5.2 Model for Gas Core Flow

To model the interaction between the gas core and the liquid layer close to the wall, we shall assume that, at some intermediate point between the slug flow and annular flow regions both the gas and liquid are flowing unidirectionally with a known temperature and velocity. Although this is a major simplifying assumption, it does not seem unreasonable that at some point before the initiation of true annular flow such flow conditions exist. We also assume that, if required, the relevant temperatures and velocities could be experimentally determined.

We assume that the gas flow is inviscid and incompressible, and, from the assumptions above irrotational. We may introduce a velocity potential for the gas flow. Since we are dealing with an inviscid flow, upon the introduction of the velocity potential the Euler equations reduce to Laplace's equation with the dependent variable being the velocity potential. This is a standard result, the details of which can be found in most fluid mechanics text books, such as Panton (1984) or Acheson (1990). The velocity potential is usually denoted by ϕ and therefore satisfies

$$\frac{\partial^2\phi}{\partial x^2} + \frac{\partial^2\phi}{\partial y^2} = 0\,. \tag{5.3}$$

The velocity components are related to the velocity potential in the usual way by

$$u = \frac{\partial\phi}{\partial x}\,, \tag{5.4}$$

$$v = \frac{\partial\phi}{\partial y}\,. \tag{5.5}$$

The problem for the gas core flow is shown schematically in figure 5.1.

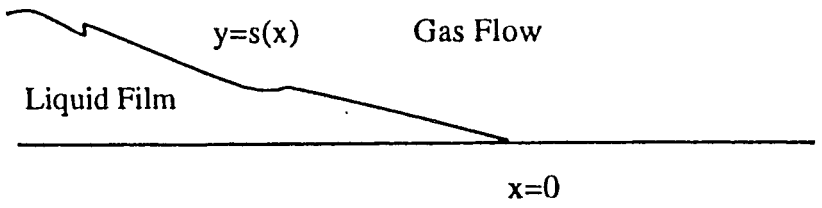

Figure 5.1: Schematic diagram of flow of gas core over the liquid film

The boundary conditions for equation (5.3) are given by an upstream condition and a tangency condition.

$$\phi \sim u_\infty x \qquad as \quad x^2 + y^2 \to \infty\,, \tag{5.6}$$

$$\frac{v}{u} = \frac{dy}{dx} \qquad on \quad y = s(x)\,. \tag{5.7}$$

If we now redefine our problem in terms of the non-dimensional scaled variables,

$$x = L\,\hat{x}\,,$$

$$y = L\,\hat{y}\,,$$

$$\phi = u_\infty L\hat{\phi}\,,$$

$$s(x) = \varepsilon L\hat{s}(\hat{x})\,,$$

where ε is a scaling factor for the film height and is known as the thickness parameter. It seems reasonable to introduce the scaling factor since the aspect ratio of the film is small; in reality, of course, the value of ε would have to be determined by some sort of experimental measurement.

The problem in non-dimensional variables is

$$\hat{\phi}_{\hat{x}\hat{x}} + \hat{\phi}_{\hat{y}\hat{y}} = 0\,, \tag{5.8}$$

$$\hat{\phi} \sim \hat{x} \qquad as \quad \hat{x}^2 + \hat{y}^2 \to \infty\,, \tag{5.9}$$

$$\hat{\phi}_{\hat{y}} = \varepsilon\hat{s}'(\hat{x})\hat{\phi}_{\hat{x}} \qquad \text{on} \quad \hat{y} = \varepsilon\hat{s}(\hat{x})\,, \tag{5.10}$$

$$\hat{\phi}_{\hat{y}} = 0 \qquad \text{on} \quad \hat{y} = 0\,. \tag{5.11}$$

We now seek an asymptotic expansion as a function of the thickness parameter, of the form

$$\hat{\phi}(\hat{x},\hat{y}) = \hat{x} + \varepsilon\hat{\phi}_1(\hat{x},\hat{y}) + \varepsilon^2\hat{\phi}_2(\hat{x},\hat{y}) + \cdots\,. \tag{5.12}$$

For the purposes of this work we will be considering only terms up to $O(\varepsilon)$. In order to employ the above expansion we need to transfer the tangency condition from the gas/liquid interface to the axis $y = 0$. This is the same technique as that used in thin aerofoil theory. Following Van Dyke (1964), the transfer is achieved by expanding the tangency condition about $y = 0$.

The $O(\varepsilon)$ problem can then be written

$$\hat{\phi}_{1\hat{x}\hat{x}} + \hat{\phi}_{1\hat{y}\hat{y}} = 0\,, \tag{5.13}$$

$$\hat{\phi}_1 = o(1) \qquad \text{as} \quad \hat{x}^2 + \hat{y}^2 \to \infty\,, \tag{5.14}$$

$$\hat{\phi}_{1\hat{y}}(\hat{x}, 0) = \hat{s}'(\hat{x})\,. \tag{5.15}$$

This elliptic problem may be solved by representing the interface as a distribution of sources and sinks along the y axis. The simplest way of doing this is to write

$$\hat{\phi}_1(\hat{x}, \hat{y}) = \frac{1}{2\pi}\int_{-\infty}^{0} g(t)\log((\hat{x}-t)^2 + \hat{y}^2)dt\,. \tag{5.16}$$

where the function $g(t)$ is to be determined. Applying the boundary condition (5.15) and noting that the source distribution becomes a delta function under differentiation, we find that $g(t) = 2\hat{s}'(t)$ and thus

$$\hat{\phi}_1(\hat{x}, \hat{y}) = \frac{1}{\pi}\int_{-\infty}^{0} \hat{s}'(t)\log((\hat{x}-t)^2 + \hat{y}^2)dt\,. \tag{5.17}$$

The solution to the original problem to order ε is therefore,

$$\hat{\phi}(\hat{x}, \hat{y}) = x + \frac{\varepsilon}{\pi}\int_{-\infty}^{0} \hat{s}'(t)\log((\hat{x}-t)^2 + \hat{y}^2)dt\,. \tag{5.18}$$

The velocity components as defined by equations (5.4) and (5.5) are

$$v_2 = 1 + \frac{2\varepsilon}{\pi}\int_{-\infty}^{0} \frac{s'(t)(x-t)}{(x-t)^2 + y^2}\,dt\,, \tag{5.19}$$

$$\nu_2 = \frac{2\varepsilon}{\pi}\int_{-\infty}^{0} \frac{s'(t)y}{(x-t)^2 + y^2}\,dt\,. \tag{5.20}$$

Note that for convenience we have dropped the hats above the non-dimensional quantities.

With the thin aerofoil approximation, the velocity along the gas/liquid interface is obtained by setting $y = 0$, leading to

$$v_{2i} = 1 + \frac{2\varepsilon}{\pi} \fint_{-\infty}^{0} \frac{s'(t)}{x-t}\, dt\,. \tag{5.21}$$

In the above the liquid film occupies the region $(-\infty, 0)$ but, for simplicity, we redefine the equations so that the film occupies the region $(0, \infty)$, with the trailing edge of the film remaining at $x = 0$. The non-dimensional interfacial velocity is now given by

$$v_{2i} = 1 + \frac{2\varepsilon}{\pi} \fint_{0}^{\infty} \frac{s'(t)}{x-t}\, dt\,. \tag{5.22}$$

To calculate the pressure along the the gas/liquid interface we apply Bernoulli's equation :

$$P_\infty + \frac{1}{2}\rho_2 v_\infty^2 = P_{2i} + \frac{1}{2}\rho_2 v_{2i}^2\,. \tag{5.23}$$

Substituting for v_{2i} and retaining terms to $O(\varepsilon)$ yields the gas pressure P_{2i} on the surface of the liquid film as

$$P_{2i} = P_\infty - \frac{1}{2}\rho_2 v_\infty^2 \left(\frac{2\varepsilon}{\pi} \fint_{0}^{\infty} \frac{s'(t)}{x-t}\, dt \right)\,. \tag{5.24}$$

5.3 Liquid Film Flow

Assuming that the liquid is irrotational and inviscid, and noting that by Kelvin's theorem the flow in the film will be irrotational we may again introduce a velocity potential $\phi(x, y)$ such that $\mathbf{U} = \nabla\phi$. The conservation of mass equation is

$$\nabla^2 \phi = 0\,. \tag{5.25}$$

Since the height of the liquid film is of $O(\varepsilon)$ we may introduce the following scalings:

$$\phi \;=\; \varepsilon^{\frac{1}{2}} v_\infty L \hat{\phi}\,, \tag{5.26}$$

$$x = L\hat{x}\,, \tag{5.27}$$

$$y = \varepsilon L\hat{y}\,, \tag{5.28}$$

which transforms equation (5.25) to

$$\hat{\phi}_{\hat{x}\hat{x}} + \frac{1}{\varepsilon^2}\hat{\phi}_{\hat{y}\hat{y}} = 0\,. \tag{5.29}$$

To $O(1)$ equation (5.29) becomes

$$\hat{\phi}_{\hat{y}\hat{y}} = 0\,. \tag{5.30}$$

The general solution to the equation (5.30) is

$$\hat{\phi}(\hat{x},\hat{y}) = A(\hat{x})\hat{y} + B(\hat{x})\,, \tag{5.31}$$

where $A(\hat{x})$ and $B(\hat{x})$ are arbitrary functions to be determined by the boundary conditions. The wall condition $\hat{\phi}_{\hat{y}}(\hat{x},0) = 0$ implies that $A(\hat{x}) = 0$ for all $\hat{x}$, which implies that $\hat{\phi}$ is only a function of $\hat{x}$ to $O(\varepsilon)$. Hence to order ε

$$u = u(x)\,, \tag{5.32}$$

and we note that the vertical velocity v is zero. The liquid film thins, and eventually disappears completely, because there is an interchange of mass between the liquid film and the gas core. In the current model, since the vertical velocity v is zero, mass is effectively transported from the liquid film via the horizontal velocity u. To determine the mass loss term, we note that the amount of liquid crossing the boundary of the liquid film between the positions x and $x + \delta x$ will be given by $s(x+\delta x)u(x+\delta x) - s(x)u(x)$. The equation for the conservation of mass for the liquid film may therefore be written

$$\rho_1 u(x)s(x) = \dot{m}(x)\,, \tag{5.33}$$

where $\dot{m}$ is a mass exchange term combining entrainment, deposition and vapourisation rates. The mass excahnge term is usually defined as the rate of change of mass per unit surface area. So strictly speaking the true mass exchange term is given by $\frac{d\dot{m}}{dx}$, but for furture calculations it is easier to work in terms of $\dot{m}$. Note that since $u = u(x)$ it satisfies the condition imposed by equation (5.32). For the remainder of this chapter, it will be tacitly assumed that $\dot{m}$ is a known function of x (determined, perhaps, from experimental measurements). In reality, of course, the mass exchange is likely to be a complicated function of s and other flow variables, including the temperature. In chapter 6, the difficult problem of formulating an independent model for $\dot{m}$ to close the system of equations is discussed.

To retain the thickness parameter ε explicitly in the equation we introduce the following scalings:

$$x = L\hat{x}\,, \tag{5.34}$$

$$y = \varepsilon L\hat{y}\,, \tag{5.35}$$

$$s(x) = \varepsilon L\hat{s}(\hat{x})\,, \tag{5.36}$$

$$\dot{m} = \epsilon^n \rho_1 u_\infty \hat{\dot{m}}(\hat{x})\,. \tag{5.37}$$

The parameter n has to be chosen such that $u^2 \sim O(\varepsilon)$. Applying these scalings to equation (5.33) we obtain

$$u = \varepsilon^{n-1} u_\infty \frac{\hat{\dot{m}}(\hat{x})}{\hat{s}(\hat{x})}\,. \tag{5.38}$$

This implies that $n = \frac{3}{2}$. The scaled velocity is thereby defined by

$$u = \varepsilon^{\frac{1}{2}} u_\infty \frac{\hat{\dot{m}}(\hat{x})}{\hat{s}(\hat{x})}\,. \tag{5.39}$$

Since the velocity does not depend on y the interfacial liquid velocity is defined by

$$u_i = \varepsilon^{\frac{1}{2}} u_\infty \frac{\hat{\dot{m}}(\hat{x})}{\hat{s}(\hat{x})}\,. \tag{5.40}$$

To calculate the pressure along the liquid/gas interface we must apply Bernoulli's equation

$$P_1 + \frac{1}{2}\rho_1 u^2 = h\,, \tag{5.41}$$

here h is the Bernoulli constant. On using equation (5.40) in the above equation we obtain

$$P_{1i} = h - \frac{1}{2}\varepsilon u_\infty^2 \rho_1 \frac{\hat{\dot{m}}(\hat{x})^2}{\hat{s}(\hat{x})^2}\,. \tag{5.42}$$

5.3.1 Equation of Free Surface

To calculate the velocities and pressures in the respective regions, we must first of all determine $s(x)$, the equation of the free surface between the liquid film and the gas phase. An equation for $s(x)$ can be formed by noting that

$$P_{1i} - P_{2i} = \frac{2\sigma}{R}\,, \tag{5.43}$$

where σ is the surface tension and R is the radius of curvature of the surface. We assume that the term $\frac{2\sigma}{R}$, suitably non-dimensionalised, is negligible. Since we are only considering terms up to $O(\varepsilon)$ equation (5.43) reduces to

$$P_{1i} - P_{2i} = 0\,. \tag{5.44}$$

Substituting for P_{1i} and P_{2i}, we have an equation for the free surface $\hat{s}(\hat{x})$:

$$h - \frac{1}{2}\varepsilon\rho_1 u_\infty^2 \frac{\hat{\dot{m}}(\hat{x})^2}{\hat{s}(\hat{x})^2} = P_\infty - \frac{1}{2}\rho_2 u_\infty^2 \left(\frac{2\varepsilon}{\pi} \fint_0^\infty \frac{\hat{s}'(t)}{\hat{x} - t}\, dt\right)\,. \tag{5.45}$$

If we define

$$h = P_\infty + \frac{1}{2}\varepsilon\rho_1 u_\infty^2 \hat{h}\,, \tag{5.46}$$

then equation (5.45) becomes

$$\hat{h} - \frac{\hat{\dot{m}}^2(\hat{x})}{\hat{s}^2(\hat{x})} = 2\frac{\rho_2}{\rho_1}\frac{1}{\pi} \fint_0^\infty \frac{\hat{s}'(t)}{t - \hat{x}}\, dt\,. \tag{5.47}$$

The above is a *nonlinear singular integro-differential equation* for the shape of the free surface that divides the liquid film and the gas core. As noted above, the equation is made even more complicated by the fact that an expression for the mass exchange between the gas core and the liquid film is required. The nonlinearity of the equation suggests that attempts to determine closed-form solutions for general mass exchange rates are likely to prove fruitless; additionally, it is not obvious what suitable boundary conditions are for the equation.

On physical grounds, it is evident that $\hat{s}(0) = 0$ since the film ceases to exist at the dryout point. A further approximation implicit in the derivation above is that the liquid film extends over a semi-infinite range; in view of the fact that the liquid film is extremely thin in the vicinity of the dryout point this is clearly valid.

5.4 Non-linear Singular Integro-differential Equations

The theory of linear first and second kind singular Fredholm integrals with Cauchy kernels dates back to the start of the century. More recently, singular integral equations have been investigated because of their use in linear elasticity, thin aerofoil theory and many other boundary value problems. Examples of such boundary value problems in the theory of linear elasticity can be found in Muskhelishvili (1953). It seems that there are very few theoretical results available concerning non-linear singular integral equations.

In general over recent years singular integral equations have received more attention then integro-differential equations, although Varley and Walker (1989) studied the linear integro-differential equation

$$u(x) = \frac{1}{\pi} \int\!\!\!\!\!\!- _0^\infty \frac{v(s)}{s - x}\, ds\,, \tag{5.48}$$

where both u and v were linear in the unknown function $S(x)$ and its derivatives. This type of integral equation often occurs when studying the motion of an interface between two incompressible fluids with different densities. Upstream, the fluids are separated by a semi-infinite plate and the interface starts at the trailing edge of the plate. Such problems are termed *dock* problems. Methods for such equations, however, rely largely on complex variable techniques that do not carry over to non-linear equations.

Nonlinear singular integro-differential equations similar to equation (5.47) also occur in the study of inviscid flows where the flow separates. Examples of such separated flows are given by Fitt, Ockendon and Jones (1985), in relation to the study of the aerodynamics of slot film cooling, and by O'Malley, Fitt et al. (1991), for high Reynolds number flow down a step.

There is a large amount of literature available concerning the numerical solution of linear integral equations. For example, Theocaris and Ioakimidis (1977) use Jacobi functions to approximate an integral equation by a system of linear equations. In general, there are no standard numerical techniques for the solution of non-linear singular integro-differential equations, and methods tend to be *ad hoc*. However Fitt (1994) has developed a numerical scheme, based on direct iteration, to solve the singular integro-differential equation

$$\frac{1}{\pi} \int\!\!\!\!\!\!- _A \frac{S'(t)}{t-x}\, dt = f(S(x))\,. \tag{5.49}$$

In Fitt's investigation of this equation he only considers functions $f(S(x))$, where x does not explicitly appear on the right hand side of the equation but only via $S(x)$. This is an extremely useful scheme since the equation (5.49) normally only admits closed-form solutions when f is a linear function of $S(x)$. For the case when f is non-linear numerical techniques must be used to determine $S(x)$. We shall explain

more about such numerical schemes in § 5.7.

5.5 Exact Solution for the Equation of the Free Surface

An exact solution to equation (5.47) can be found for the special case when the mass exchange rate is proportional to $\sqrt{x}$. Although physically this solution maybe of little relevance, it has the benefit of illustrating that at least one solution exists. This analytical solution could also be used for comparison with any numerical results obtained. For this particular form of the mass exchange rate (with a constant of proportionality of one) the shape of the free surface is obtained by solution of

$$h - \frac{x}{s(x)^2} = \lambda \fint_0^\infty \frac{s'(t)}{t-x}\, dt\,, \tag{5.50}$$

where λ is defined by

$$\lambda = 2\,\frac{\rho_2}{\rho_1 \pi}\,. \tag{5.51}$$

For ease of notation we have dropped the $\hat{}$ symbols from above the non-dimensional variables. To solve equation (5.50) we use properties of the eigenfunctions of the Hilbert transform on the semi-infinite interval. As quoted by Pipkin (1991), the eigenfunctions are of the form x^{-p}, where $0 < p < 1$, with respective eigenvalues $\pi \cot(p\pi)$. Hence the eigenfunctions satisfy the equation

$$\fint_0^\infty \frac{t^{-p}}{t-x}\, dt = \pi \cot(p\pi) x^{-p}\,. \tag{5.52}$$

In particular, $x^{-1/2}$ has the eigenvalue zero:

$$\fint_0^\infty \frac{t^{-1/2}}{t-x}\, dt = 0\,. \tag{5.53}$$

We therefore observe that there is a solution of equation (5.50) of the form $s(x) = A\,x^{1/2}$. Substituting the proposed form of solution into equation (5.50), and applying

equation (5.53), we obtain

$$h - \frac{1}{A^2} = 0\,. \tag{5.54}$$

This implies that the solution for the free surface between the liquid film and gas core when the mass exchange rate is $x^{1/2}$, is

$$s(x) = \sqrt{\frac{x}{h}}\,. \tag{5.55}$$

It should be noted that this solution has infinite slope at the dryout point and is unbounded for large x.

5.6 Asymptotic Analysis

Before considering the numerical solution of the equation for $s(x)$, we note that some progress may be made in determining the asymptotic solution for large and small values of x. In fact, it transpires that knowledge of the relevant asymptotic behaviour is essential if accurate numerical schemes are to be constructed. Suitable asymptotic methods may be illustrated by considering particular forms for the mass exchange term $\dot{m}(x)$.

5.6.1 Constant Mass Exchange Rate

We investigate the behaviour of the free surface asymptotically when the mass exchange rate is constant. Details of the asymptotic analysis, when the mass exchange is constant are given, since a similar analysis may be used to investigate situations where the mass exchange rate is a function of the variables involved. The integral

equation may be written

$$h - \frac{1}{s(x)^2} = \lambda \oint_0^\infty \frac{s'(t)}{t-x}\, dt\,, \tag{5.56}$$

where

$$\lambda = 2\frac{\rho_2}{\rho_1}\frac{1}{\pi}\,. \tag{5.57}$$

$\underline{x \to 0}$

If we assume that $s(x)$ is an algebraic function of x as $x \to 0$ then we may substitute $s(x) = Ax^n$ (where A is a constant) for small x into equation (5.56), giving

$$h - \frac{1}{A^2}x^{-2n} = \lambda \left(\oint_0^\delta \frac{Ant^{n-1}}{t-x} dt + \oint_\delta^\infty \frac{s'(t)}{t-x} dt \right)\,. \tag{5.58}$$

In the above equation δ and x satisfy the inequalities

$$0 < x \ll \delta \ll 1\,. \tag{5.59}$$

By substituting $t = ux$ into the first integral it is easily seen that to balance both sides of the equation we need to set $n = \frac{1}{3}$, yielding

$$-\frac{1}{A^2}x^{-\frac{2}{3}} = \lambda \left(\frac{1}{3}A \oint_0^\delta \frac{1}{t^{2/3}(t-x)} dt + \int_\delta^\infty \frac{s'(t)}{t} dt \right) + O(x)\,. \tag{5.60}$$

The first integral is a Cauchy principal value integral which needs to be expanded.

$$\oint_0^\delta \frac{1}{t^{2/3}(t-x)}\, dt = \lim_{\epsilon \to 0} \left(\int_0^{x-\epsilon} \frac{1}{t^{\frac{2}{3}}(t-x)} dt + \int_{x+\epsilon}^\delta \frac{1}{t^{\frac{2}{3}}(t-x)} dt \right) \tag{5.61}$$

$$= \lim_{\epsilon \to 0} \frac{1}{x^{2/3}} \log \mid -(x-\epsilon)^{1/3} + x^{1/3} \mid - \frac{1}{2x^{2/3}} \log \mid (x-\epsilon)^{2/3} + x^{1/3}(x-\epsilon)^{1/3} \mid$$

$$- \frac{\sqrt{3}}{x^{2/3}} \arctan \left(\frac{(x-\epsilon)^{1/3}\sqrt{3}}{2x^{2/3} + (x-\epsilon)^{1/3}} \right) + \frac{1}{x^{2/3}} \log \mid \delta^{1/3} - x^{1/3} \mid$$

$$- \frac{1}{2x^{2/3}} \log \mid \delta^{2/3} + x^{1/3}\delta^{1/3} + x^{2/3} \mid - \frac{\sqrt{3}}{x^{2/3}} \arctan \left(\frac{\delta^{1/3}\sqrt{3}}{2x^{1/3} + \delta^{1/3}} \right)$$

$$-\frac{1}{x^{2/3}}\log\mid -(x+\epsilon)^{1/3}+x^{1/3}\mid \frac{1}{2x^{2/3}}\log\mid (x+\epsilon)^{2/3}+x^{1/3}(x-\epsilon)^{1/3}+x^{2/3}\mid$$

$$\frac{\sqrt{3}}{x^{2/3}}\arctan\left(\frac{(x+\epsilon)^{1/3}\sqrt{3}}{2x^{1/3}+(x+\epsilon)^{1/3}}\right)$$

$$=\frac{1}{x^{2/3}}\log\left|\frac{x^{1/3}-\delta^{1/3}}{(\delta^{2/3}+x^{1/3}\delta^{1/3}x^{2/3})^{1/2}}\right|-\frac{\sqrt{3}}{x^{2/3}}\arctan\left(\frac{\delta^{1/3}\sqrt{3}}{2x^{1/3}+\delta^{1/3}}\right)$$

Expanding the above expression as a Taylor series in x,

$$⨍_0^{\delta}\frac{1}{t^{2/3}(t-x)}dt=-\frac{\sqrt{3}\pi}{3x^{2/3}}-\frac{3}{2\delta^{2/3}}+O(x). \tag{5.62}$$

Substituting this result into equation (5.60) gives

$$-\frac{1}{A^2}x^{-2/3}=\lambda\left(-\frac{\sqrt{3}A\,\pi}{9}x^{-2/3}-\frac{A}{2}\delta^{-2/3}+\int_{\delta}^{\infty}\frac{s'(t)}{t}dt\right)+O(x)\,. \tag{5.63}$$

To complete the asymptotic expansion we need to show that

$$\int_{\delta}^{\infty}\frac{s'(t)}{t}dt=\frac{A}{2}\delta^{-2/3}\,, \tag{5.64}$$

which can be achieved by studying the integral

$$⨍_0^{\infty}\frac{s'(t)-\frac{1}{3}t^{-2/3}}{t-x}\,dt. \tag{5.65}$$

Splitting the above integral, gives

$$⨍_0^{\infty}\frac{s'(t)-\frac{1}{3}t^{-2/3}}{t-x}\,dt=⨍_0^{\delta}\frac{s'(t)-\frac{1}{3}t^{-2/3}}{t-x}\,dt+⨍_{\delta}^{\infty}\frac{s'(t)-\frac{1}{3}t^{-2/3}}{t-x}\,dt$$

$$=0+⨍_{\delta}^{\infty}\frac{s'(t)-\frac{1}{3}t^{-2/3}}{t-x}\,dt\,.$$

Since $x\ll\delta$ we may expand the above integral as a Taylor series in x, giving

$$\int_{\delta}^{\infty}\frac{s'(t)-\frac{1}{3}t^{-2/3}}{t}dt+O(x)$$

Integrating by parts, it follows that the above integral equals

$$\frac{s(\delta)-\delta^{1/3}}{\delta}+\int_{\delta}^{\infty}\frac{s(t)-t^{1/3}}{t^2}\,dt\,.$$

Since δ is small we may use the asymptotic expansion for small x to evaluate $s(\delta)$. The above expression then reduces to

$$\int_{\delta}^{\infty}\frac{s(t)-t^{1/3}}{t^2}\,dt\,.$$

By continually expanding the above integral by parts, and using the asymptotic expansion, it is easily seen that the integral is zero. This then implies that

$$\int_{\delta}^{\infty}\frac{s'(t)-\frac{1}{3}t^{-2/3}}{t-x}\,dt=0\,,$$

which is equivalent to equation (5.64). Using this result equation (5.63) reduces to

$$-\frac{1}{A^2}x^{-2/3}=\frac{\sqrt{3}\,A\pi}{9}x^{-2/3}+O(x)\,. \tag{5.66}$$

By equating like terms we can determine the value of A. This leads to the following asymptotic expansion for equation (5.56), as $x\to 0$

$$s(x)\sim\sqrt{3}\left(\frac{x}{\lambda\pi}\right)^{1/3}. \tag{5.67}$$

This asymptotic expansion for small x is not too dissimilar from the solution for the interface when the mass exchange rate is equal to $\sqrt{x}$ since the slope at the dryout front is infinite. On physical grounds it might be expected that $\dot{m}(x)=1$ does not provide a very accurate estimate of the mass exchange.

<u>$x\to\infty$</u>

Some informal experimentation suggests that a suitable asymptotic form for $s(x)$ when x is large is given by

$$s(x)\sim A-B\frac{1}{x^n}-C\frac{\log(x)}{x^n}\,. \tag{5.68}$$

On substituting into equation (5.56) we obtain

$$h - \frac{1}{\left(A - Bx^{-n} - Cx^{-n}\log(x)\right)^2} = \tag{5.69}$$

$$\lambda\left(\fint_0^{\delta} \frac{s'(t)}{t-x}dt + \fint_{\delta}^{\infty} \frac{1}{t-x}\left(\frac{Bn}{t^{n+1}} - \frac{C}{t^{n+2}} + \frac{2Cn\log(t)}{t^{n+2}}\right)dt\right).$$

The integral has been split on the assumption that δ and x satisfy the inequality

$$1 \ll \delta \ll x\,. \tag{5.70}$$

Expanding equation (5.6.1) to lowest order terms in x as $x \to \infty$ we obtain

$$\left(h - \frac{1}{A^2}\right) - 2\frac{B}{A^3x^n} - \frac{2C\log(x)}{A^3x^{n+1}} + O(\frac{1}{x^{n+1}}) =$$

$$\lambda\left(-\frac{1}{x}\int_0^{\delta} s'(t)dt - \fint_{\delta}^{\infty} \frac{1}{t-x}\left(\frac{Bn}{t^{n+1}} - \frac{C}{t^{n+1}} + \frac{2Cn\log(t)}{t^{n+1}}\right)dt\right) + O(\frac{1}{x^2}).$$

To balance both sides of the equation we choose $A = \frac{1}{\sqrt{h}}$ (thus relating the final thickness of the fluid layer to the Bernoulli constants) and $n = 1$, in which case

$$-2\frac{Bh^{3/2}}{x} - \frac{2Ch^{3/2}\log(x)}{x^2} = \lambda\left(-\frac{s(\delta)}{x} - \fint_{\delta}^{\infty} \frac{1}{t-x}\left(\frac{B}{t^2} - \frac{C}{t^3} + \frac{2C\log(t)}{t^3}\right)dt\right). \tag{5.71}$$

Evaluating the Cauchy principal value integral and expanding the above expression we obtain

$$-\frac{2Bh^{3/2}}{x} - \frac{2Ch^{3/2}\log(x)}{x^2} = \lambda\left(-\frac{s(\delta)}{x} - \frac{B}{x\delta} - \frac{C\log(\delta)}{x\delta^2} - \frac{B\log(x)}{x^2}\right) + O(\frac{1}{x^2}). \tag{5.72}$$

Since $\delta \gg 1$ we may use the asymptotic expansion to evaluate $s(\delta)$ in the form

$$s(\delta) = \frac{1}{\sqrt{h}} - \frac{B}{\delta} - \frac{C\log(\delta)}{\delta^2}\,. \tag{5.73}$$

The above expression can then be substituted into equation (5.72) to give

$$-\frac{2Bh^{3/2}}{x} - \frac{2Ch^{3/2}\log(x)}{x^2} = -\lambda\left(\frac{1}{x} + \frac{B\log(x)}{x^2}\right). \tag{5.74}$$

For the above equation to balance we require $B = \frac{\lambda}{2h^{3/2}}$ and $C = \frac{\lambda^2}{4h^3}$. The leading order terms in the asymptotic expansion of equation (5.56) as $x \to \infty$ are then

$$s(x) \sim \frac{1}{\sqrt{h}} - \frac{\lambda}{2h^{3/2}x} - \frac{\lambda^2 \log(x)}{4h^3x^2}. \tag{5.75}$$

A key difference between the derived forms of the interface for the different mass exchange rates considered is that as x tends to infinity, $s(x)$ becomes infinite when $\dot{m}(x) = \sqrt{x}$, whilst when $\dot{m}(x) = 1$ $s(x)$ tends to a constant value.

5.6.2 General Mass Exchange Rate

By using similar techniques to the ones developed in the previous section we can formulate asymptotic solutions for some particular forms of $\dot{m}(x)$. If $\dot{m}(x) = x^m$ for $0 < m < 1$ then it can be shown that

$$s(x) \sim -\left(\frac{3\tan(\frac{2\pi}{3}(1-m))}{\lambda\pi(2m+1)}\right)^{\frac{1}{3}} x^{\frac{2m+1}{3}} \quad \text{as } x \to 0\,, \tag{5.76}$$

$$s(x) \sim \frac{x^m}{\sqrt{h}} \quad \text{as } x \to \infty\,. \tag{5.77}$$

The asymptotic formula as $x \to 0$ is valid only for values of m that satisfy $0 < m < 1/4$. For values outside this range the asymptotic formula becomes *unphysical* since $s(x) < 0$. There are no such restrictions upon the asymptotic formula as $x \to \infty$. Once again, it is seen that $s(x) \to \infty$ as x tends to infinity.

For $\dot{m}(x) = x^m$ with $m > 1$ we find that

$$s(x) \sim \frac{x^m}{\sqrt{h}} \quad \text{as } x \to 0\,. \tag{5.78}$$

It would appear from the forms of $\dot{m}(x)$ studied that in general $s(x)$ tends to infinity as $x \to \infty$, with $\dot{m} = 1$ being the exception.

Further examples of mass exchange rate can be constructed by using the formulae derived above. For example the mass exchange rate

$$\dot{m}(x) = \frac{\sqrt{x}}{1+\sqrt{x}}, \tag{5.79}$$

behaves like as $\sqrt{x}$ as x tends to zero and approaches 1 as x becomes large. Thus it is possible to construct other forms of $\dot{m}(x)$ that generate an interface $s(x)$ which tends to a constant as x tends to infinity. For practical purposes, some details of the function $\dot{m}(x)$ would be required in order to determine the values of ε and other such variables.

As far as the pressure is concerned, the asymptotic results that have been established above predict an infinite slope at the dryout point which corresponds to an infinite pressure. Clearly this is not physically realistic. Near to the dryout point, however, there will be a small region where the assumption that the aspect ratio is small will not be justified. Analysis of the flow within this 'inner' region would be necessary in order to make accurate pressure predictions. We do not consider this matter further, but simply note that the prediction of such infinite pressures is commonly encountered (see, for example, O'Malley et. al. (1991)) in simple separated flow models.

5.7 Numerical Solution

We will develop the general approach to solving the film equation numerically and then apply this approach to the case when $\dot{m} = 1$. The first step is to invert the integral equation so that we can then integrate with respect to x. We do this since the use of numerical differentiation can lead to inaccuracies. The inverted integral

equation is

$$s'(x) = \frac{C}{\sqrt{x}} + \frac{1}{\lambda\pi} \int_0^\infty \left(\frac{\dot{m}(t)^2}{s(t)^2} - h \right) \left(\frac{x}{t} \right)^{\pm 1/2} \frac{1}{t-x} dt. \tag{5.80}$$

For details of the inversion of the Hilbert transform on the semi-infinite interval see the Appendix B. C is an arbitrary constant that arises owing to the fact that the transformation does not possess a unique inverse. The value of C has to be calculated by using the asymptotic series developed for equation (5.45). The exact form of the kernel is also determined by the asymptotic solutions. If C is taken to be non-zero and the kernel taken to be $\sqrt{(t/x)}$ then $s(x)$ will become unbounded as x tends to infinity. Where as if C is zero and the kernel $\sqrt{(t/x)}$ then $s(x)$ will be bounded as x tends to infinity. So the value C really corosponds to weither $s(x)$ is bounded or unbounded as x tends to infinity. We illustrate the numerical scheme for $s(x)$ bounded as x tends to infinity when $C = 0$ and the kernel is

$$k(x,t) = \sqrt{\frac{t}{x}} \frac{1}{t-x}. \tag{5.81}$$

The numerical scheme for C non-zero could also be developed using a similar approach. The integral equation for $s(x)$ therefore becomes

$$s'(x) = \frac{1}{\lambda\pi} \int_0^\infty \left(\frac{\dot{m}(t)^2}{s(t)^2} - h \right) \left(\frac{t}{x} \right)^{1/2} \frac{1}{t-x} dt. \tag{5.82}$$

Integrating equation (5.82) with respect to x yields

$$s(x) = D + \frac{1}{\lambda\pi} \int_0^\infty \left(\frac{\dot{m}(t)^2}{s(t)^2} - h \right) \log \frac{\sqrt{t} + \sqrt{x}}{|\sqrt{t} - \sqrt{x}|} dt. \tag{5.83}$$

The parameter D is an arbitrary constant that is determined by the initial condition $s(0) = 0$, implying that $D = 0$.

Equation (5.83) is more suitable for numerical evaluation since it no longer contains a Cauchy principal value integral. Assuming that s is piecewise constant on the

intervals (ξ_k, ξ_{k+1}) we may write the equation in the discrete form

$$\lambda\pi s(x_i) \approx \int_0^{\xi_1} \left(\frac{\dot{m}(t)^2}{s(t)^2} - h\right) \log \frac{\sqrt{t}+\sqrt{x_i}}{|\sqrt{t}-\sqrt{x_i}|}\, dt \tag{5.84}$$

$$+ \sum_{k=1}^{N} \frac{1}{s(\xi_k)^2} \int_{\xi_k}^{\xi_{k+1}} \dot{m}(t)^2 \log \frac{\sqrt{t}+\sqrt{x_i}}{|\sqrt{t}-\sqrt{x_i}|}\, dt$$

$$-h\int_{\xi_1}^{\xi_{N+1}} \log \frac{\sqrt{t}+\sqrt{x_i}}{|\sqrt{t}-\sqrt{x_i}|} dt + \int_{\xi_{N+1}}^{\infty} \left(\frac{\dot{m}(t)^2}{s(t)^2} - h\right) \log \frac{\sqrt{t}+\sqrt{x_i}}{|\sqrt{t}-\sqrt{x_i}|}\, dt\,.$$

The first and last integrals above can be approximated by using the relevant asymptotic expansions. Numerical experiments have indicated that some form of relaxation is invariably required to ensure convergence of the scheme. Therefore we use the iterative numerical relaxation scheme

$$\lambda\pi \overline{s}_{j+1}(x_i) = A_{i1} + \sum_{k=1}^{N} s_j^{-2}\,(\xi_k)\, B_{ik} - hC_{iN} + D_{iN}\,, \tag{5.85}$$

$$s_{j+1}(x_i) = s_j(x_i) + \theta(\overline{s}_{j+1}(x_i) - s_j(x_i))\,, \tag{5.86}$$

$$(i = 1, ...N, j = 1, ...N)\,,$$

where

$$B_{ik} = \int_{\xi_k}^{\xi_{k+1}} \dot{m}(t)^2 \log \frac{\sqrt{t}+\sqrt{x_i}}{|\sqrt{t}-\sqrt{x_i}|} dt,$$

$$C_{iN} = (\xi_{N+1} - \xi_1) \log \frac{\xi_{N+1}^{1/2} + x_i^{1/2}}{|\,\xi_{N+1}^{1/2} - x_i^{1/2}\,|} - (\xi_1 - x_i) \log \frac{\xi_1^{1/2} + x_i^{1/2}}{|\,\xi_1^{1/2} - x_i^{1/2}\,|}\,.$$

The terms A_{iN} and D_{iN} are the approximations to the integrals for small and large t respectively, and the scheme is begun with an estimate for $s(x)$.

The same analysis could be performed on the integral equation if we had the inverted film equation with the kernel

$$k(x,y) = \sqrt{\frac{x}{t}} \frac{1}{t-x}\,. \tag{5.87}$$

The important point to recognise about our numerical scheme is that we need to know the asymptotic expansions of $s(x)$ as $x \to 0$ and as $x \to \infty$. Having the asymptotic expansion for large x allows us to truncate the integral at a finite value and then use the asymptotic expansion to estimate the remaining part of the integral. The asymptotic expansion as x tends to zero is required by virtue of the initial condition $s(0) = 0$ and the fact that terms of the form $1/s(x)$ appear in the scheme.

5.7.1 Application of Numerical Scheme to Constant Mass Exchange Rate

By using the previous asymptotic results for the film equation with $\dot{m} = 1$ it may easily be shown that the corresponding inverted equation is

$$s(x) = \frac{1}{\lambda\pi}\int_0^\infty \left(\frac{1}{s(x)^2} - h\right)\log\frac{\sqrt{t}+\sqrt{x}}{|\sqrt{t}-\sqrt{x}|}\,dt\,. \tag{5.88}$$

We may now apply the iterative relaxation scheme described in the previous section to obtain

$$\lambda\pi\overline{s}_{j+1}(x_i) = A_{i1} + \sum_{k=1}^{N} s_j^{-2}(\xi_k)B_{ik} - hC_{iN} + D_{iN}\,, \tag{5.89}$$

$$s_{j+1}(x_i) = s_j(x_i) + \theta(\overline{s}_{j+1}(x_i) - s_j(x_i))\,, \tag{5.90}$$

$$(i = 1,\ldots N, j = 1,\ldots N)\,,$$

$$A_{i1}\lambda^{-2/3} = \xi^{1/3}\log\frac{\sqrt{\xi_1}+\sqrt{x_i}}{|\sqrt{\xi_1}-\sqrt{x_i}|} - \frac{3}{2}x_i^{1/3}\log\frac{\xi_1^{1/6}+x_i^{1/6}}{|\xi_1^{1/6}-x_i^{1/6}|}$$

$$+\sqrt{3}x_i^{1/3}\left(\arctan\left(\frac{2\xi_1^{1/6}+x_i^{1/6}}{\sqrt{3}x_i^{1/6}}\right) - \arctan\left(\frac{-2\xi_1^{1/6}+x_i^{1/6}}{\sqrt{3}x_i^{1/6}}\right)\right)$$

$$B_{iN} = (\xi_{k+1}-\xi_k)\log\frac{\xi_{k+1}^{1/2}+x_i^{1/2}}{|\xi_{k+1}^{1/2}-x_i^{1/2}|} - (\xi_k - x_i)\log\frac{\xi_k^{1/2}+x_i^{1/2}}{|xi_k^{1/2}-x_i^{1/2}|}\,,$$

$$C_{iN} = (\xi_{N+1}-\xi_1)\log\frac{\xi_{N+1}^{1/2}+x_i^{1/2}}{|\xi_{N+1}^{1/2}-x_i^{1/2}|} - (\xi_1 - x_i)\log\frac{\xi_1^{1/2}+x_i^{1/2}}{|xi_1^{1/2}-x_i^{1/2}|}\,,$$

$$D_{iN} = \frac{4\lambda}{\pi}\left(\frac{x_i}{\xi_{N+1}}\right)^{1/2}.$$

When running the code an exponentially increasing mesh was used. The numerical results compare favourably with the asymptotic results. A plot of $s(x)$ and the asymptotic results is shown in figure (5.5). The sequence of solutions S_j converged rapidly for all initial guesses for $S_0(x)$ when the relaxation parameter θ was chosen to be less than 0.1. It was found that in general the closer the initial guess was to $\frac{1}{\sqrt{h}}$ then the better the convergence. The scheme was deemed to have converged when the L_∞ norm of the relative errors in successive iterates fell below 5×10^{-4}. The table in figure (5.2) shows the convergence of $S(1)$ given a range of initial guesses. In generating this table an exponential grid over the range $(0, 2)$ was used with the relaxation parameter equal to 0.1. For an initial guess $S_0(x) = 1$ with 100 node

Number of Iterations	Initial Guess S(1)=1	S(1)=2	S(1)=10
2	0.93272	1.53085	8.63425
10	0.94927	0.94050	1.77693
20	0.94942	0.94955	0.93092
40	0.94935	0.94935	0.94941
50	0.94935	0.94935	0.94935

Figure 5.2: Table showing convergence of S(1) given different initial guesses

points over the range $(0, 2)$ and an exponentially increasing grid, the solution was found to converge in 44, 78 and 268 iterations respectively, for relaxation parameters 0.1, 0.05 and 0.01. In addition to exponentially increasing grids we can also use a grid with constant step size. Exponential grids are usually preferred to equally spaced

meshes since they usually converge more rapidly and fewer mesh points are required to encompass large values of x.

Calculations were carried out with an equally spaced mesh using 20, 40, 80 and 100 mesh points, with associated step-lengths 0.2, 0.1, 0.05 and 0.04 respectively, so that the mesh stretched from 0 to 4. A relaxation parameter of 0.1 was applied and the number of iterations (NIT) required for convergence was recorded. The results from these calculations along with asymptotic values for large x are shown in figure 5.3. The numerical values even for 20 mesh points are encouraging and all the calculated values for large x compare favourably with the asymptotic values. It is interesting to note that the agreement with the asymptotic results becomes slightly *less* accurate as the number of mesh points increases; this may be attributed to mesh truncation effects. Further calculations were carried out with the same convergence criterion and initial approximation but using 40, 80 and 160 mesh points with step sizes 0.2, 0.1 and 0.05 respectively so that the mesh now stretched over (0,8). The results of these calculations are shown in figure 5.4. In contrast to the results of figure 5.3, the agreement with the asymptotic results is now improved as the number of points increases.

Plots of the variation of film the thickness are shown in figures (5.5) and (5.6). Evidently the numerical solution compares favourably with the asymptotic solutions for both large and small values of x.

x	20	40	80	100	*large* x
0.0	0.0	0.0	0.0	0.0	-
0.2	0.70009	0.87127	0.83057	0.82912	-
0.4	0.87478	0.89684	0.89331	0.89265	-
0.6	0.90972	0.92367	0.92205	0.92166	-
0.8	0.94641	0.93974	0.93868	0.93841	-
1.0	0.95065	0.95026	0.94951	0.94932	0.94695
1.2	0.95913	0.95768	0.95712	0.95700	0.95543
1.4	0.96413	0.96318	0.96275	0.96264	0.96163
1.6	0.96832	0.96741	0.96708	0.96699	0.96632
1.8	0.97158	0.97077	0.97051	0.97043	0.97002
2.0	0.97426	0.97350	0.97328	0.97322	0.97298
2.2	0.97647	0.97575	0.97557	0.97552	0.97543
2.4	0.97833	0.97764	0.97749	0.97541	0.97747
2.6	0.97991	0.97925	0.97912	0.97908	0.97920
2.8	0.98126	0.98063	0.98052	0.98048	0.98068
3.0	0.98242	0.98182	0.98172	0.98168	0.98198
3.2	0.98342	0.98284	0.98275	0.98272	0.98310
3.4	0.98429	0.98372	0.98363	0.98360	0.98410
3.6	0.98500	0.98445	0.98435	0.98431	0.98498
3.8	0.98554	0.98499	0.98486	0.98480	0.98578
4.0	0.98586	0.98542	0.98616	0.98684	0.98650
NITS	110	65	55	53	

Figure 5.3: Table of convergences for different step sizes over the range (0,4)

x	40	80	160	*large* x
0.0	0.0	0.0	0.0	-
0.2	0.70083	0.86373	0.83061	-
0.4	0.86807	0.89652	0.89356	-
0.6	0.91581	0.92390	0.92229	-
0.8	0.94289	0.93995	0.93890	-
1.0	0.95157	0.95049	0.94974	0.94695
1.2	0.95878	0.95793	0.95737	0.95543
1.4	0.96490	0.96345	0.96302	0.96163
1.6	0.96822	0.96771	0.96737	0.96632
1.8	0.97450	0.97109	0.97081	0.97002
2.0	0.97417	0.97384	0.97361	0.97298
2.2	0.97639	0.97612	0.97592	0.97543
2.4	0.97827	0.97803	0.97787	0.97747
2.6	0.97987	0.97967	0.97952	0.97920
2.8	0.98125	0.98108	0.98095	0.98068
3.0	0.98245	0.98230	0.98219	0.98198
3.2	0.98351	0.98338	0.98328	0.98310
3.4	0.98445	0.98434	0.98425	0.98410
3.6	0.98529	0.98519	0.98511	0.98498
3.8	0.98604	0.98595	0.98588	0.98578
4.0	0.98672	0.98664	0.98657	0.98650
NITS	55	53	51	

Figure 5.4: Table of convergences for different step sizes over the range (0,8)

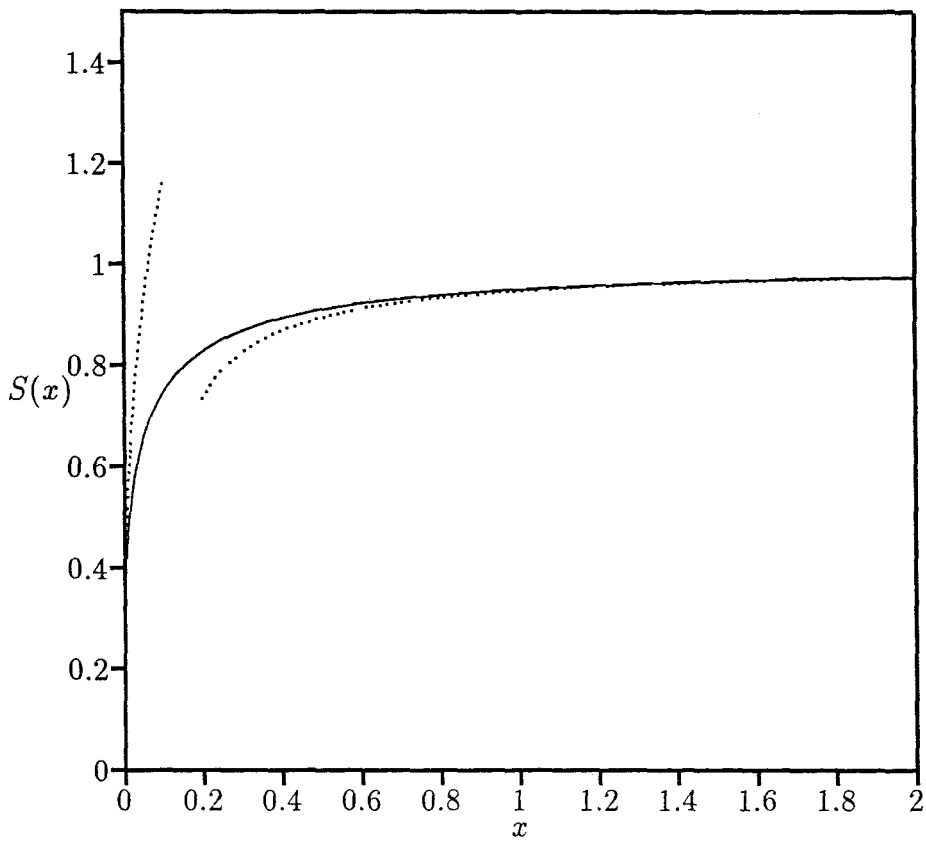

Figure 5.5: Variation of film thickness along the heated surface

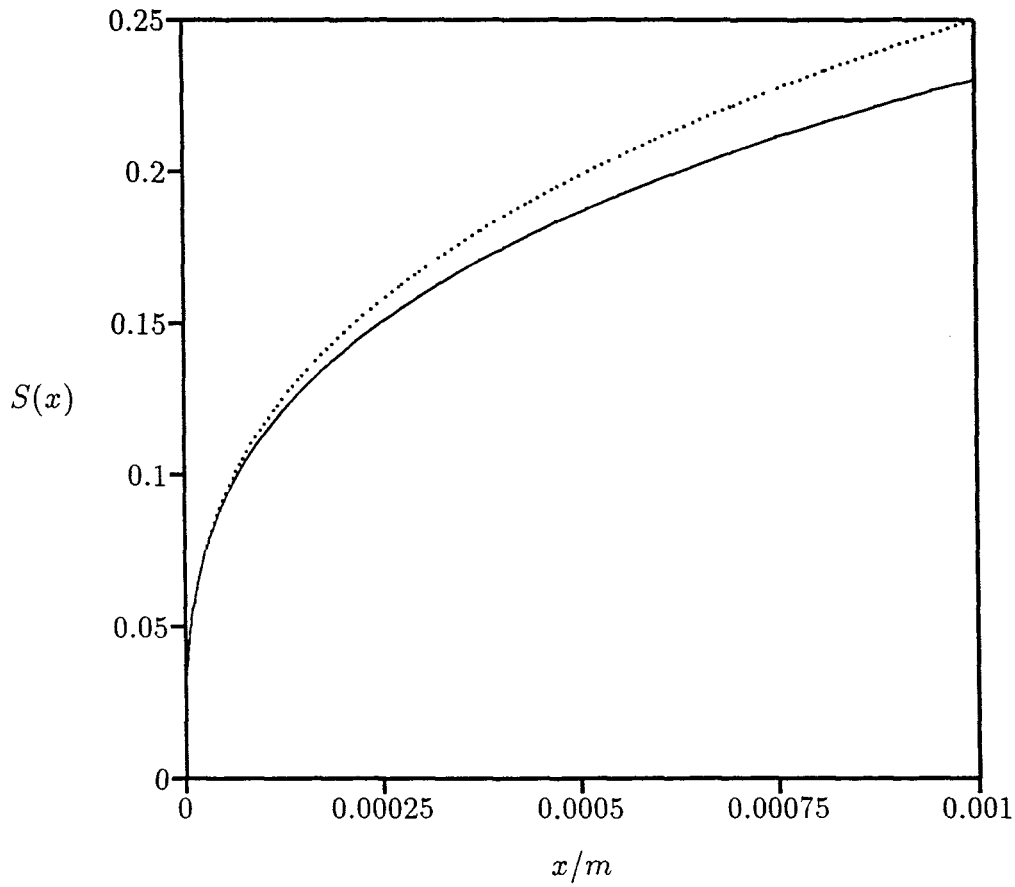

Figure 5.6: Comparison of variation of film thickness along heated surface with asymptotic approximation for small x

Chapter 6

INVESTIGATION OF MASS EXCHANGE RATE

It was noted in the previous chapter that, in order to close the model for the liquid film region properly, the dependence of the mass exchange rate needs to be *determined* in terms of $s(x)$ and the other flow quantities. The mass exchange between the film and the gas core is due to entrainment, deposition and evaporation; in the work presented below, we consider only the evaporation as it is clearly the dominant mechanism. Heat is conducted from the channel wall to the liquid film. Bubbles of steam are produced at nucleation sites along the channel wall. In reality the bubbles would then rise up through the film and join the gas core. To indicate how a model could be proposed for the mass exchange rate, we will make a number of approximations. In particular, we will assume that the steam produced at the nucleation sites appears 'instantaneously' in the gas core. This is a reasonable approximation to make since the film is thin and the time taken for the bubble to pass through the film would be very short. Since the film is inviscid any mixture effects due to the bubble rising up through the film are also neglected.

In the model presented in the previous chapter, the vertical velocity v was found to be zero to lowest order (§ 5.3). In the model described below for the temperature in the film, the assumption that the evaporation occurs at the wall means that the streamlines cannot be horizontal; therefore the vertical velocity will not be zero. Physically, the vertical velocity acts to replace the fluid that has been evaporated at

the wall. We still assume, however, that u is given by (§ 5.3).

6.1 Temperature Distribution Within the Film

Assuming that the flow is steady, the equations governing the flow of heat within the film are

$$\rho c_p \left(u \frac{\partial T}{\partial x} + v \frac{\partial T}{\partial y} \right) = k \left(\frac{\partial^2 T}{\partial x^2} + \frac{\partial^2 T}{\partial y^2} \right) , \tag{6.1}$$

where, in this chapter, k denotes the thermal conductivity of the liquid layer. This equation must be solved in the liquid layer and the problem is thus of free boundary type since we do not know the position of the liquid/gas interface. We therefore require enough boundary conditions to specify the solution completely. Since the thermal conductivity of steam is far less than the thermal conductivity of water there will be negligible heat loss from the liquid film to the gas core. This boundary condition is represented by the equation

$$k \frac{\partial T}{\partial n} = 0 \quad \text{on } y = s(x) , \tag{6.2}$$

where $\frac{\partial}{\partial n}$ denotes differentiation in the direction of the outward normal to the interface. Expanding equation (6.2) in terms of $s(x)$ and the derivatives of T we obtain

$$- s'(x) \frac{\partial T}{\partial x} + \frac{\partial T}{\partial y} = 0 . \tag{6.3}$$

Consider now the boundary conditions on the channel wall. As explained previously we are modelling the evaporation of the liquid film by assuming that the phase change occurs at the wall. Because of the fact that water is being evaporated at the wall, the liquid film must move towards the wall to replace the water that has been evaporated. The boundary condition at the wall is therefore

$$- k \frac{\partial T}{\partial y} = q - \rho \lambda v. \tag{6.4}$$

Here q is the heat flux through the wall, ρ the density of water, and λ the latent heat of vaporisation of water. The other boundary condition on the wall is that the water along the film/wall interface is at its saturation temperature.

$$T = T_s \quad \text{on } y = 0\,. \tag{6.5}$$

Our final boundary condition is based on the fact that the fluid entering the annular flow regime is at a temperature that is close to, but below the saturation temperature. Denoting this temperature by T_0 we have

$$T = T_0 \quad \text{at } x = L\,, \tag{6.6}$$

where L denotes the point at which the upstream measurements are made. For clarity we list the equations and boundary conditions together.

$$\rho\, c_p\, (u\, T_x + v\, T_y) = k\, (T_{xx} + T_{yy})\,, \tag{6.7}$$

$$-\, s'(x)\, T_x + T_y = 0 \quad \text{on } y = s(x)\,, \tag{6.8}$$

$$T = T_s \quad \text{on } y = 0\,, \tag{6.9}$$

$$-\, k\, T_y = q - \rho\, \lambda\, v \quad \text{on } y = 0\,, \tag{6.10}$$

$$T = T_0 \quad \text{at } x = L\,. \tag{6.11}$$

The thermodynamical problem for the liquid film is displayed in figure 6.1.

6.1.1 Simplified Analysis of Mass Exchange Rate

To make progress with the previous equations we need to non-dimensionalize and scale to exploit the fact that the film is thin compared to the channel diameter. The scaled variables are therefore

$$T = T_s\, (1 + \varepsilon^{\tau} \theta)\,,$$

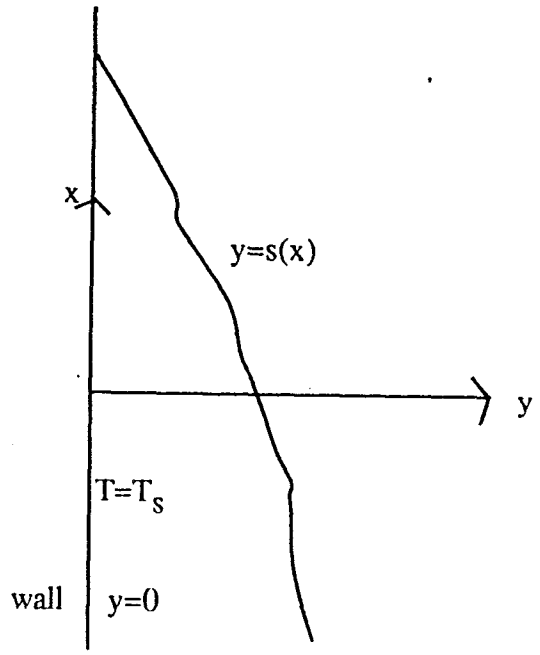

Figure 6.1: Schematic diagram of evaporation of the liquid film

$$y = \varepsilon L Y ,$$

$$x = L X ,$$

$$s(x) = \varepsilon L S(X) ,$$

$$v = \varepsilon^{3/2} u_\infty V ,$$

$$u = \varepsilon^{1/2} u_\infty U .$$

The scalings have been chosen such that they are consistent with the scalings used previously when modelling the film flow. The scaled equations are therefore

$$\varepsilon^{1/2} \left(U \theta_X + V \theta_Y \right) = \frac{1}{Pe} \left(\theta_{XX} + \frac{1}{\varepsilon^2} \theta_{YY} \right) , \tag{6.12}$$

$$\varepsilon^{3/2} S'(X) T_X + \frac{1}{\varepsilon} T_Y = 0 \text{ on } Y = S(X), \tag{6.13}$$

$$\theta = 0 \text{ on } Y = 0, \tag{6.14}$$

$$\varepsilon^{r-1} \theta_Y = -q^* + Pe \left(\frac{\lambda}{c_p T_s} \right) \varepsilon^{3/2} V \text{ on } Y = 0, \tag{6.15}$$

$$\theta = \theta_0 = \frac{1}{\varepsilon^2} \frac{T_0 - T_s}{T_s} \text{ at } X = 1. \tag{6.16}$$

As in the previous set of equations Pe is the Peclet number and q^* the non-dimensional heat flux, which are defined by respectively

$$Pe = \frac{\rho c_p L u_\infty}{k}, \tag{6.17}$$

$$q^* = \frac{q L}{k T_s}. \tag{6.18}$$

For this particular problem the Peclet number has a typical value of 6×10^6 and q^* a value of 10. The non-dimensional number $\frac{\lambda}{c_p T_s}$ has a value of 4.6×10^{-2}. A possible balance for equation (6.12) is

$$\varepsilon^{1/2} \sim \frac{1}{Pe\, \varepsilon^2}. \tag{6.19}$$

This implies that $\varepsilon \sim 0.002$ and gives us an estimation for the thickness parameter from a thermodynamic argument. Using this balance also implies that $r = 1$. To lowest order our system of equations is now

$$U \theta_X + V \theta_Y = \theta_{YY}, \tag{6.20}$$

$$\theta_Y = 0 \text{ on } Y = S(X), \tag{6.21}$$

$$\theta = 0 \text{ on } Y = 0, \tag{6.22}$$

$$\theta_Y = -q^* + \alpha V \text{ on } Y = 0, \tag{6.23}$$

$$\theta = \theta_0 \text{ at } X = 1. \tag{6.24}$$

6.1.2 Simplification of Velocity

In our previous analysis of the film we calculated that, to lowest order, the component parallel to the pipe wall of the velocity, u, was only a function of x. This allows us to integrate the continuity equation for the fluid with respect to Y to obtain

$$V = C(X) - U_X\, Y\,, \tag{6.25}$$

where $C(X)$ is an arbitrary function of X. In contrast to the model of the previous chapter, $Y = S(X)$ is now a streamline of the flow. Applying the standard kinematic boundary condition leads to

$$V(X,Y) = (U(X)\, S(X))' - U'(X)\, Y\,. \tag{6.26}$$

Equation (6.26) can now be used to simplify the equations (6.20)-(6.24) to obtain

$$U\,\theta_X + \left[(U\,S)' - U'\,Y\right]\theta_Y = \theta_{YY}\,, \tag{6.27}$$

$$\theta_Y = 0 \ \text{ on } Y = S(X)\,, \tag{6.28}$$

$$\theta = 0 \ \text{ on } Y = 0\,, \tag{6.29}$$

$$\theta_Y = -q^* + \alpha\,(U\,S)' \ \text{ on } Y = 0\,, \tag{6.30}$$

$$\theta = \theta_0 \ \text{ at } X = 1\,. \tag{6.31}$$

Equation (6.27) can be simplified considerably by a change of independent variable. Consider the change of variable

$$\theta = \theta(X,\eta)\,, \tag{6.32}$$

where

$$\eta = \eta(X,Y)\,. \tag{6.33}$$

Substitution of the above into equation (6.27) gives

$$U\,\theta_X + U\,\theta_\eta\,\eta_X + \left[(U\,S)' - U'\,Y\right]\,\theta_\eta\,\eta_Y = \theta_{\eta\eta}\,\eta_Y^2 + \theta_\eta\,\eta_{YY}\,, \tag{6.34}$$

and rearranging this and collecting like terms yields

$$U\,\theta_X + \left[U\,\eta_X + \left((U\,S)' - U'\,Y\right)\,\eta_Y\right]\,\theta_\eta = \theta_{\eta\eta}\,\eta_Y^2 + \theta_\eta\,\eta_{YY}\,. \tag{6.35}$$

We now choose $\eta\,(X,Y)$ such that it satisfies the relation

$$U\,\eta_X + \left[(U\,S)' - U'\,Y\right]\,\eta_Y = 0\,. \tag{6.36}$$

We look for a solution of the form

$$\eta\,(X,Y) = A(X)\,Y + B(X)\,. \tag{6.37}$$

Substitution of the above into equation (6.36) yields

$$U\,\left(A'\,Y + B'\right) + \left[(U\,S)' - U'\,Y\right]\,A = 0\,. \tag{6.38}$$

The constraints on A and B for the above equation to be satisfied are

$$U\,A' - U'\,A = 0\,, \tag{6.39}$$

$$U\,B' + (U\,S)'\,A = 0\,. \tag{6.40}$$

A suitable choice of $\eta\,(X,Y)$ is therefore

$$\eta\,(X,Y) = U\,(S - Y)\,. \tag{6.41}$$

This reduces the problem to:

$$\theta_X = U\,\theta_{\eta\eta}\,, \tag{6.42}$$

$$\theta_\eta = 0 \;\text{ on }\; \eta = 0\,, \tag{6.43}$$

$$\theta = 0 \text{ on } \eta = U\,S\,, \tag{6.44}$$

$$U\,\theta_\eta = q^* - \alpha\,(U\,S)' \text{ on } \eta = U\,S\,, \tag{6.45}$$

$$\theta = \theta_0 \text{ at } X = 1\,. \tag{6.46}$$

In the previous analysis for the equation of the free surface we defined the non-dimensional mass exchange rate by

$$\dot{m}(X) = U\,S(X)\,. \tag{6.47}$$

This notation allows us to construct the thermodynamic problem for the liquid film in terms of the mass exchange rate and the free surface function. The thermodynamic problem is therefore:

$$\theta_X = \frac{\dot{m}(X)}{S(X)}\,\theta_{\eta\eta}\,, \tag{6.48}$$

$$\theta_\eta = 0 \text{ on } \eta = 0\,, \tag{6.49}$$

$$\theta = 0 \text{ on } \eta = \dot{m}(X)\,, \tag{6.50}$$

$$\frac{\dot{m}(X)}{s(X)}\,\theta_\eta = q^* - \alpha\,(\dot{m}(X))' \text{ on } \eta = \dot{m}(X)\,, \tag{6.51}$$

$$\theta = \theta_0 \text{ at } X = 1\,. \tag{6.52}$$

This seems to be the simplest form in which the free boundary problem may be written; if equation (6.48) could be solved subject to the boundary conditions (6.49), (6.50) and (6.52) then the extra condition (6.51) would presumably determine $\dot{m}$ in terms of S. We note, however, that in contrast to many other problems of this type the 'extra' condition is applied not on the free boundary but on the pipe wall. This is a consequence of the form of the flow streamlines.

In general, of course, the submodel for the determination of $\dot{m}$ that has been presented above constitutes a complicated free boundary problem which would require a numerical solution. It seems unlikely that any progress can be made in proving

existence and uniqueness for general $\dot{m}$ and S, but we note that there is one special case in which some progress may be made.

6.1.3 Special Case: Upstream Liquid at Saturation Temperature

Consider now the case where θ_0 is zero. Physically, this corresponds to the fact that all of the incoming fluid is already at saturation temperature. The solution of the thermodynamic problem is therefore trivial and is given by $\theta = 0$. To satisfy the complete problem it thus only remains to satisfy

$$q = \alpha(\dot{m})' .$$

If q is a given function of x, then a simple integration immediately gives $\dot{m}$ and therefore η. We now solve the non-linear singular integro-differential equation of the previous chapter to determine S and finally use the relationship $US = \dot{m}$ to find U. Although physically this case is not very realistic, it can be regarded as corresponding to the case where the θ_η term in (6.51) is small. In any case, it does at least have the virtue of showing that, in this simple case, the problem possesses a sensible solution.

Chapter 7

CONCLUSIONS AND POSSIBLE FUTURE WORK

From our analysis we have been able to make predictions of the lengths of the subcooled and bubbly flow regimes and also of the pressure drop across the bubbly flow regime. Although a detailed comparison with experiment has not been carried out (mainly owing to the lack of suitable experimental results) it is clear that the predictions are generally in agreement with the few experimental results that are available. Using asymptotic techniques we have developed simple formulae for predicting the length of the subcooled regime. By considering a set of one dimensional averaged two phase flow equations for the bubbly flow regime we have been able to relate such quantities as gas velocity to the void fraction.

These results have a number of practical uses; first, they may enable estimates to be made of flow regime size in large and small scale experiments. Also, they increase the physical understanding of how the different flow regimes interact in a LMBFR.

From the analysis of the lengths of the flow regimes we were able to confirm that the annular flow regime is the dominant flow regime in length, a fact that is once again in agreement with experimental evidence. The annular flow regime is the most important region since it is the region in which dryout occurs. Modelling the annular flow regime is complicated by the fact that there is an exchange of mass between the liquid film and gas core. We have developed a model to predict the position of the

interface between the liquid film and the gas core. This model describes both the fluid flow in the liquid layer near to the pipe wall and the thermal problem in the fluid layer. The shape of the interface between the liquid and gas phase within the annular flow regime is governed by a non-linear singular integro-differential equation. Progress has been made in solving this equation both asymptotically and numerically for various mass exchange rates.

All the analysis that has been carried out has been for the steady flow of water and steam in a steam generating pipe. An extension to the work would be to consider related unsteady problems. This would involve investigating the hyperbolicity of the unsteady system of equations for bubbly flow. Because of the large number of variables involved this would require the assistance of a symbolic manipulator package. The model for the dryout front could also be extended to encompass the case of unsteady flow. This would allow analysis of a case that is of particular physical significance, namely the oscillations in dryout front position that have sometimes been observed in boiler pipes. The main results of such analysis would be predictions of the speed of the dryout front and its sensitivity to changes in conditions at the entrance to the boiler pipe. Another extension to the modelling of the annular flow regime would be to consider the axially symmetric problem.

Future work will involve an investigation of the behaviour at the interface between the gas and the liquid as $x \longrightarrow 0$ since near the dryout point the assumption that the aspect ratio is small is no longer justified. To do this it will be necessary to consider the 'inner' solution at the dryout point and asymptotically match this to the 'outer' solution obtained in chapter 5. The indications are, however, that this may be a formidable problem.

Appendix A

PHYSICAL PARAMETERS

A.1 Subcooled Flow Regime

$T_0 = 240\ °C$

$q = 595\ Kw/m^2$

$\rho = 800\ Kg/m^3$

$\omega = 2.0\ m/s$

$K = 6.39 \times 10^{-4}\ Kw/mK$

$a = 7 \times 10^{-3}\ m$

A.2 Bubbly Flow Regime

$T_s = 365.0\ °C$

$p_s = 200.0\ Bar$

$q = 595.0\ Kw/m^2$

$\rho_1 = 600.0\ Kg/m^3$

$\rho_{2s} = 110.0\ Kg/m^3$

$v_0 = 2.0\ m/s$

$L = 6.0\ m$

$a = 7 \times 10^{-3}\ m$

$g = 9.81\ \ m/s^2$

c_{p1}= $21.044 KJ/KG°C$

c_{p2}= $20.125 KJ/KG°C$

R_0= $8.3143\ KJ/mol°C$

$\lambda = 587.1\ KJ/Kg$

A.3 Annular Flow Regime

$\rho_1 = 600\ Kg/m^3$

$\rho_2 = 110\ Kg/m^3$

$\lambda = 587.1\ KJ/Kg$

Appendix B

INVERSION OF THE HILBERT TRANSFORM ON THE SEMI-INFINITE INTERVAL

The Hilbert transform of a function $\phi(x)$ on the semi-infinite strip is defined by

$$\mathcal{H}[\phi(x)] = \barint_0^\infty \frac{\phi(t)}{t-x}\,dt\,, \tag{B.1}$$

where the *bar* through the integral sign indicates that it is a *Cauchy principal value integral.* A Cauchy principal value integral on the interval (a,b) is defined as

$$\barint_a^b \frac{\phi(t)}{t-x}\,dt = \lim_{\epsilon\to 0}\left(\int_a^{x-\epsilon}\frac{\phi(t)}{t-x}\,dt + \int_{x+\epsilon}^b \frac{\phi(t)}{t-x}dt\right)\,. \tag{B.2}$$

The inversion of the Hilbert transform on a semi-infinite interval can be achieved by the application of Fourier transforms. Before doing so we shall briefly outline the relevant properties of the Fourier transform.

The Fourier transform and its inverse on the infinite strip are defined respectively by

$$\mathcal{F}(\psi) = \frac{1}{\sqrt{2\pi}}\int_{-\infty}^{\infty} e^{\imath sx}\psi(x)\,dx\,, \tag{B.3}$$

$$\mathcal{F}^*(\psi) = \frac{1}{\sqrt{2\pi}}\int_{-\infty}^{\infty} e^{-\imath sx}\psi(x)\,dx\,. \tag{B.4}$$

For the Fourier transform of $\psi(x)$ to exist the integral of $|\psi(x)|$ over the range $(-\infty,\infty)$ needs to be finite. If $f(x)$ and $g(x)$ are two functions in $L_2[-\infty,\infty]$ then

the convolution of $f(x)$ and $g(x)$ is defined to be

$$(f * g)(x) = \int_{-\infty}^{\infty} f(y)g(x-y)\,dy\,. \tag{B.5}$$

Two important properties of the convolution are

1. $(f * g)(x) = (g * f)(x)$

2. $\mathcal{F}(f * g) = \sqrt{2\pi}\mathcal{F}(f)\mathcal{F}(g)$

We now have enough information about Fourier transforms and the convolution theorem to be able to invert the integral equation

$$\frac{1}{\pi} \int_0^{\infty} \frac{\phi(t)}{x-t}\,dt = f(x)\,. \tag{B.6}$$

To be able to take the Fourier transform of equation (B.6) we first need to change the variables so that the integral is taken over the range $(-\infty, \infty)$. This is achieved by the using the following change in variables

$$x = e^{2\xi}\,, \tag{B.7}$$

$$t = e^{2\eta}\,. \tag{B.8}$$

Upon introduction of the new variables (B.7) and (B.8) equation (B.6) becomes

$$\frac{1}{\pi} \int_{-\infty}^{\infty} \frac{\phi(e^{2\eta})2e^{2\eta}}{e^{2\xi} - e^{2\eta}}\,d\eta = f(e^{2\xi})\,. \tag{B.9}$$

To simplify equation (B.9) we redefine the dependent variables as

$$\psi(\eta) = \phi(e^{2\eta})e^{\eta}\,, \tag{B.10}$$

$$g(\xi) = f(e^{2\xi})e^{\xi}\,. \tag{B.11}$$

Upon further algebraic manipulation, equation (B.9), in terms of the new dependent variables ψ and g, becomes

$$\frac{1}{\pi} \int_{-\infty}^{\infty} \frac{\psi(\eta)}{\sinh(\xi - \eta)} d\eta = g(\xi) . \tag{B.12}$$

Application of the Fourier transform to equation (B.12) yields

$$\frac{\sqrt{2\pi}}{\pi} \mathcal{F}(\psi) \mathcal{F}\left(\frac{1}{\sinh(\eta)}\right) = \mathcal{F}(g). \tag{B.13}$$

To proceed further we need to expand the Fourier transform

$$\mathcal{F}\left(\frac{1}{\sinh(\eta)}\right) = \int_{-\infty}^{\infty} \frac{e^{is\eta}}{\sinh \eta} d\eta ,$$

and this can be accomplished by integrating the complex function

$$F(z) = \frac{e^{isz}}{\sinh z} , \tag{B.14}$$

around the closed contour depicted in figure B. Integrating around the contour we obtain

$$\int_{\gamma} F(z)\, dz = \int_{-R}^{-\rho} F(x)\, dx - \int_{\Gamma_\rho} F(z)\, dz + \int_{\rho}^{R} F(x)\, dx + \int_{\Gamma_R} F(z)\, dz \tag{B.15}$$

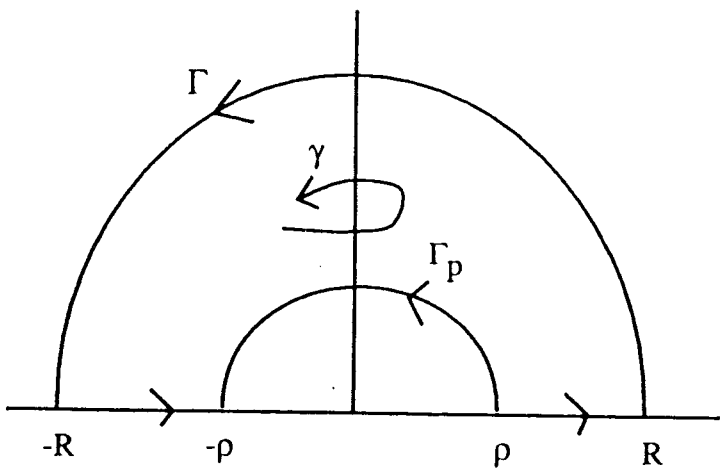

Figure B.1: Contour of integration

In the limit as $\rho \to 0$

$$\int_{\Gamma_\rho} F(z)\,dz = Re_0 \imath(\pi - 0) = \pi\imath\,, \tag{B.16}$$

where Re_0 is the residue at $z = 0$. To evaluate the integral of $F(z)$ over the contour Γ we apply Jordan's lemma. Jordan's lemma (Chillingworth 1972) states:

> Let $f(z)$ be meromorphic in the upper half-plane and let $f(z)$ approach zero uniformly for all θ in $0 < \theta < \pi$ as $|z|$ approaches infinity. Then, for all $m > 0$,
>
> $$\int_{\Gamma_R} e^{\imath m z} f(z)\,dz \to 0, \tag{B.17}$$
>
> where Γ is the upper semi-circle $|z| = R$.

A function whose only singularities in a domain D are poles is said to be meromorphic in D.

The poles of $f(z)$ are all of order 1 and are given by solving

$$\sinh(z) = 0\,. \tag{B.18}$$

The roots of the above are trivial to find and can be expressed

$$z = n\pi\imath \quad , n = 1, 2, \ldots\,. \tag{B.19}$$

and the residue at each pole is given by

$$\begin{aligned} Re_n &= \lim_{z \to n\pi\imath} \frac{(z - n\pi\imath)e^{\imath s z}}{\sinh(z)} && \text{(B.20)} \\ &= \lim_{z \to n\pi\imath} \frac{e^{\imath s z}}{\cosh(z)} && \text{(B.21)} \\ &= (-1)^n e^{-sn\pi}\,. && \text{(B.22)} \end{aligned}$$

Thus the integral of $F(z)$ over γ is equal to the sum of the residues given by equation (B.22), ie

$$\int_\gamma F(z)\,dz = 2\pi\imath \sum_{n=1}^{\infty}(-1)^n e^{-sn\pi}. \tag{B.23}$$

Here, as $\rho \to 0$ and $R \to \infty$ equation(B.15) reduces to

$$\int_{-\infty}^{\infty} \frac{e^{\imath s\eta}}{\sinh(\eta)}\,d\eta = 2\pi i\left(\frac{1}{2} + \sum_{n=1}^{\infty}(-1)^n e^{-sn\pi}\right). \tag{B.24}$$

This can be simplified further by noting that

$$\begin{aligned}
\frac{1}{2} + \sum_{1}^{\infty}(-1)^n e^{-sn\pi} &= -\frac{1}{2} + \sum_{0}^{\infty}(-1)^n e^{-sn\pi} && \text{(B.25)}\\
&= -\frac{1}{2} + \frac{1}{1+e^{-s\pi}} && \text{(B.26)}\\
&= \frac{1-e^{-s\pi}}{2\,(1+e^{-s\pi})} && \text{(B.27)}\\
&= \frac{1}{2}\tanh\left(\frac{s\pi}{2}\right). && \text{(B.28)}
\end{aligned}$$

So equation (B.24) reduces to

$$\int_{-\infty}^{\infty} \frac{e^{\imath s\eta}}{\sinh\eta}\,d\eta = \pi\imath \tanh\left(\frac{s\pi}{2}\right). \tag{B.29}$$

Substituting the above result into equation (B.13) leads to

$$\mathcal{F}(\psi) = \frac{1}{\imath\pi}\frac{\cosh\left(\frac{s\pi}{2}\right)}{\sinh\left(\frac{s\pi}{2}\right)}\mathcal{F}(g), \tag{B.30}$$

and applying the inverse Fourier transform then gives

$$\psi(\xi) = C + \frac{1}{2\imath\pi}\int_{-\infty}^{\infty} g(\xi-\eta)d\eta \int_{-\infty}^{\infty} e^{-\imath s\eta}\frac{\cosh\left(\frac{\pi s}{2}\right)}{\sinh\left(\frac{\pi s}{2}\right)}\,ds. \tag{B.31}$$

To simplify the above we need to evaluate the integral

$$\int_{-\infty}^{\infty} e^{-\imath s\eta}\frac{\cosh\left(\frac{\pi s}{2}\right)}{\sinh\left(\frac{\pi s}{2}\right)}\,ds. \tag{B.32}$$

By substituting $s = -t$ the above integral becomes

$$-\int_{-\infty}^{\infty} e^{it\eta} \frac{\cosh\left(\frac{\pi t}{2}\right)}{\sinh\left(\frac{\pi t}{2}\right)} ds\,. \tag{B.33}$$

This integral can then be evaluated by integrating

$$F(z) = e^{iz\eta} \frac{\cosh\left(\frac{\pi z}{2}\right)}{\sinh\left(\frac{\pi z}{2}\right)} \tag{B.34}$$

about the closed contour depicted in figure B:

$$\int_{\gamma} F(z)dz = \int_{-R}^{-\rho} F(x)\,dx - \int_{\Gamma_\rho} F(z)\,dz + \int_{\rho}^{R} F(x)\,dx + \int_{\Gamma_R} F(z)\,dz\,. \tag{B.35}$$

The poles of $F(z)$ are obtained by solving

$$\sinh\left(\frac{\pi z}{2}\right) = 0\,. \tag{B.36}$$

The poles are therefore located at

$$z = 2n\imath \quad n = 0 \cdots \infty\,, \tag{B.37}$$

and for the corresponding residues are given by

$$Re_n = \frac{2}{\pi} e^{-2n\eta}\,. \tag{B.38}$$

These residues then allow us to calculate the following integrals

$$\int_{\gamma} F(z)\,dz = 4\imath \sum_{n=1}^{\infty} e^{-2n\eta}\,, \tag{B.39}$$

$$\int_{\Gamma_\rho} F(z)\,dz = 2\imath\,. \tag{B.40}$$

Application of Jordan's lemma then gives

$$\int_{-\infty}^{\infty} F(x)\,dx = 2\imath\left(1 + 2\sum_{n=1}^{\infty} e^{-2n\eta}\right) \tag{B.41}$$

$$= 2\imath \frac{\cosh(\eta)}{\sinh(\eta)}\,. \tag{B.42}$$

Substituting this result into equation (B.31) we obtain

$$\psi(\xi) = C - \frac{1}{\pi} \fint_{-\infty}^{\infty} g(\xi - \eta) \frac{\cosh(\eta)}{\sinh(\eta)} \, d\eta. \tag{B.43}$$

By using the properties of the convolution this may then be written as

$$\psi(\xi) = C - \frac{1}{\pi} \fint_{-\infty}^{\infty} g(\eta) \frac{\cosh(\xi - \eta)}{\sinh(\xi - \eta)} \, d\eta. \tag{B.44}$$

In terms of our original variables the integral equation is

$$\phi(x) = \frac{C}{\sqrt{x}} - \frac{1}{2\pi} \int_0^{\infty} \frac{f(t)}{\sqrt{xt}} \frac{x+t}{x-t} \, dt \,. \tag{B.45}$$

This expression, (B.45), can be simplified by using the fact that

$$\frac{x+t}{x-t} = -1 + \frac{2x}{x-t}, \tag{B.46}$$

$$= 1 + \frac{2t}{x-t}. \tag{B.47}$$

Substituting equation (B.46) into equation (B.45) and simplifying the integral we obtain the relationship

$$\phi(x) = \frac{C}{\sqrt{x}} - \frac{1}{\pi} \int_0^{\infty} \sqrt{\left(\frac{x}{t}\right)} \frac{f(t)}{x-t} \, dt \,. \tag{B.48}$$

If we substitute equation (B.47) into equation (B.44) and simplify the resulting integral we obtain

$$\phi(x) = \frac{C}{\sqrt{x}} - \frac{1}{\pi} \int_0^{\infty} \sqrt{\left(\frac{t}{x}\right)} \frac{f(t)}{x-t} \, dt \,. \tag{B.49}$$

Both the above equations are valid alternatives for the inverse of the Hilbert transform on a semi-infinite interval. The properties of the function $f(t)$ may be used to dictate which form is relevant This is determined by which of the integrals is convergent when given a particular function $f(t)$. The integral equation for the inverse of the Hilbert

transform on the semi-infinite interval is usually written as

$$\boxed{\phi(x) = \frac{C}{\sqrt{x}} - \frac{1}{\pi} \int_0^\infty \left(\frac{x}{t}\right)^{\pm 1/2} \frac{f(t)}{x-t}\, dt\,.} \tag{B.50}$$

REFERENCES

ACHESON, D., J, *Elementary Fluid Dynamics* , 1990, Clarendon Press, Oxford.

ATKIN, R. J., CRAINE, R. E., *Continuum Theories of Mixtures: Basic Theory and Historical Development*, Q. Jl. Mech. appl. Math., Vol XXIX, pt 2, (1976), pp 209–244.

ATTHEY, D. R., SCRUTON, B., CHOJNOWSKI, B., *A Model to Predict the Transient Behaviour of The Dryout Front in a Steam Generating Tube*, Proc. Uk. Second National Heat Transfer Conf., Vol. 1, (1988), pp 285–298.

ATTHEY, D. R., *Private Communication*, (1992).

CARSLAW, H. S., JAEGER, J. C., *Conduction of Heat in Solids*, Oxford University Press, (1946).

CHILLINGWORTH, H.R., *Complex Variables*, Oxford Pergamon press, (1973)

CHISHOLM, D., *Two Phase Flow in Pipelines and Heat Exchangers*, Longman Group Limited, (1983).

COLLIER, J. G., *Convective Boiling and Condensation*, Mcgraw Hill, (1972)

DREW, D. A., *Mathematical Modelling of Two-Phase Flow*, Ann. Rev. Fluid Mech., Vol , (1983), pp 363–409.

DREW, D. A., WOOD, R. T., *Overview and Taxonomy of Models and Methods for Workshop on Two-Phase Flow Fundamentals*, (1988)

FITT, A. D., *Private Communication*, (1994).

FITT, A. D., OCKENDON, J. R., JONES, T. V., *Aerodynamics of Slot-Film Cooling: Theory and Experiment*, J. Fluid. Mech., Vol. 160, (1985), pp 15–27.

FOWLER, A. C., LISSETER, P. E., *Flooding and Flow Reversal in Annular Two-Phase Flows*, Int. J. Multiphase Flow, Vol. 18, No. 2, (1992), pp 195–204.

GRIFFITH, P., WALLIS, G., B., *Two-Phase Slug Flow*, J. Heat Trans., (1961), 83, 307.

ISHII, I., ZUBER, N., *Drag Coefficient and Relative Velocity in Bubbly, Droplet or Particulate Flows*, AIChE J., Vol. 25, No. 5, (1976), pp 843–855.

ISHII, M., GROLMES, M.A, *Inception criteria for Droplet Entrainment in Two-phase Concurrent Film Flow*, AIChe J., Vol. 21, No 2, 308318,(1975), pp 308–318.

JOESPH, D. D., SHAEFFER, D.G., *Two-Phase Flows and Waves*, Springer–Verlang, (1989).

KEENAN, J. H., KEYES, F. G., HILL, P. G., MOORE., J. G., *Steam Tables*, John Wiley and Sons Inc.,(1969)

LISSETER, P. E., FOWLER, A. C., *Bubbly Flow – 1 A Simplified Model*, Int. J. Multiphase Flow, Vol. 18, No. 2, (1992), pp 195–204.

MAGEE, P. M., CASEY, D. F., CHU, C. L., DILLMAN, C. W., ROBERTS, J. M., WOLF, S., *An Evaluation of Strain Cycling Effects in the Dnb Zone of the CRBR Evaporators*, General Electric Internal Report, (1976)

MAO, Z.–S., DUKLER, A. E., *The Motion of Taylor Bubbles in Vertical Tubes—II. Experimental Data and Simulation for Laminar and Turbulent Flow*, Chem. Eng. Sci., Vol. 46, No. 8, pp 2055–2064.

MCLAIN, S., *Reactor Handbook Volume 4*, 2nd edition, Interscience, (1964).

MUSKHELISHVILI, N. I., *Singular Integral Equations*, Dover Publications Inc, sec-

ond edition 1992.

NAKORYAKOV, V. E., KASHINSKY, O. N., KOZMENKO, B. K., *Experimental study of gas-liquid slug flow in a small diameter vertical pipe*, Int. J. Multiphase Flow, Vol 12, No 3, pp 337-355, (1986).

NAYFEH, A. H., *Perturbation Methods*, New York Wiley-Interscience, (1973).

NAVARRO-VALENTI, S., CLAUSSE, A., DREW, D. A., LAHEY, R. T., *A Contribution to the Mathematical Modelling of Bubbly/Slug Flow Regime Transistion*, Chem. Eng. Comm., Vol. 102, (1991), pp 69–85.

NEWITT, D. M., DOMBROWSKI, N., KNELMAN, F. H.,*Liquid Entrainment: The Mechanism of Droplet Formation from Gas or Vapour Bubbles*, Trans. Inst. Chem. Eng., 32, (1954), 244.

OLIEMANS, R. V. A., POTS, B. F. M., TROMPE, N., *Modelling of Annular Dispersed Two-Phase flow in Vertical Pipes*, Int. J. Multiphase Flow, Vol. 12, No. 5, pp 711-732, (1986).

O'MALLEY, K., FITT, A. D., JONES, T. V., OCKENDON, J. R., WILMOTT, P., *Models for High Reynolds Flow Down a Step*, J. Fluid. Mech., Vol 222, (1991), pp 139-155.

PANTON, R.L., *Incompressible Flow* , Wiley, New York, (1984)

PEDERSEN, E. S., *Nuclear Power Volume 2*, Ann Arbor Science Publishers Inc., (1978)

PIPKIN, A. C., *A Course on Integral Equations*, Springer-Verlag, (1991).

PROSPERETTI, A., SATRAPE, J. V.,*Stability of Two-Phase Flow Models*,Two Phase Flows and Waves, Springer-Verlag,(1990).

RANSOM, V. H., HICKS, D. L., *Hyperbolic Two-Pressure models for Two-Phase Flow*, J. Comp. phys., Vol. 53, (1984), pp 124–151.

RODGERS, G. F. C., MAYHEW, Y. R., *Engineering Thermodynamics: Work and Heat Transfer*, 2nd ed, Longman Text, (1967).

SOO, S. L., *Fluid Dynamics of Multiphase Systems*, Wiley Interscience, (1967).

SOO, S. L., *Multiphase Fluid Dynamics*, Ist ed, Beijing Science Press, (1990).

STEWART, H. B., WENDROFF, B., *Review Article, Two-Phase Flow: Models and Methods*, J. Comp. phys., Vol. 56, (1984), pp 363–409.

TAITEL, Y., BORNEA, D., DUKLER, A. E., *Modelling Flow Pattern Transitions for Steady Upward Gas-Liquid Flow in Vertical Tubes*, AIChe J., Vol. 26, No. 3, (1980), pp 345–354.

THEOCARIS, P.S, IOAKIMIDIS, N.I *Numerical Integration Methods for the Solution of Singular Integral Equations*, Quart. Appl. Math. Vol 35, pp 173–187, 1977.

VAN DYKE, M., *Perturbation Methods in Fluid Mechanics*, Parobolic Press, (1975).

VAN ROSSUM, J. J.,*Experimental Investigation of Horizontal Liquid Films*, Chem. Eng. Sci., 11, 35 (1959).

VARLEY, E., WALKER, J. D. A., *A Method for Solving Singular Integrodifferential Equations*, IMA Journal of Applied Mathematics, Vol 43, (1989), pp 11-45.

WALLIS, G. B., *One Dimensional Two-Phase Flow*, McGraw Hill, (1969).

WHALLEY, P. B., *Boiling Condensation and Gas-Liquid Flows*, Oxford Science Publications, (1987).